TECHNICAL REPORT STANDARD TITLE PAGE

1. Report No.	2. Government Accession No.	3. Recipient's Catalog No.
TTI-2-5-75-195-1F		

4. Title and Subtitle	5. Report Date
THE MEASUREMENT OF PILE DRIVING FORCES AND ITS APPLICATION TO WAVE EQUATION ANALYSIS OF PILES	September 1975
	6. Performing Organization Code
7. Author(s)	8. Performing Organization Report No.
Francis X. Kaiser, Jr., Harry M. Coyle, Lionel J. Milberger and Richard E. Bartoskewitz	Research Report No. 195-1F
9. Performing Organization Name and Address	10. Work Unit No.
Texas Transportation Institute Texas A&M University College Station, Texas 77843	11. Contract or Grant No. Study No. 2-5-75-195
	13. Type of Report and Period Covered
12. Sponsoring Agency Name and Address	Final - September, 1974 September, 1975
Texas State Department of Highways and Public Transportation; Transportation Planning Division P. O. Box 5051 Austin, Texas 78763	14. Sponsoring Agency Code

15. Supplementary Notes

Research performed in cooperation with DOT, FHWA.
Study Title: "Field Evaluation of a Dynamic Peak-Force Read-out Apparatus for Use in Analysis of Piling Behavior"

16. Abstract

A new, dynamic peak force readout device was tested and found to be accurate, reliable, and easily used with a proposed new method of analysis of driven piles. Model pile, pile stub in a pendulum loading facility, and actual field pile driving tests are described. The data from the tests are presented for the new device and for a standard carrier amplified system which was also used during the tests. Comparison of the output data shows that the new device measures peak force values which are within 4% of the values obtained with the standard carrier amplifier system. Tests conducted under various temperature conditions demonstrate the stability of the new device.

The traditional wave equation technique of pile driving analysis is very briefly introduced and a proposed standard method of analysis using measured peak force is presented in a step-by-step manner. A sample problem is presented using the proposed standard method and data obtained from the new device field-evaluation tests. The sample problem is used to demonstrate the use of the new device in conjunction with the proposed method of analysis. Good agreement is indicated between the proposed standard method and the use of measured force in the pile with time when predicting total resistance at the time of driving. Studies of hammer simulation and parameter variations, and test results of a proposed aluminum force transducer are appended.

17. Key Words	18. Distribution Statement
Pile Driving, Pile Bearing Capacity, Measured Dynamic Peak Force, Wave Equation Analysis.	No Restrictions. This document is available to the public through the National Technical Information Service, Springfield, Virginia 22161.

19. Security Classif. (of this report)	20. Security Classif. (of this page)	21. No. of Pages	22. Price
Unclassified	Unclassified	146	

Form DOT F 1700.7 (8-69)

THE MEASUREMENT OF PILE DRIVING FORCES AND ITS APPLICATION TO WAVE EQUATION ANALYSIS OF PILES

by

Francis X. Kaiser, Jr.
Research Assistant

Harry M. Coyle
Research Engineer

Lionel J. Milberger
Research Associate

and

Richard E. Bartoskewitz
Engineering Research Associate

Research Report 195-1F

Field Evaluation of a Dynamic Peak-Force Read-out Apparatus for Use in Analysis of Piling Behavior
Research Study Number 2-5-75-195

Sponsored by the
State Department of Highways and Public Transportation
in Cooperation with the
U.S. Department of Transportation
Federal Highway Administration

September 1975

TEXAS TRANSPORTATION INSTITUTE
Texas A&M University
College Station, Texas

DISCLAIMER

The contents of this report reflect the views of the authors who are responsible for the facts and the accuracy of the data presented herein. The contents do not necessarily reflect the official views or policies of the Federal Highway Administration. This report does not constitute a standard, specification, or regulation.

NOTE

Until recently the State Department of Highways and Public Transportation (SDHPT) was known as the Texas Highway Department (THD). Various tests mentioned in this report are identified with the former name.

ABSTRACT

A new, dynamic peak force readout device was tested and found to be accurate, reliable, and easily used with a proposed new method of analysis of driven piles. Model pile, pile stub in a pendulum loading facility, and actual field pile driving tests are described. The data from the tests are presented for the new device and for a standard carrier amplifier system which was also used during the tests. Comparison of the output data shows that the new device measures peak force values which are within 4% of the values obtained with the standard carrier amplifier system. Tests conducted under various temperature conditions demonstrate the stability of the new device.

The traditional wave equation technique of pile driving analysis is very briefly introduced and a proposed standard method of analysis using measured peak force is presented in a step-by-step manner. A sample problem is presented using the proposed standard method and data obtained from the new device field-evaluation tests. The sample problem is used to demonstrate the use of the new device in conjunction with the proposed method of analysis. Good agreement is indicated between the proposed standard method and the use of measured force in the pile with time when predicting total resistance at the time of driving. Studies of hammer simulation and parameter variations, and test results of a proposed aluminum force transducer are appended.

KEY WORDS: Pile Driving, Pile Bearing Capacity, Measured Dynamic Peak Force, Wave Equation Analysis.

SUMMARY

The information presented in this report has been developed during a one year type B study on the evaluation of a new Dynamic Peak-Force Read-out device for use in Wave Equation analysis of piling behavior. The new device has been evaluated by conducting laboratory model tests, full scale pile stub tests in a pendulum loading facility, and actual pile driving tests at a bridge site. Data taken with the new device are compared with data measured by a standard carrier amplifier system. Peak force measurements obtained from the new device are found to be accurate and reliable.

A proposed standard method of analysis using measured peak force in conjunction with the wave equation computer program is also presented in this report. An example problem is included to demonstrate the use of the proposed standard method of analysis. Data taken during the actual pile driving test at Gouchy Creek in Red River County, Texas are used in the example problem. The example problem illustrates how the peak force obtained from the new read-out device is used to analyze a pile driving problem and to prepare a "bearing graph" for predicting pile bearing capacity by wave equation analysis.

IMPLEMENTATION STATEMENT

The dynamic peak-force read-out device is available to State Department of Highways and Public Transportation personnel for immediate use and implementation. Tests conducted during this study have shown that the device is durable, easy to use under field conditions, and suitable for production pile driving work. Data taken with the new device can be used to improve the accuracy of wave equation analyses of piling behavior.

It should be noted that the device must be used with strain gage instrumentation of test piling at this time. A new Type B research project has been approved for this year (Sept. 1975 thru Aug. 1976) to develop a portable transducer or externally bonded strain gage system that can be used with the read-out device. Development of a portable transducing system will result in easier and more efficient implementation of the use of the device.

TABLE OF CONTENTS

	Page
INTRODUCTION	1
Present Status of the Question	1
Objectives	3
PEAK FORCE MEASUREMENT SYSTEMS	4
Dynamic Pile Force Readout Device (DYROD)	4
Standard Carrier Amplifier System (STDSYS)	5
DESCRIPTION OF EVALUATION TESTS	11
Model Pile Test	11
Pile Stub and Pendulum Test	14
Gouchy Creek Test	17
EVALUATION TESTS -- DATA REDUCTION, ANALYSIS AND ACCURACY	31
Calibration Factors and Data Reduction	31
Analysis of Output Data from the Measurement Systems Evaluation Tests	36
USE OF PEAK FORCE MEASUREMENT SYSTEM DATA	54
Wave Equation Technique for Simulation of a Pile Driving Operation	54
Proposed Standard Method of Analysis Using Measured Peak Force Data	59
Sample Problem Using Standard Method of Analysis - Gouchy Creek Data	61
CONCLUSIONS AND RECOMMENDATIONS	70
Conclusions	70
Recommendations	71
APPENDIX I - REFERENCES	74
APPENDIX II - NOTATION	77
APPENDIX III - CORRELATION OF DRIVING RATES AND PEAK FORCE	80
APPENDIX IV - TABULAR AND GRAPHICAL PRESENTATION OF DATA USED IN EVALUATING MEASUREMENT SYSTEMS INCLUDING PERCENT DIFFERENCES	87
APPENDIX V - TEST OF PERFORATED, ALUMINUM FORCE TRANSDUCER	110

TABLE OF CONTENTS (CONTINUED)

	Page
APPENDIX VI - ACTUALLY MEASURED FORCE - TIME DATA AND PARAMETER VARIATION STUDIES	121
APPENDIX VII - LINEARITY AND CALIBRATION RESISTORS	130

LIST OF TABLES

Table		Page
1	TENTATIVE SPECIFICATIONS FOR MODEL 2174 DYNAMIC PILE FORCE READOUT	6
2	COMPARATIVE SPECIFICATIONS FOR STDSYS HONEYWELL MODEL 119	9
3	STRAIN GAGE INSTRUMENTATION SPECIFICATIONS	10
4	STANDARD SPECIFICATIONS FOR DELMAG -- DIESEL PILE HAMMER, MODEL D-12	26
5	PROPERTIES USED IN COMPUTATIONS OF CALIBRATION SIGNAL EQUIVALENT VALUES	32
6	FINAL DETERMINATION OF WEIGHTED AVERAGE PERCENT DIFFERENCE OF DYROD GALVO FROM STDSYS	38
7	FINAL DETERMINATION OF WEIGHTED AVERAGE PERCENT DIFFERENCE OF DYROD DPM FROM STDSYS	41
8	FINAL DETERMINATION OF WEIGHTED AVERAGE PERCENT DIFFERENCE OF DYROD GALVO FROM DPM	45
9	SUMMARY OF STANDARD METHOD OF ANALYSIS INPUT DATA FOR GOUCHY CREEK PILES	65

LIST OF FIGURES

Figure		Page
1	MODEL PILE TEST SET-UP	12
2	AVAILABLE OUTPUTS FROM MEASUREMENT SYSTEMS	13
3	PILE STUB AND PENDULUM TEST FACILITY	15
4	GOUCHY CREEK BRIDGE - PLAN	19
5	GOUCHY CREEK BRIDGE - FOUNDATION	20
6	GOUCHY CREEK BORING PROFILES	21
7	TEST PILE INSTRUMENTATION	23
8	MODULUS OF ELASTICITY OF CONCRETE CYLINDERS	24
9	PENETRATION OF TEST PILES	28
10	AVERAGE DYROD READING VS. STDSYS READING	39
11	AVERAGE DYROD DPM READING VS. STDSYS READING	42
12	AVERAGE GALVO READING VS. DPM READING	46
13	SCALING ERROR - MAXIMUM PROBABLE	50
14	INDICATED ERROR OVER TEMPERATURE RANGE	52
15	PILE AND SOIL SIMULATION	55
16	HAMMER SIMULATION	57
17	FORCE-TIME FOR VELMI = 17.8 FT/SEC ASSUMING NO CAPBLOCK.	66
18	RAM VELOCITY VS. COMPUTED PEAK FORCE IN THE TOP OF A PILE.	67
19	BEARING GRAPH FOR PILE B-17	68

INTRODUCTION

Present Status of the Question.

The wave equation method of analysis has become a rather well-known technique over the last decade for the simulation of piles during driving. It is a realistic representation of a dynamic problem and, as such, can provide accurate analyses. However, the method has not found widespread use to-date. One of the principal reasons for this has been the inability to verify the assumed hammer simulation data during normal driving operations. A promising solution to that problem has recently been suggested by Coyle, et al. (5)* using an instrument designed by Milberger and Zimmer (12). The new instrumentation, joined with the wave equation method of analysis, will provide a feasible and improved approach to general pile driving analyses, after some investigation and standardization of the combined approach.

Pile foundation design and analyses of pile driving have been performed by engineers through the years using a myriad of theories and formulas (4). Most of these have been empirical relationships with correction factors for unknown parameters and/or their unknown influence. Others more or less reflect the actual behavior of the pile-soil system (3, 11), as does the wave equation method of analysis.

The "traveling wave" nature of impact on rods, from which the wave equation originates, was reported to have been first studied by St. Venant about 1865 (3). In the 1930's, others performed extensive mathematical and experimental studies of wave propagation behavior in piles, but it was not until Smith (15) developed an accurate, numerical method of simulating the dynamic, interactive behavior of the pile driving system that use of this form of analysis started to pick up momentum. During the last fifteen years considerable research has been performed using the wave equation theory. Efforts have been directed toward the

*Numbers in parentheses refer to references listed in Appendix I.

development of a general, adequate modeling of pile driving system components for the computer analysis of pile driving behavior and determination of ultimate static bearing capacity. Several studies have included attempts to determine the effect of various parameter changes (18). Case records have also been studied to develop generalized relationships between the wave equation parameters and component types and/or commonly obtained properties of the soil-pile-hammer system (2, 6, 11). Simulation of new hammers, materials, and geometries are also subject to on-going unpublished research.

Throughout the wave equation research studies, one of the recurring problems has been the simulation of the pile driving hammer and associated driving accessories. The difficulty of accurately modeling and measuring force transmission thru capblocks and cushions is compounded by the variety of materials used, and the changing condition and properties of those components, during the driving operation. Inroads have been made into these areas yielding some approximate or average recommended values (10). The diesel hammer assembly simulations however, have not met with as much success as other hammer types.

To adequately model the pile driving assemblies, a technique has been used which involves adjustment of various assumed values until computed force-time input being delivered to the pile agrees with measured force-time input delivered to the pile (6). Obtaining the actual force-time records at several points along the pile has necessitated elaborate electronic recording devices. Such set-ups are not practical nor economical for general usage during production pile driving operations. That problem, however, has been solved. It is now possible to predict accurate values of bearing capacity and driving stresses, using adjusted input parameters which are obtained by matching the computed and measured peak forces alone (5), at the head of the pile.

The wave equation method of analysis when coupled with the actual peak driving force at the head of the pile, as input, would appear to offer a more reasonable and direct approach to the analysis of pile behavior. Potential application of the method to widespread usage in

production pile driving has been further enhanced by recent research and design of a simply operated and portable, peak force read-out instrument (12). The device prior to this study, had been bench-tested but had not undergone field tests.

Objectives.

The broad objective of the research is to develop a better method for predicting the static bearing capacity of driven piles by wave equation analysis.

The specific objectives of this research effort are, first, to investigate and expand the wave equation method of analysis using peak driving force as input, and second, to test a new instrument which will actually measure the peak driving force.

To meet those objectives, it was necessary to accomplish the following tasks:

A. Determine the suitability of a dynamic peak force read-out apparatus designed by Milberger and Zimmer (12) for use in routine wave equation analysis.
B. Establish and document the accuracy and repeatability of the apparatus by comparison with a standard measuring system.
C. Determine modifications or changes that might be made to optimize the device as an investigative tool.
D. Provide additional peak force and force-time data for future use in wave equation analysis of driven piles.

PEAK FORCE MEASUREMENT SYSTEMS

Two peak force measurement systems were compared in this study. The new, dynamic pile force readout device (DYROD) was compared with a standard carrier amplifier system (STDSYS). A separate description of each peak force measurement system follows.

Dynamic Pile Force Readout Device (DYROD).

General description.-- A dynamic, pile-driving compressive force readout device (DYROD) has recently been designed and built by researchers of the Texas Transportation Institute at Texas A&M University. The device was developed during research sponsored by the Texas State Department of Highways and Public Transportation (SDHPT) in cooperation with the Federal Highway Administration. The device is basically "an electronic readout unit for displaying the maximum dynamic force on the head of a pile at the time the pile is being driven" (12).

The Model 2174 Dynamic Pile Force Readout is intended for use with a universal transducer, placed on top of the pile or pile cap. The readout has also been used with strain gages embedded at any point within concrete piles. It can be used equally well with bonded or weldable strain gages which are typically attached to pipe piles and H-piles. The readout unit is designed for use with a full Wheatstone bridge configuration, thus enabling cancellation of bending and temperature effects at the time of pile driving. An acceptable universal transducer for use with the DYROD has not yet been developed and will be the subject of research in the near future. A Belden 8723 interconnect cable (1.5 ohm) is presently used for connection to a transducer or strain gage.

Output available.-- The normal output mode for the DYROD is the lighted digital panel meter (DPM). The DPM displays the peak compressive impact force delivered to a pile during driving directly in "KIPS" (4.45 kN). Any number of blows between 0 and 99 may be skipped between samplings, as the operator desires. The DPM display may be interpreted

in any units of force, stress, strain, or deflection if an appropriate calibration number is used. In the normal manner of interpretation, the DPM will not be triggered to display below 50 kips (222 kN).

Two additional output modes are provided. A front panel Oscilloscope BNC connection is available as voltage output for driving high impedance instruments of 1 megohm or higher. Galvonometer binding posts are also available on the front panel as current output for driving low impedance devices. The DYROD can be powered by an internal, sealed and rechargeable, lead-acid 5 amp-hour battery, a 12 V d-c external battery, or a 117 V a-c line. The device is lightweight and completely self-contained.

Tentative specifications and accuracy.-- Tentative specifications according to the designers (12) of the instrument are summarized in Table 1. On the basis of laboratory tests during construction of the DYROD and assembly of electrical components, the accuracy of the readout is expected to be 1% of full scale.

Standard Carrier Amplifier System (STDSYS).

General description.-- The standard carrier amplifier system (STDSYS) has long been used to obtain dynamic strain measurements on piles at the Texas Transportation Institute. The system is composed of four separate pieces of equipment: an a-c power source, a "power supply"/oscillator unit, a carrier amplifier unit, and a Visicorder oscillograph. The equipment is of the vacuum tube type and is expensive, cumbersome, complex, and difficult to maintain for field use. Complete technical operations manuals are available for each device (7, 8). With proper transducer input the system is capable of measuring both tension and compression. Only some of the more salient features will be described.

Power source.-- Where no suitable on site power source is available, some alternate source must be brought with the instrumentation or provided by a contractor at additional cost. Use of the standard carrier amplifier system in the past has necessitated trailering of a

TABLE 1.-- TENTATIVE SPECIFICATIONS FOR MODEL 2174
DYNAMIC PILE FORCE READOUT (12)

Component	Rating of Type	Remarks
Input Transducer	120-500 ohms	Full-bridge strain gage type.
Signal Conditioner	Carrier type	*
Carrier Freq.	10 kHz	Amplitude stabilized.
Excitation Volt.	3-4.5 Vrms	----------
Freq. Response	d-c to 1 kHz	Pass-band flatness ± 0.2db.
Range	50-1000 kips	Direct reading.
Noise	0.1% rms	Of full scale (F.S.).
BNC Output	approx. +2V	At F.S.
Binding Posts	25 mA	F.S., into 27 ohms impedance.
Bal. Rnage**	3000 μ-strain	Resistive balance.
	0.0005 μF	Capacitive balance.
Nonlinearity	<1%	Of F.S.
Input Impedance	5000 ohms	----------
Display	3-1/2 digits	Digital panel meter.
Cal. Resistors	10	***
Coarse & Fine Gain	2 ten turn pots	----------
Internal Power	lead-acid battery	Sealed & rechargeable.
Case (sealed)	10"x16"x12"	(25x41x30 cm)
Weight	26 lbs. (12 kg)	----------
Operating Range	0-70°C	32-158°F
Warm-up Time	5 sec	----------

* Will suppress self-generating responses of moving strain gages.

** Included is a special automatically compensating "balance error correction amplifier" (BECA), such that imbalance during operation is not critical.

*** Pre-selected shunt to simulate known effect of selected, probable impact force.

Note - Percents error may be additive. See Tables 2 and 3 also.

military PE-95 power unit. The PE-95 power unit is a 2800 lb. (1300 kg), gasoline driven portable generator, capable of delivering 110 volts a-c at a steady 60 cycles. Accuracy of timing indicator circuits which indicate time on system output records is very dependent upon a steady power input frequency.

Power supply unit.-- The power supply unit is a three component device. Incoming alternating current first must go through the rectifier, where it is rectified to d-c. Then the current goes to the second component, the regulator, which provides constant d-c voltage to the oscillator and amplifiers, regardless of changes in load and line voltage. The third component, the oscillator provides a 5000 Hz carrier voltage to energize the strain gage bridges or transducer. It also supplies a 5000 Hz reference voltage to a discriminator circuit in the amplifiers.

Carrier amplifier unit.-- The carrier amplifier unit contains six, single-channel amplifiers, each equiped with attenuation, gain, resistive and capacitive balance, and discriminator balance controls, with an internal 60K ohm (±0.1%) calibration switch. A channel selector, on the regulator component of the power supply unit, connects the amplifiers one at a time with a voltmeter and milliammeter, for balancing. The milliammeter may also be used for reading amplifier output during a static strain test.

The carrier amplifier unit will accept two or four-arm external resistance strain gage bridges, or variable reluctance transducers, or differential transformer gages as "pickup" devices to provide a signal input. After amplification of the voltage output of a bridge, the 5000 Hz carrier frequency is removed from the signal by the discriminator and filter circuit of the amplifier unit. The amplified signal is then output to a galvonometer or other low impedance device. In the case of dynamic measurements, a Visicorder oscillograph receives the signal.

Visicorder oscillograph unit.-- The Visicorder oscillograph is a Honeywell, Model 1508, direct writing oscillograph capable of simultaneously recording up to 24 channels of data at frequencies ranging from

d-c to 5000 Hz. The device used fluid-damped galvonometers. Ultraviolet light from a high pressure mercury vapor lamp is passed through collecting and focusing lenses and is reflected off a number of mirrors to eventually produce a continuous tracing on light sensitive paper. Drive speeds of up to 80 in. (200 cm) per second (8) are used with 8 in. (20 cm) by 100 ft (30 m) rolls of paper. A separate synchronized paper take-up unit is also required. Timing lines can be printed at 0.01 sec intervals (±2%), and recording spot velocities range from static to 25,000 inches per second (640 m/sec). Longitudinal grid (scale) lines are printed at 0.1 inch (2.5 mm) spacing for determining the values of trace deflections. The trace, timing, and grid lines become visible after "latensification" (latent image intensification), by exposure to sunlight or fluorescent light. The exposed Visicorder tracing is the normal output mode for the standard carrier amplifier system when dynamic measurements are to be obtained from one or more locations in a pile during driving.

Comparative specifications and accuracy.-- Specifications of the standard carrier amplifier system are listed in Table 2. Similar information is presented in Table 3 for strain gage instrumentation used with the standard carrier amplifier system. Based upon component accuracies including that of the galvonometer as indicated by the system manufacturers in the referenced technical manuals, and from the experience of user's of the system, the overall error of the standard carrier amplifier system is no better than ±3%.

TABLE 2.-- COMPARATIVE SPECIFICATIONS FOR STDSYS-
HONEYWELL MODEL 119

Component	Rating or Type	Remarks
Input Transducer	100-1000 ohms	2 or 4 arm bridge.
Signal Conditioner	Carrier type	6 channel.
Carrier Freq.	5 kHz	----------
Gage Voltage	1-5 Vrms	Oscillator carrier output.
Freq. Response	d-c to 1000 Hz	3-db. point at 1 kHz.
Crosstalk	Less than 1%	At F.S. output.
Amp. Output	± 3%	Current output.
Binding Posts	± 50 mA	F.S., 18 ohm load**.
Nonlinearity	± 2%	Of F.S. (± 50 mA).
Input Impedance	350 ohms	----------
Display	Film trace	Visicorder trace.
Cal. Resistor	1	60,000 ohm
Attenuation	7 settings	0-1.0, each with full gain.
Power Source	115 V a-c	None internally.
Visicorder GALVO.	± 2%	----------
Power Supply	10"x17"x12"	Weight: 55 lbs. (25 kg)
Amplifier Unit	6"x17"x12"	Weight: 39 lbs. (18 kg)
Visicorder	12"x19"x17"	----------
Operating Range	10-46^{o}C	50-115^{o}F
Warm-up Time	1/2 hour	----------

* 0-1000 Hz range.

** Output to galvonometers in oscillograph.

*** Data obtained from Ref. 7 and 8.

Note - Percents error may be additive. See Table 3 also.

TABLE 3

STRAIN GAGE INSTRUMENTATION SPECIFICATIONS

Type	Use & Rating
Model Pile Test W.T. Bean. Inc., Detroit, Mich. BAE-13-125TB-120	120 ± ohm resistance 1/8" long Half-bridge, bonded GF = 2.05 (± 1%)
Pile Stub & Pendulum Test --Pile Stub Tokyo Sokki Kenkyujo Co., LTD, Japan PML-100S	300 ± 0.9 ohm resistance 100 mm long Quarter-bridge, embedded GF = 2.10
--Alum. Transducer W.T. Bean, Inc., Detroit, Mich. BAE-13-125TB-120	120 ± 0.2 ohm resistance 1/8" long Half-bridge, bonded GF = 2.02 (± 1%)
Gouchy Creek Test Tokyo Sokki Kenkyujo Co., LTD, Japan PML-100S	300 ± 0.9 ohm resistance 100 mm long Quarter-bridge, embedded GF = 2.11
Note - Errors for various combinations of instrumentation equipment may be additive.	

DESCRIPTION OF EVALUATION TESTS

Model Pile Test.

General.-- Initial testing of the dynamic pile force readout device was performed on 27 March 1975 in a structural research laboratory at the Texas A&M University Research Annex.

Description of pile.-- A model pile was fabricated from Alcoa seamless aluminum tubing for the laboratory testing. A smooth, hemispherical steel cap was installed on the top end of the tubular model pile. The solid steel cap minimized the bending effects of any unintended eccentricities during impact loading. A 1/2 in. (13 mm) thick steel plate was welded to the base of the pile to serve as a non-bending reaction base. Other dimensions are shown in Fig. 1(a).

Hammer and cushion assembly.-- For the model pile tests, a steel weight mounted on two-by-four was used to simulate the hammer and cushion assembly. The weight was dropped from various heights and additional cushioning materials were placed above the pile cap. Various combinations of heights and cushions were tried in an effort to obtain a variety of loading wave magnitudes and shapes.

Instrumentation.-- Two full-strain gage bridges were attached to the surface of the model pile in order to measure axial strain and cancel strains due to bending stresses.

The strain gages were 120 ohm resistance type, manufactured by W. T. Bean, Inc. The gages had 1/8 in. (3 mm) gage lengths.

One pair of opposing gages was connected to the DYROD and the other pair to the STDSYS. The galvonometer (GALVO) binding posts of the DYROD were additionally connected to a free channel on the Visicorder. The Visicorder oscillograph thus printed two traces simultaneously. One trace recorded the continuous force time output signal of the STDSYS and the other trace recorded the continuous output signal of the DYROD galvonometer binding posts. This configuration allowed comparison of both the DYROD DPM output and GALVO output with the output of the STDSYS. Those system outputs are shown diagrammatically in Fig. 2.

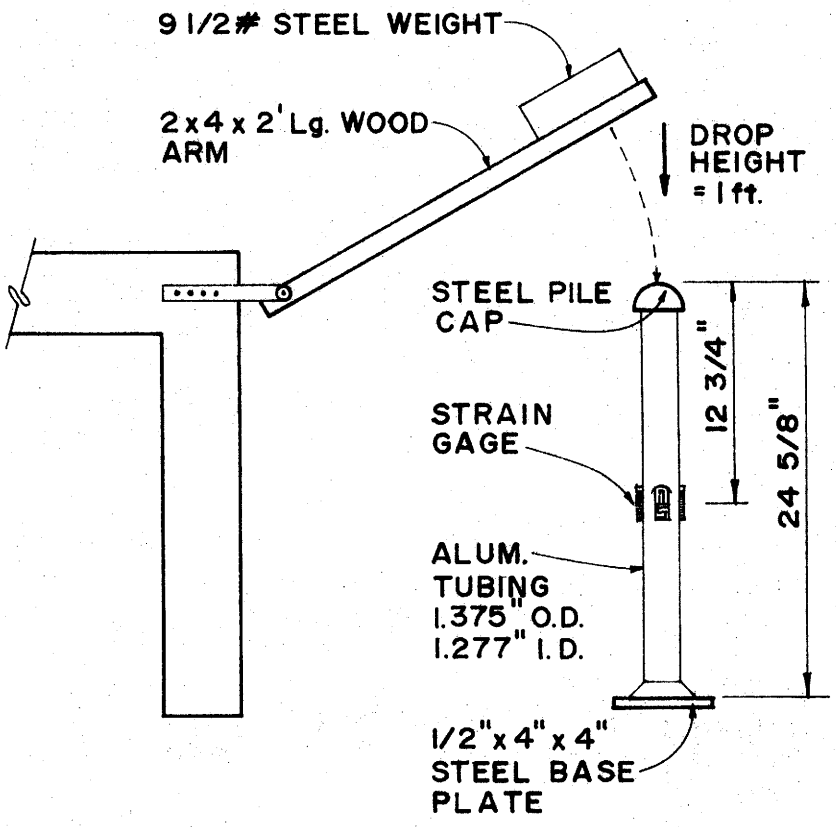

(a) Elevation

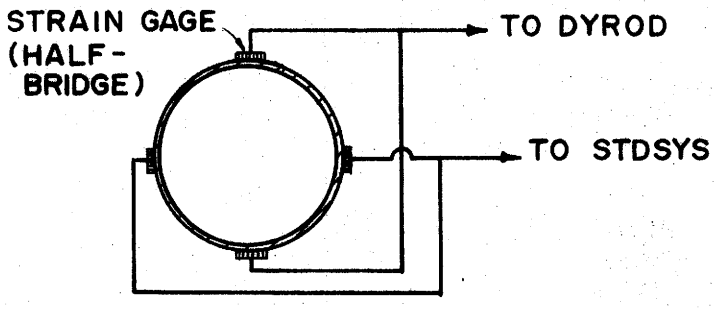

(b) Section Thru Pile At Gages

FIG. 1. - MODEL PILE TEST SET-UP.

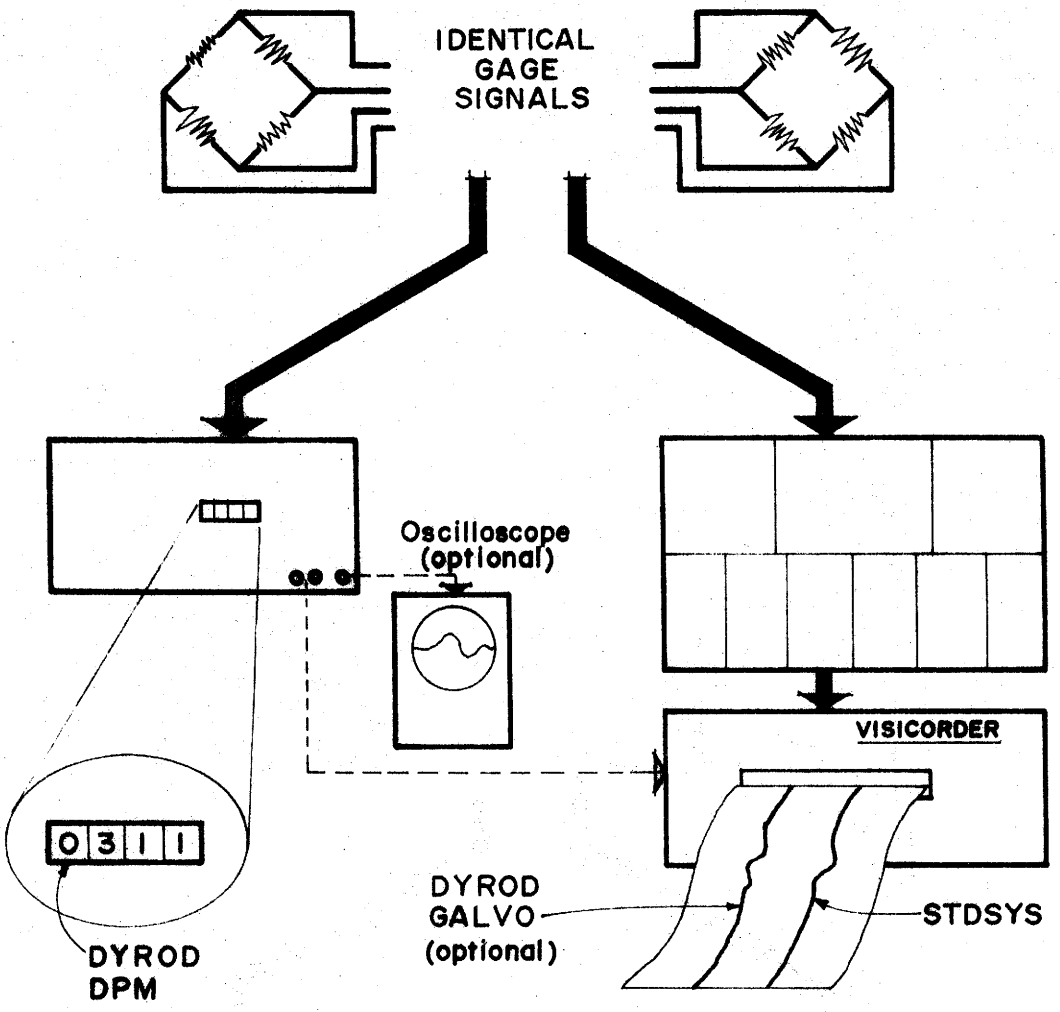

FIG. 2.- AVAILABLE OUTPUTS FROM MEASUREMENT SYSTEMS.

Loading program.-- In addition to varying the magnitude of the impact loadings, a number of cushion materials were tried. A slow push load was attempted, but this test load only provided a comparison of DYROD GALVO and STDSYS outputs.

The loading mechanism and procedures were obviously not capable of delivering peak forces in the magnitude of kips. Instead, a suitable calibration number was computed and the DPM then correctly displayed peak force in terms of pounds which was easily converted to micro-strain later for comparative purposes.

Use of aluminum tubing, from a material standpoint, allowed a lower modulus of elasticity than steel, and thus required less force to develop the desired range of dynamic strain. Geometrically, the thin wall tube configuration also served to reduce the required force, in contrast to a solid bar model pile of similar outside diameter and height. Flexibility in drop heights, and pile material and geometry combined to give a test which covered a much broader portion of the total range of the DYROD's output, than any of the other tests conducted during this study.

Pile Stub and Pendulum Test.

General.-- Tests were performed on November 14 and 20, 1974 at the Texas Transportation Institute Proving Grounds using a full-scale pendulum loading facility and an adjacent instrument house. The pile stub and pendulum tests were actually dual purpose tests. The DYROD system was being compared with the STDSYS, and at the same time, a top-of-pile perforated aluminum force transducer was being evaluated. The results of the aluminum force transducer tests are presented separately in Appendix V.

Description of pile stub.-- A 3 ft (92 cm) long section of a concrete pile was cast at the research facility and later mounted on a back-up plate as shown in Fig. 3. Four 1 in. (25 mm) diameter, steel mounting bolts had been embedded in the bottom of the pile stub, at the time of casting.

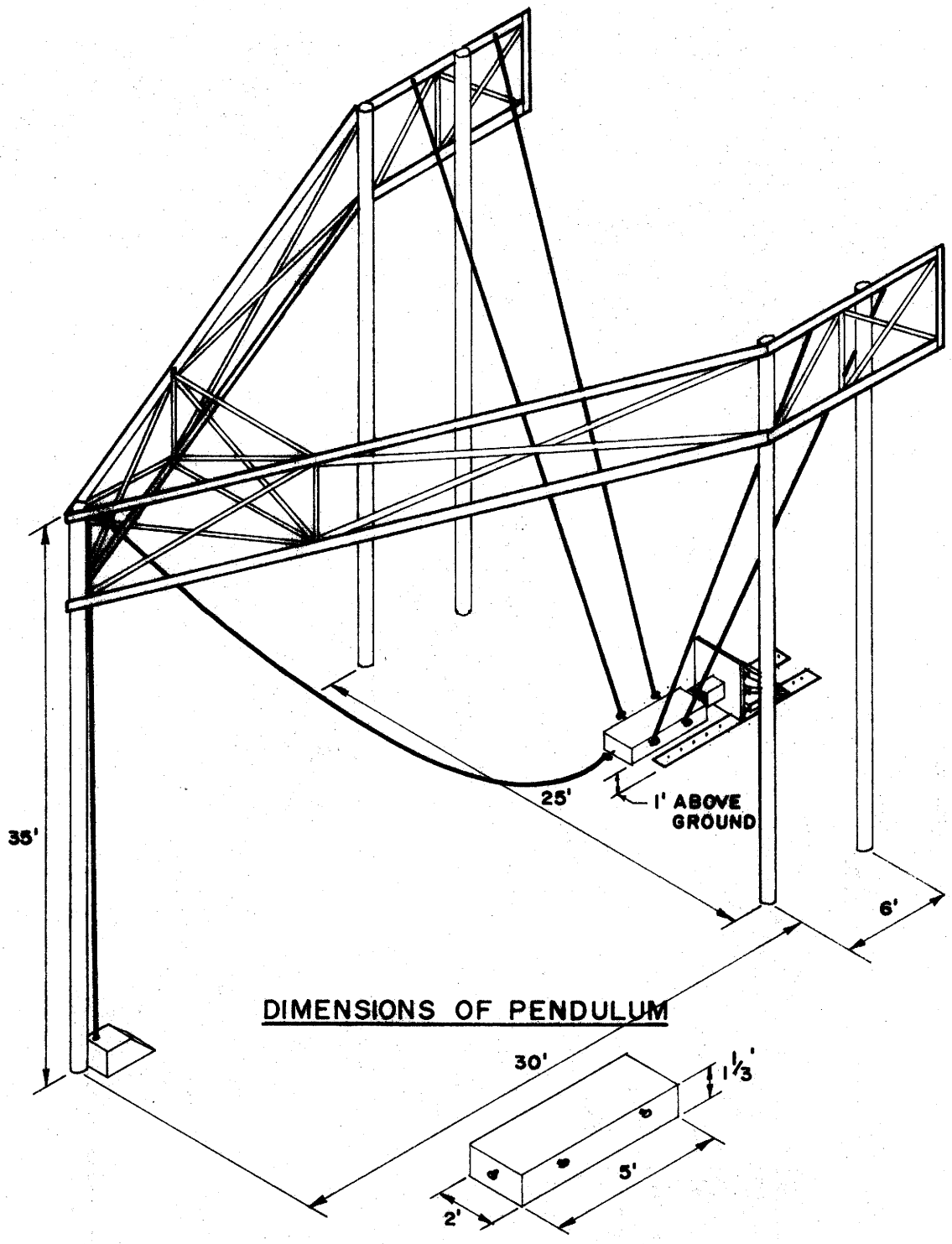

FIG. 3. - PILE STUB AND PENDULUM TEST FACILITY.

The pile was 16 in. (41 cm) square with four #8 reinforcing bars spaced 12 in. (30 cm) c to c. The design mix was for approx. 3000 psi (21 MN/m^2) concrete and the pile stub was approximately 30 days old when the DYROD tests were conducted.

The 1/2 in. (13 mm) thick steel back-up plate was reinforced with three horizontal, spot welded I-beams. The back-up plate, with the pile stub mounted horizontally on its face, was then bolted to a concrete foundation. Despite the reinforcing, the back-up plate buckled under pendulum-pile impact. Pendulum drop-heights and the number of loadings were then limited in magnitude and quantity.

Hammer simulation and pile cushion.-- The full-scale pendulum loading facility was used to dynamically load the reinforced concrete pile stub. The pendulum facility was used to test the DYROD system under impact loadings closely simulating that produced by pile driving hammers.

The one ton (907 kg) pendulum used in these tests is made of solid concrete, encased in steel, and suspended on four steel cables approximately 35 ft (11 m) long. The pendulum itself is not instrumented. During operation, it is leveled using turnbuckles and a 3 ft (92 cm) carpenters level and may be oriented to give an eccentric impact, if that is desirable. Pendulum dimensions are shown in Fig. 3. The pendulum is pulled back and up with an electric winch to the desired release position. It is then allowed to swing forward striking the target at the bottom of its arc. Thus, the weight is at its maximum velocity at the moment of impact, and maximum energy is delivered to the pile.

Eight pieces of 1/2 x 16 x 16 in. (1x41x41 cm) plywood, the steel-covered aluminum transducer, and two more pieces of 1/2 x 16 x 16 in. plywood were used on the top end of the pile stub to serve as the pile cushion. Six pieces of one-by-three wood strip, held along the pile with metal bands around the pile, aligned and supported the cushion and load cell.

Instrumentation.-- Four active strain gages were embedded in the concrete pile stub, two longitudinally and two horizontally. The gages were attached to the reinforcing steel in the required manner (12) for support during concrete placement. Longitudinal gages were placed on opposites sides of the pile and horizontal gages were located on the remaining two sides. All gages were centered 1.5 ft (46 cm) from the end of the pile stub. Gages were of the 300 ohm resistance type. Proper connection of the gages provided a full Wheatstone bridge suitable as input to any one measurement system used during these tests. Because only one complete bridge was installed in the pile stub, comparison of simultaneous DYROD and STDSYS outputs was not possible.

Though the DYROD system and STDSYS could not be connected to the pile stub simultaneously, both systems were used individually as in the aforementioned aluminum transducer check-out. The use of the DYROD in the pile stub and pendulum test did, however, afford an opportunity to compare the various available outputs of the DYROD. An oscilloscope was connected to the BNC connection and a Visicorder oscillograph was connected to the GALVO binding posts. The signals from the BNC oscilloscope connection and GALVO binding posts were then compared for a number of blows. As expected the signals from those optional output modes were identical in magnitude and shape.

Use of the DYROD measuring system in the pile stub and pendulum test also provided additional data for comparison of the galvonmeter binding posts output with the digital panel meter output.

Near the end of the pile stub and pendulum tests, a standard Vishay BA-4 portable bridge amplifier (1) was also connected to the pile stub strain gages. This portable device served as a further check on all of the other measurement systems used in the pendulum and pile stub tests.

Gouchy Creek Test.

General.-- The Gouchy Creek test was performed on May 21, 1975 and was an actual field test on a production pile driving project. Piles

were being driven at Gouchy Creek as part of a pair of Texas State Department of Highways and Public Transportation (SDHPT) contracts to grade and widen 8 existing bridges. The bridges are located on State Highway 37 between Bogota and Clarksville in Red River County. Gouchy Creek is 4.2 miles (6.8 km) NNE of the U.S. 271 - S.H. 37 intersection in Bogota.

The bridge over Gouchy Creek, a standard Highway Dept. type CS-18-110, was being widened from 25 ft (7.6 m) to 46 ft 3 in. (14.1 m) overall, with consequent extension of variable depth concrete bents beneath. The existing bridge is supported by H-piles but concrete piles were chosen to support the new, widened portion of the bridges. Foundation and bridge plans are shown in Figs. 4 and 5.

As is normally the case for small routine Texas Highway Department bridge widening projects, the length and bearing capacity of the existing foundation piles are also used for the new additional piles. Since the existing bridge foundation seemed to be performing well, 34 ft (10.4 m) piles were again chosen for use beneath the widening at bent #2. The instrumented piles were interior piles designated B-16 and B-17.

On-site soils.-- Descriptions of soil types beneath the existing bridge were available from two old and two recent borings as shown in Figs. 5 and 6. Soft to stiff, moist, gray, black, blue, and yellow clays are indicated in the first 20 ft (6.1 m) of depth. These clays overlay 7 to 18 feet (2.1 - 5.5 m) of dark, blue gray or black shale, which overlay about 10 feet (3 m) of slightly firm to slightly stiff gray clays. Beneath the gray clays lie gray shales slightly harder than the previous blue gray to black shales.

Available information about the local soils was limited to basic type and color descriptions for the "Old Test Holes". Soil consistency and Texas Highway Department Cone Penetrometer blow counts were additionally obtained for the two recent on-site test holes. Piles supporting the bridge are founded on the upper, blue gray shale layer. Penetrometer penetrations averaged 1-1/2 in. (3.8 cm) for 50 blows for that material, implying almost 400 blows per foot (0.3 m).

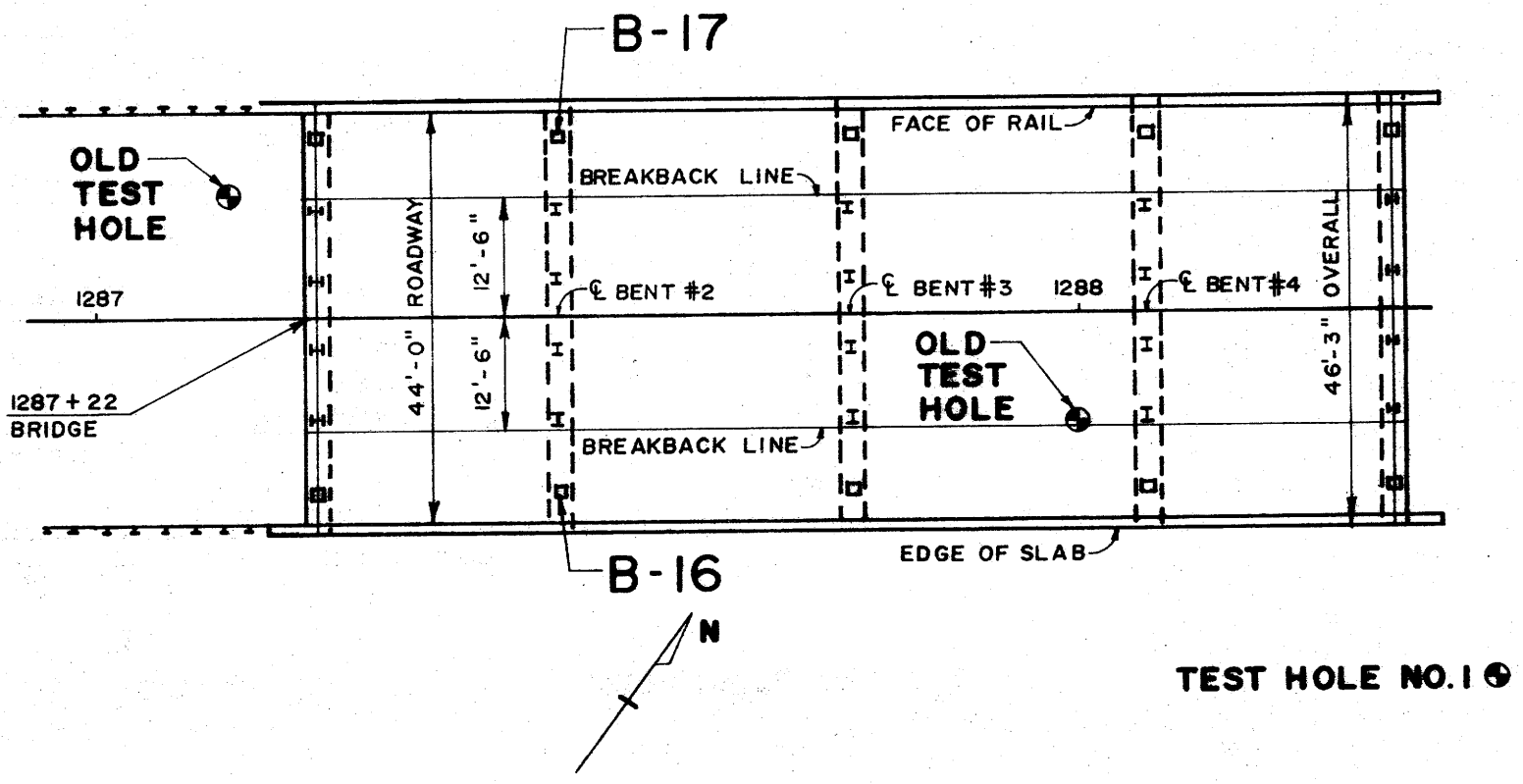

FIG. 4. - GOUCHY CREEK BRIDGE - PLAN.

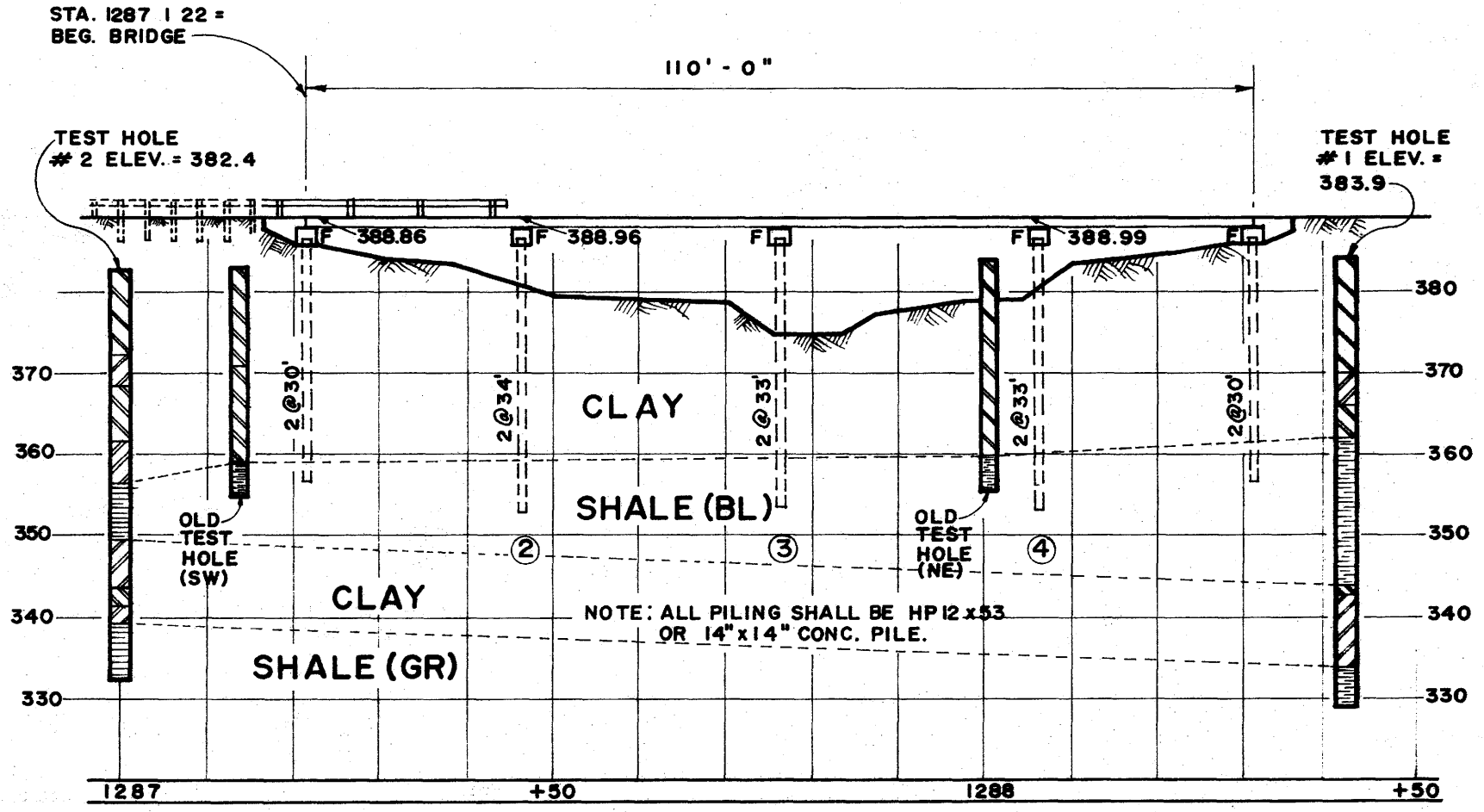

FIG. 5. - GOUCHY CREEK BRIDGE - FOUNDATION.

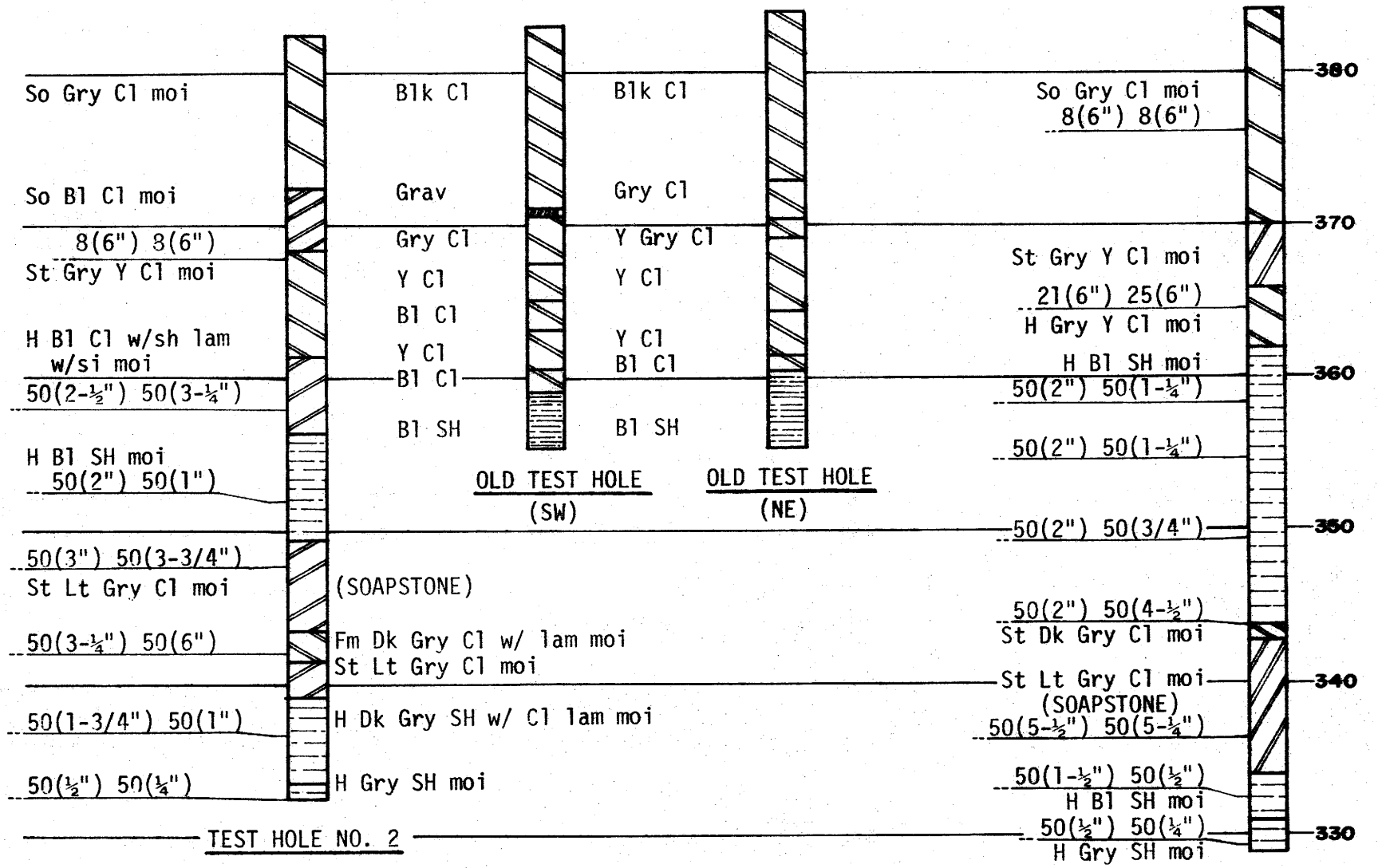

FIG. 6. - GOUCHY CREEK BORING PROFILES.

Pile casting and instrumentation.-- The test piles were formed February 18, 1975 at a casting yard, near Eagle Lake, Texas. The dimensions of each of the two instrumented test piles were 34 ft (10.4 m) long by 14 in. (36 cm) square. A 3/4 in. (1.9 cm) chamfered edge was formed all around the tops and bottoms of the piles. The piles had a metal form finish on three sides and a troweled surface of medium roughness on the side where the instrument leads exited. Six, 1/2 in. (13 mm) diameter steel cables were embedded in the pile to allow pre-tensioning to 173,400 lbs (772 kN). Pre-tensioning was released when the concrete reached a strength of 4600 psi (32 MN/m^2). The spacing of the reinforcing (tensioning) cables is shown in Fig. 7.

Instrumentation embedded in each pile consisted of two separate and complete Wheatstone bridge circuits. The separate, full bridges were each composed of four strain gages, two gages placed longitudinally and two placed horizontally. The two horizontal gages were dummy "pillow" gages which provided automatic temperature compensation for the bridge. They were designed and installed in the prescribed manner (12). Use of such a strain gage configuration eliminated a need to use Poisson's ratio, which is difficult to determine for concrete, in the later test data reduction calculations. The instrumentation also provided the capability for simultaneous hook-up of different readout systems for comparison of forces from any given hammer blow. Additional information concerning the strain gages is presented in Fig. 7. Gage specifications are included in the previously presented Table 3.

Cylinder test results.-- At the time of pile casting and embedment of the sensing instrumentation, six standard 12 in. (30 cm) long by 6 in. (15 cm) diameter concrete cylinders were made. The cylinders were cured wet for 7 days and thereafter were allowed to air dry, as was done for the piles themselves. The cylinders were then tested to determine an average static modulus of elasticity for the two instrumented pre-cast concrete piles. Results of the tests are shown in Fig. 8, and an average chord modulus of 6.2×10^6 psi (4.3×10^7 kN/m^2) compression was computed. The cylinders were tested at approximately 180 days

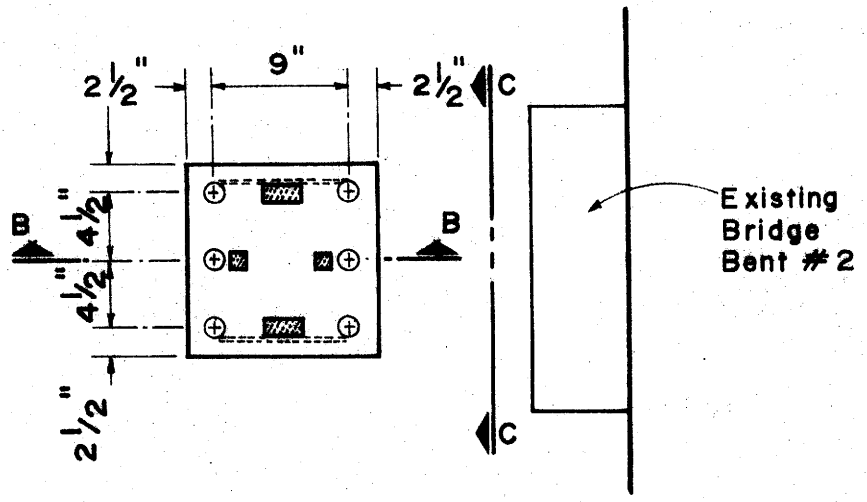

(a) SECTION A-A

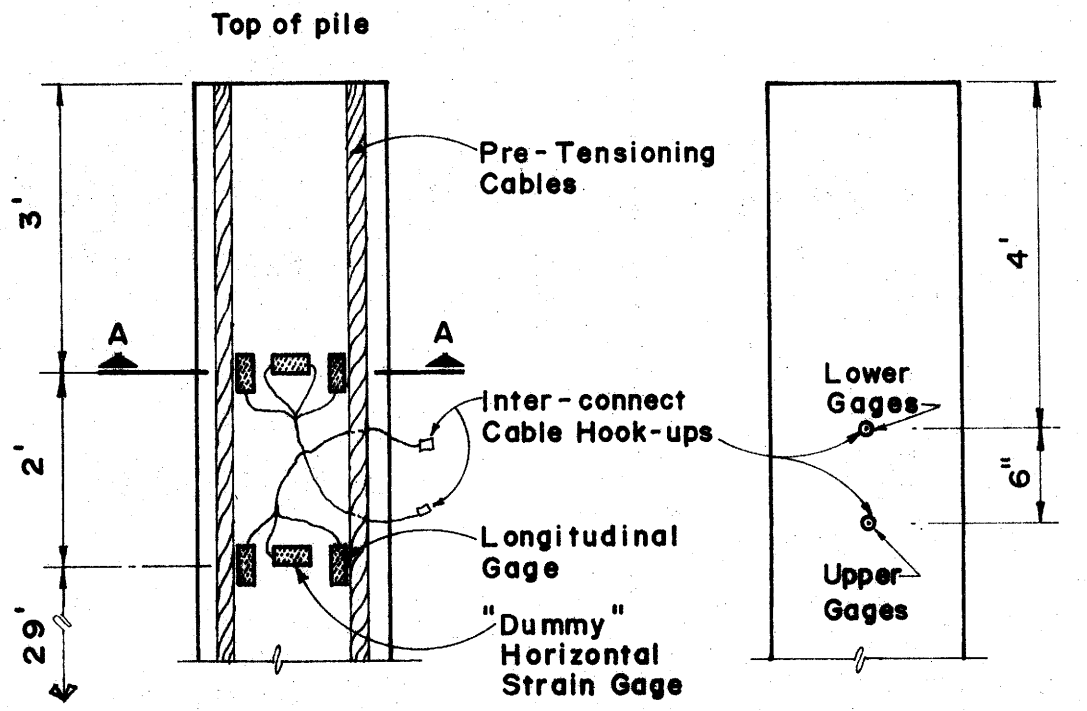

(b) SECTION B-B

(c) SECTION C-C

FIG. 7.- TEST PILE INSTRUMENTATION.

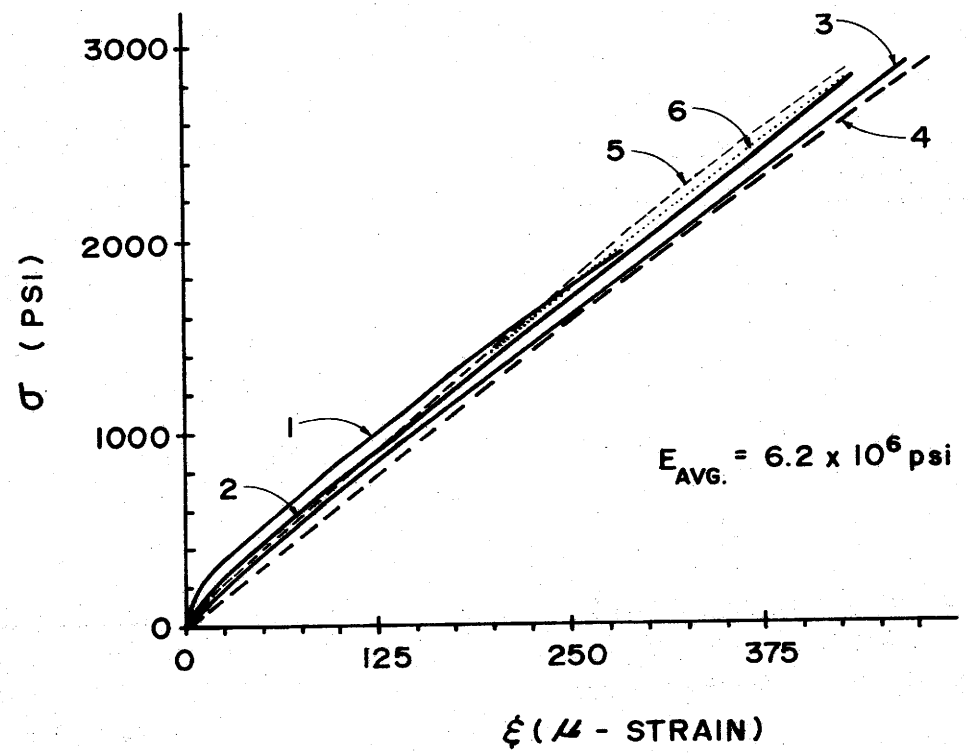

CYLINDER NO.	E (PSI x 10^6)
1	6.19
2	6.24
3	5.98
4	6.13
5	6.62
6	6.32

COMPRESSIVE STRENGTH OF CYLINDER NO. 1 WAS 7780 PSI AT 180 DAYS

FIG. 8. - MODULUS OF ELASTICITY OF CONCRETE CYLINDERS.

after casting. It should be noted that the evaluation of the Highway Dept. Dynamic Pile Force Readout (DYROD) was purposely done on a strain basis rather than stress or force.

Readout equipment.-- The readout systems used in the Gouchy Creek test were the DYROD and the STDSYS. The DYROD was connected to the upper set of strain gages (Wheatstone bridge) and the STDSYS was connected to the lower set as shown in Fig. 7. One hundred feet (30.5 m) of Belden #8723 was used as interconnect cable in each case. Since only one input signal was being monitored by the STDSYS, it was decided to connect the GALVO output of the DYROD to one of the other 23 available channels on the Visicorder. Two continuous force-time signal traces were then output by the Visicorder in this test: one from the STDSYS (normal) and one from the THD DYROD GALVO binding posts (optional).

The signal from the upper gages and the signal from the lower gages were treated as equal and simultaneous for all practical purposes of systems evaluation. A 14,000 feet per second (4300 m/sec) compressive force wave would traverse the 2 ft. (60 cm) between the two sets of gages in 0.1 milliseconds. Such a small time difference was detected on some peak force traces from the Visicorder but was less than the width of a pencil line, and too small to be measured or significant. Time between blow peaks is presented in Appendix III.

Pre-drilling and driving equipment.-- Pile driving at Gouchy Creek was delayed several times because of heavy rains and high water. After noon, on May 21, the foundations sub-contractor moved equipment onto the bridge to begin the work. All drilling and driving was performed with truck-mounted rigs operating from and over the side of the existing bridge. Predrilling was accomplished using a Hughes LDH drilling rig with a 18 in. (46 cm) diameter flight auger. A Delmag-diesel hammer, model D-12, burning Mobil #2 diesel oil, was used for driving the piles. Hammer specifications supplied by the subcontractor are shown in Table 4. Seven pieces of 3/4 in. (18 mm) plywood, reported to be old "form" wood, were used as a cushion. The wood was thought to be fir; it remained in good condition even after the pile driving. The weather was hot and humid after a rain the day before.

TABLE 4.-- STANDARD SPECIFICATIONS FOR DELMAG - DIESEL PILE HAMMER, MODEL D-12 *

Ram weight (piston)	2750 lbs, 1250 kg
Energy per blow	22,500 ft lbs
Number of blows	42-60/min
Max. explosion pressure on pile	93,700 lbs
Jumpheight "h" to be used in the ramming formula	98 27/64", 2500 mm
Fuel consumption per hour	1.76 Imp gals
Oil consumption per hour	0.17 Imp gals
Fuel tank capacity	3.41 Imp gals
Oil tank capacity	0.66 Imp gals
Area of bottom of "impact block" **	254 $in.^2$

* Supplied to Texas State Highway Department by Martin & Martin, Foundation Drilling Contractors, Fort Worth, Texas, 5/21/75.

** Supplied by hammer manufacturer by telecon, 8/75. "Slightly ball shaped surface."

Instrumentation problems.-- The heat caused the standard carrier amplifier system to overheat while waiting for the driving to begin. The system requires a half-hour warm-up time and thus had to be activated ahead of time. The offending amplifier was slid forward out of the case and allowed to cool; a large umbrella was erected to provide shade before proceeding.

One other instrument related problem occurred but was quickly though not permanently solved. There had been no supervision of the piles to the job site, and considerable time had past since casting of the piles. It was thus desirable to check the condition of the embedded strain gages prior to start of driving. On the day before driving, the DYROD was connected to the upper set of gages on B-16, balanced and a calibration attempted. The edgewise panel meter needle, however, would drop whenever the carrying handle was touched, and then would return to its original value when the operator's hand was removed from the handle. (The edgewise panel meter indicates bridge balance during normal operation of the DYROD.) The apparent transient imbalance was caused by a lack of grounding. During pile driving the next day, a piece of wire was run, from the "Neg" post of the 12 V external power input connection to the bridge guardrail, providing the necessary ground for the system. Such grounding may be necessary during routine use of the DYROD.

Driving procedure.-- Pile B-16 was driven first. A 18 in. (46 cm) diameter hole had been predrilled to a depth of 28.3 ft (8.6 m), existing ground surface being approximately El. 380 as shown in Fig. 9. There appeared to be no water in the hole. The pile was set in the hole but had to be pulled up and down and pushed laterally to center it with respect to the pile cap and to move it 3 in. (8 cm) further away from the bridge. When it was finally set down, a hole had to be dug beside the pile to free the crane hook from the lifting eye embedded in the pile. The leads and hammer were then set over the pile and driving proceeded.

The pile was hit about 6 blows to determine whether the predicted forces used in calibration computations were within the ballpark, to

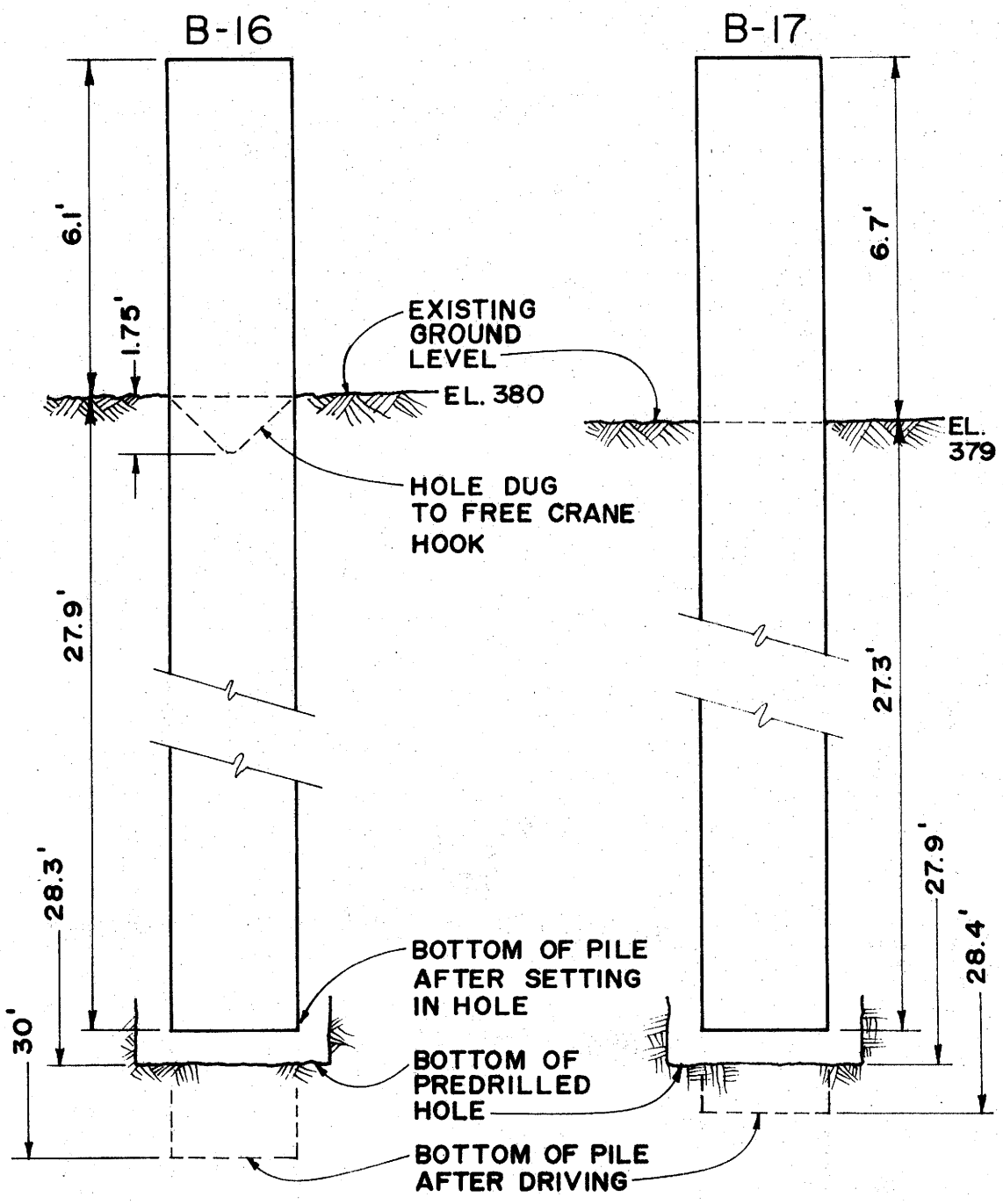

FIG. 9. PENETRATION OF TEST PILES.

make certain that both the DYROD and STDSYS were functioning, and to check the magnitude of the Visicorder trace deflections. The DYROD DPM was set to read every second blow. The pile was then driven for approximately 220 blows. Penetration for the last 20 blows was 1/8 inch (3.1 mm). The hammer bounce height was observed to average between 5-1/2 and 5-3/4 ft (1.75 m). The SDHPT inspector stated that the bounce height for similar driving had averaged 6 ft (1.8 m).

The hole for pile B-17 was then drilled and extended to a depth of 27.9 feet (8.5 m), with existing ground surface at El. 379 as shown in Fig. 9. Water was seeping into the hole only slightly. The pile was lowered into the hole and pieces of soil could be heard being knocked off the sides of the hole and falling to the bottom. Dust was also seen to be rising out of the hole. The pile did not have to be lifted out of the hole again as for B-16.

This pile was also hit 6 times to check instrument readings and then was driven about 200 more blows. The DYROD DPM was set to read every third blow. The bounce height of the hammer was between 4 1/2 and 5 1/2 feet (1.7 m) for the first 6 calibration blows and greater than 5 1/2 feet (1.7 m) for all subsequent blows. Driving was stopped 20 blows short of 200 for about a minute before the additional 20 were requested. Successive twenty blow penetrations were 1 1/2, 1, (unknown), 1/2, 3/8, 1/4, 1/2, 3/8, and 3/4 inches, as recorded by the inspector using chalk marks and a carpenter's rule. Bearing (resistance) computations were based upon 3/8 inches (10 mm) because of apparent error in the 3/4 in. (19 mm) reading due to some jumping of the leads and overlapping chalk marks.

Bearing capacity.-- The piling was required to be driven to a resistance of at least 42 tons (38 Mg). This was checked by the SDHPT inspector with the Engineering News-Record (ENR) formula (3) in the form:

$$\text{Bearing capacity (resistance) in tons} = \frac{2\,P\,H}{S + 0.1} \qquad (1)$$

in which P = pile driving hammer ram weight, in tons (2750/2000); H = average ram bounce height, in feet; and S = permanent set of the pile point, in inches.

Assuming that no plastic deformation of the pile takes place, and that no strain is locked into the pile by the soil surrounding it, the set may be measured at the pile top. That was the technique used at Gouchy Creek. According to Bowles (3) the ENR formula can be obtained by assuming that one-half of the elastic compression of cap [and anvil, etc.], pile, and soil sums to 0.1 inches and hammer efficiency equals 100%, for single-acting steam hammers. A conversion factor of 12 inches/foot to make the units consistent, and division by a safety factor of 6 yields the constant 2 used in the ENR equation.

The ENR equation has found widespread use in the past not because of its correctness, but rather because of its simplicity in use. The assumptions aforementioned were made for single-acting steam hammers and not necessarily for open-ended diesel hammers. Nor, according to Bowles (3), is the original equation valid if a pile tip is on rock or other relatively impenetrable material. The Gouchy Creek shale was relatively impenetrable.

The final set of B-16 and B-17 was deemed 1/8 in. (3 mm) and 3/8 in. (10 mm) respectively for 20 blows. Using a 6 ft (1.8 m) bounce height and 2750 lb (1250 kg) weight for the D-12 ram, the ENR formula indicated 155 tons (141 Mg) and 139 tons (126 Mg) static bearing capactiy (resistance) for the two test piles.

EVALUATION TESTS -- DATA REDUCTION, ANALYSIS AND ACCURACY

Calibration Factors and Data Reduction.

General.-- It should be recalled that the various force measurement systems used in the evaluation tests had individual calibration functions available for calibrating the various system outputs. While the magnitudes of the calibration factors were different from system to system and test to test, the equation used to compute those calibration factors was basically the same. It was of the following form (12):

$$P = \frac{(R + 2R_l)^2 (AI + 2R_l) (E) (A) \times 10^{-3}}{\text{cal } R (N_{eff}) R (AI) GF} \qquad (2)$$

where P = force in kips, R_l = leadwire resistance in ohms, AI = amplifier impedance in ohms, E = Young's modulus of elasticity in psi, A = cross-sectional area of pile material in inches squared, cal R = value of the shunt calibration resistor in ohms, N_{eff} = number of effective longitudinal gages, R = manufacturer's stated gage resistance in ohms, and GF = gage factor (sensitivity factor) for the strain gage.

Table 5 shows the various values computed and used in the reduction of test data. Poisson's ratio for aluminum was assumed to be 0.33 for computing N_{eff} (13).

The force computation equation derivation includes an adjustment for gage factor desensitization due to amplifier input impedance, as well as a correction for long leadwires.

By rearranging equation (2) and using Hooke's Law (ref. 17 and 19), the following equation can be obtained for use in determining all data in terms of strain:

$$\epsilon = \frac{(R + 2R_l)^2 (AI + 2R_l) \times 10^6}{\text{cal } R (N_{eff}) R (AI) GF} \qquad (3)$$

TABLE 5
PROPERTIES USED IN COMPUTATIONS
OF CALIBRATION SIGNAL EQUIVALENT VALUES

Test	Data	R ohms	R_l ohms	AI ohms	E psi $\times 10^6$	A in^2	Cal ohms $\times 10^3$	N_{eff}	GF	cal P kips	cal σ psi	cal ϵ micro-strain
MODEL PILE												
DYROD [2]	Box 1	120	1.5 [1]	5000	10	0.2041	60	2.5 [2]	2.05	0.837	4100	410
STDSYS	Box 1	120	1.5	350	10	0.2041	60	2.5 [2]	2.05	0.844	4140	414
DYROD [3]	Box 1	120	1.5	5000	10	0.2041	60	2.67 [3]	2.05	0.784	3840	384 [3]
STDSYS	Box 1	120	1.5	350	10	0.2041	60	2.67 [3]	2.05	0.790	3870	387 [3]
DYROD [2]	Box 2	120	1.5	5000	10	0.2041	60	2.5	2.05	0.837	4100	410
STDSYS	Box 2	120	4.5 [4]	350	10	0.2041	60	2.5	2.05	0.944	4620	462
DYROD [3]	Box 2	120	1.5	5000	10	0.2041	60	2.67	2.05	0.784	3840	384 [3]
STDSYS	Box 2	120	4.5	350	10	0.2041	60	2.67	2.05	0.884	4330	433 [3]
PILE STUB & PENDULUM												
DYROD	Nov. 20	300	1.125 [5]	5000	5	256	332	2.5	2.10	224 [6]	875	175
STDSYS	Nov. 20	300	1.125	350	5	256	60	2.5	2.1	123 [7]	480	96.3
BA-4	Nov. 20	300	1.125	--[8]	5	256	200	2.5 [2]	2.10	371 [9]	1450	290
STDSYS [10]	Nov. 14	120	1.125	(350)	(10)	(138)	60	1.25 [2]	2.02	-	-	807

TABLE 5 (CONTINUED)

Test	Data	R ohms	R_l ohms	AI ohms	E psi $\times 10^6$	A $in.^2$	Cal R ohms $\times 10^3$	N_{eff}	GF	cal P kips	cal σ psi	cal ϵ micro-strain
GOUCHY CREEK												
DYROD [11]	—	300	1.5	5000	4.5 [11]	196	60	2.0	2.11	1066 [11]	—	1209
STDSYS [11]	—	300	1.5	350	4.5 [11]	196	60	2.0	2.11	1075 [11]	—	1219
DYROD	ALL	300	1.5	5000	6.2	196	60	2.0	2.11	1470	7498	1209
STDSYS	ALL	300	1.5	350	6.2	196	60	2.0	2.11	1481	7558	1219

1. 100 ft. of 1.5 ohm/100 ft. Belden #8723 cable for leadwires.
2. Using erroneous μ for aluminum (=0.25) prior to test.
3. Used for data reduction using correct μ=0.33 for aluminum pile.
4. Used 100 ft. of 4.5 ohm/100 ft. Belden #8434 cable for leadwires.
5. 75 ft. of Belden #8723 inter-connect cable.
6. Pre-test calibration computation; erroneously used $1R_l$ instead of $2\ R_l$ yielding an erroneous calibration of 222 kips; correct value was used in data reduction, however.
7. Same error as in note 6 above; erroneous calibration 122 kips. Gain was increased x 10 for small strain signal.
8. $(AI = 2R_l)/(AI)$ terms were not used in this computation.
9. Same error as in note 6; erroneous calibration 366 kips.
10. Half-bridge configuration; see Appendix V for explanation of computation.
11. Assumed prior to test; not used in data reduction.

where ϵ = represented strain in units of micro-strain (ie. 10^{-6}).

Reduction of system evaluation test data was actually done on a strain basis. This seemed a better technique since it eliminated the need for and use of a factor which was rather arbitrary and actually unknown, as the modulus of elasticity was at the time of data reduction. A modulus of elasticity and pile cross-sectional area had been assumed at the time of of actual test calibration. Knowing those two assumed numbers, the DYROD digital panel meter readings (units of force) were later converted to strain, for system readout comparisons and evaluation. Performance specifications for these types of dynamic measuring systems are traditionally stated in terms of indicated strain.

Reduction of DYROD DPM data.-- The digital panel meter (DPM) of the DYROD is direct reading in units of peak force and that is the form in which the original data was recorded. It was desired, however, to evaluate the various measurement systems and their outputs on the basis of strain. DPM data reduction thus involved the following simple equation:

$$\begin{matrix}\text{DYROD DPM peak} \\ \text{strain for any} \\ \text{given hammer blow}\end{matrix} = \frac{\text{DPM reading in units of force}}{A \times E} \qquad (4)$$

in which A = cross-sectional area of pile, and E = modulus of elasticity assumed in computing an equivalent force value, P, for the calibration signal.

DYROD readings from the Model Pile test also required a special correction for an erroneously assumed μ for aluminum. Too large a number was used when calibrating the DYROD prior to the test. With the gain set too high, all subsequent DPM readings during the test were displayed larger than they actually were. In reducing the DYROD DPM data to strain, a correction factor was first applied to the Model Pile test readings:

$$N_{eff} \text{ using assumed } \mu \ (=0.25) = 2.50$$

$$N_{eff} \text{ using correct } \mu \ (=0.33) \text{ for aluminum} = 2.67$$

$$\text{Correction factor} = \frac{2.67}{2.50} = 1.068$$

$$\text{Corrected DPM reading in units of peak force} = \frac{\text{Original DPM reading in units of force}}{1.068} \quad (5)$$

The original DPM readings of peak force shown in Table IV-1 for the Model Pile test are not corrected. The peak strain values are corrected.

Reduction of DYROD GALVO data.-- The DYROD GALVO output was connected to one of the channels of the Visicorder continuous-recording oscillograph. Generating a calibration signal with the DYROD triggered a short, constant deflection of the GALVO tracing on the Visicorder recording paper. When several of these calibration deflections were recorded, they could be measured with dividers and Engineer's scale and an average deflection determined. Having previously computed the equivalent value of the calibration signal in force, stress, or strain, and having determined an average corresponding trace deflection, a calibration factor could be computed, as follows:

$$\text{Calibration factor} = \frac{\text{Equivalent value of calibration signal}}{\text{Trace deflection caused by calibration signal}} \text{ eg. } \frac{\text{micro-inches}}{\text{inches}} \quad (6)$$

Data reduction for the DYROD GALVO data was then a simple matter of measuring the pile-driving, force-induced trace deflections, and multiplying by the appropriate calibration factor:

$$\text{DYROD GALVO reading in strain} = \text{Trace deflection} \times \text{Calibration factor} \quad (7)$$

Since the measurement systems were evaluated on the basis of indicated strain, a calibration factor in units of strain (cal ϵ) was used in reducing data for those system comparisons.

An additional multiplicative correction factor was necessary in reducing DPM data. In reducing the Model Pile test data from the DYROD GALVO, a correct equivalent calibration signal strain was used; and a correction factor was then unnecessary.

The wave equation method of pile analysis, presented later in this investigation, is performed in units of force. Test data, used with the wave equation, was reduced in the same manner as just described with one difference. Instead of computing calibration factors using strain equivalents for the calibration trace deflections, force equivalents were used. See Table 5 for equivalent values of calibration signals in units for force (cal p).

Reduction of STDSYS data. -- The normal output for the standard carrier amplifier system (STDSYS) is the Visicorder oscillograph. The STDSYS data was reduced in the same manner as the DYROD GALVO data, previously described. Equivalent values for the calibration signal for the STDSYS are also presented in Table 5.

Analyses of Output Data from the Measurement Systems Evaluation Tests.

Comparison of DYROD GALVO AND STDSYS. -- The output for the DYROD GALVO and STDSYS is the Visicorder oscillograph recording. Measurements (scalings) of corresponding trace deflections were reduced to units of indicated strain as described in previous sections. Over a hundred such records were generated during the Model Pile and Gouchy Creek tests. Each record was analyzed by measuring trace deflections, reducing the measurements to indicated strain, and comparing the pairs of indicated peak strain from each record. Some of the tracings also indicated clear, smaller additional relative peaks. A number of those relative peaks were also measured, reduced, and compared, providing additional data for comparing the DYROD GALVO and STDSYS outputs. All of the data obtained from all of the system evaluation tests is presented in Appendix IV. Corresponding strains indicated by the DYROD GALVO and STDSYS are shown in Tables IV-1, IV-3, and IV-4. Summary plots of the data are presented in Fig. IV-3 through IV-5.

DYROD GALVO and STDSYS indicated strains were first compared by determining the percent difference between the output of each system

$$\text{\% Difference of GALVO output from STDSYS} = \frac{\text{DYROD GALVO strain reading} - \text{STDSYS strain reading}}{\text{STDSYS strain reading}} \times 100 \qquad (8)$$

The percent differences were then plotted versus the STDSYS Indicated Strain (Fig. IV-6) to determine whether a trend existed. The data showed much scatter. No significant pattern of increasing or decreasing % difference was apparent with indicated strain.

Since a meaningful trend was not apparent in the % differences plot, the decision was made to check the distribution of the percent differences (Δ%) with frequency of occurrence. Details of the technique are presented later in this report under the heading, Normality check. The percent differences fit a standard normal distribution curve well. It was thus apparent that the best way to represent the data was by computing the means and standard deviations of the system output percent differences. Those means and standard deviations are presented in Table 6. The weighted average of the means, combined (pooled) variance (14), and standard deviation were then computed.

In summary, a single, constant, average percent difference may be quoted for the DYROD GALVO as compared to the STDSYS. The DYROD GALVO averaged 3.8% less strain (signal output) than the STDSYS indicated. A 99+% confidence interval of +3.7% (high) to -11% (low) was indicated, meaning that better than 99%-of-the-time, the DYROD GALVO will average between 3.7% higher than the STDSYS to 11% lower than the STDSYS reading. This error band is shown in Fig. 10.

Comparison of DYROD DPM and STDSYS.-- As previously described, the digital panel meter (DPM) will normally be the sole output mode of the DYROD. The DPM is labeled in units of force, "KIPS." The DPM readings were converted to units of strain for purposes of measurement system evaluation in the manner previously described. The reduced DPM readings in terms of strain, however, represent only values of peak strain for any given hammer blow. Therefore, for purposes of comparing the DYROD DPM and STDSYS, only values of indicated absolute peak strain are considered from the STDSYS output data.

TABLE 6.-- FINAL DETERMINATION OF
WEIGHTED AVERAGE PERCENT DIFFERENCE
OF DYROD GALVO FROM STDSYS

Sampling	Mean (%)	Std. Dev.	Number of Data Points
Model Pile Test Data	-2.54	5.96	25
Gouchy Creek Test Data			
B-16	-3.68	1.38	50
B-17	-4.44	1.27	52
Weighted Average	-3.77		
Combined (Pooled) Variance	8.40		
Std. Deviation	2.90		

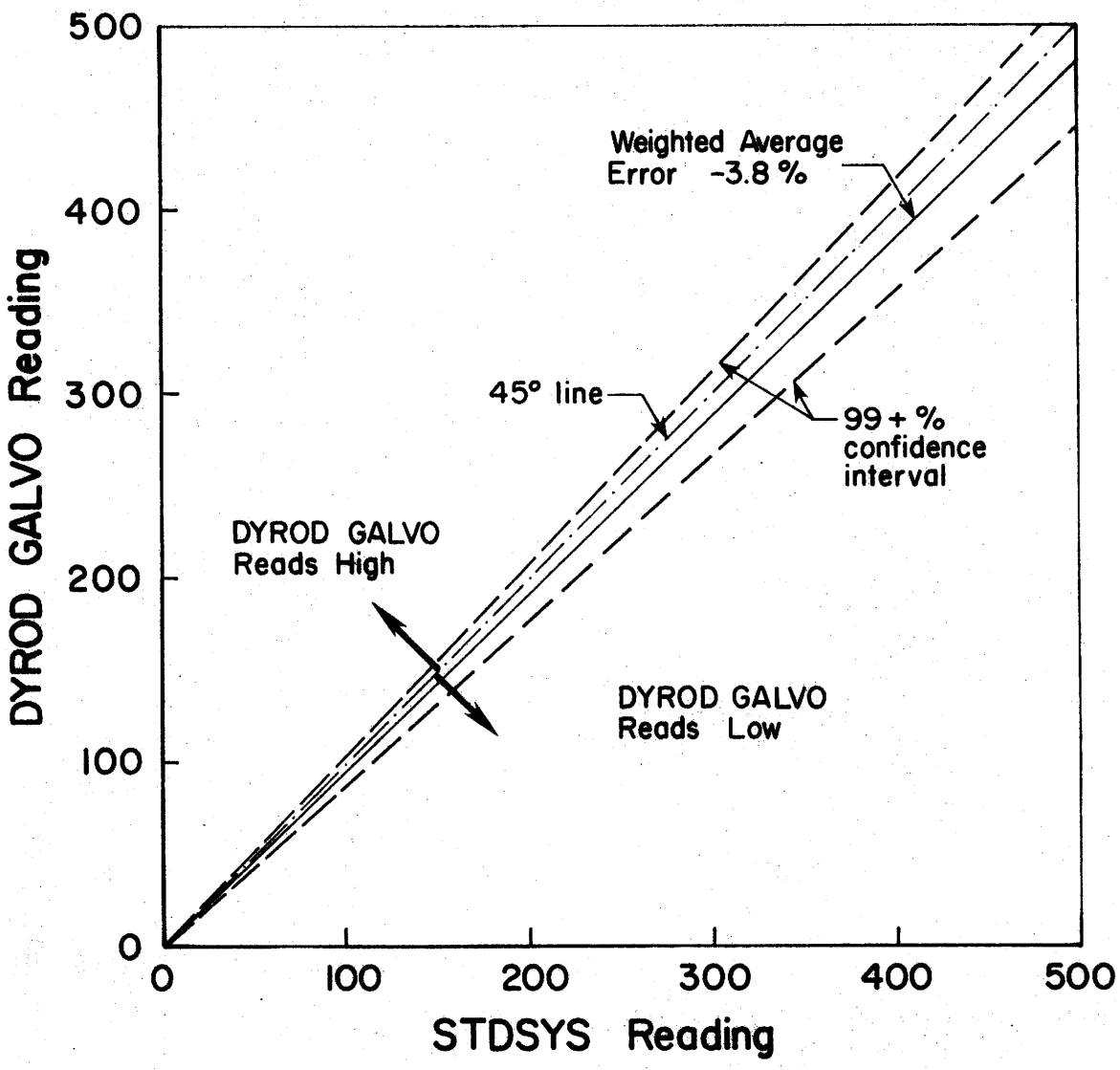

FIG. 10 - AVERAGE DYROD GALVO READING VS STDSYS READING

Comparative data were available from the Model Pile test (Table IV-1) and the Gouchy Creek test (Tables IV-3 and VI-4). Summary plots comparing these data are shown in Fig. IV-7 and Fig. IV-8.

The DYROD DPM data were compared with the STDSYS peak strain data in a manner similar to that just described for the DYROD GALVO and STDSYS comparison. The percent difference between the DYROD DPM indicated strain and the STDSYS indicated strain was computed for all of the available records.

$$\text{\% Difference of DPM output from STDSYS} = \frac{\text{DYROD DPM strain} - \text{STDSYS strain}}{\text{STDSYS strain}} \times 100 \qquad (9)$$

The percent differences were then plotted versus the DYROD DPM indicated peak strain (Fig. IV-9) to observe any patterns in the apparent system differences, with increasing values of strain. The DYROD DPM strain was chosen for the ordinate since that mode of system output was not affected by potential inaccuracies in data reduction. Possible scaling errors are discussed in a subsequent section entitled Scaling error and apply only to the data reduction of the STDSYS and DYROD GALVO output modes.

The percent difference data showed considerable dispersion, but was not as widespread as the previously analyzed DYROD GALVO vs. STDSYS data in Fig. IV-6. No significant trend in the percent differences was apparent as shown in Fig. IV-9, nonetheless. Since no obvious patterns were detected, and since the "normality" of the DYROD DPM and STDSYS data was also found to be acceptable, a weighted average of the means, combined (pooled) variance, and standard deviation were felt to be the most meaningful and useful representation of the data. The results of those computations are shown in Table 7.

Analysis of the output of the DYROD DPM with respect to the output of the STDSYS thus indicated a constant relationship with normally expected departures. That relationship is shown in Fig. 11. It indicates that on the average for these tests, the DYROD DPM read 4.4% lower than the STDSYS.

TABLE 7.-- FINAL DETERMINATION OF
WEIGHTED AVERAGE PERCENT DIFFERENCE
OF DYROD DPM FROM STDSYS

Sampling	Mean (%)	Std. Dev.	Number of Data Points
Model Pile Test Data	-3.10	2.54	9
Gouchy Creek Test Data	-4.72	1.14	37
Weighted Average	-4.40		
Combined (Pooled) Variance	2.31		
Std. Deviation	1.52		

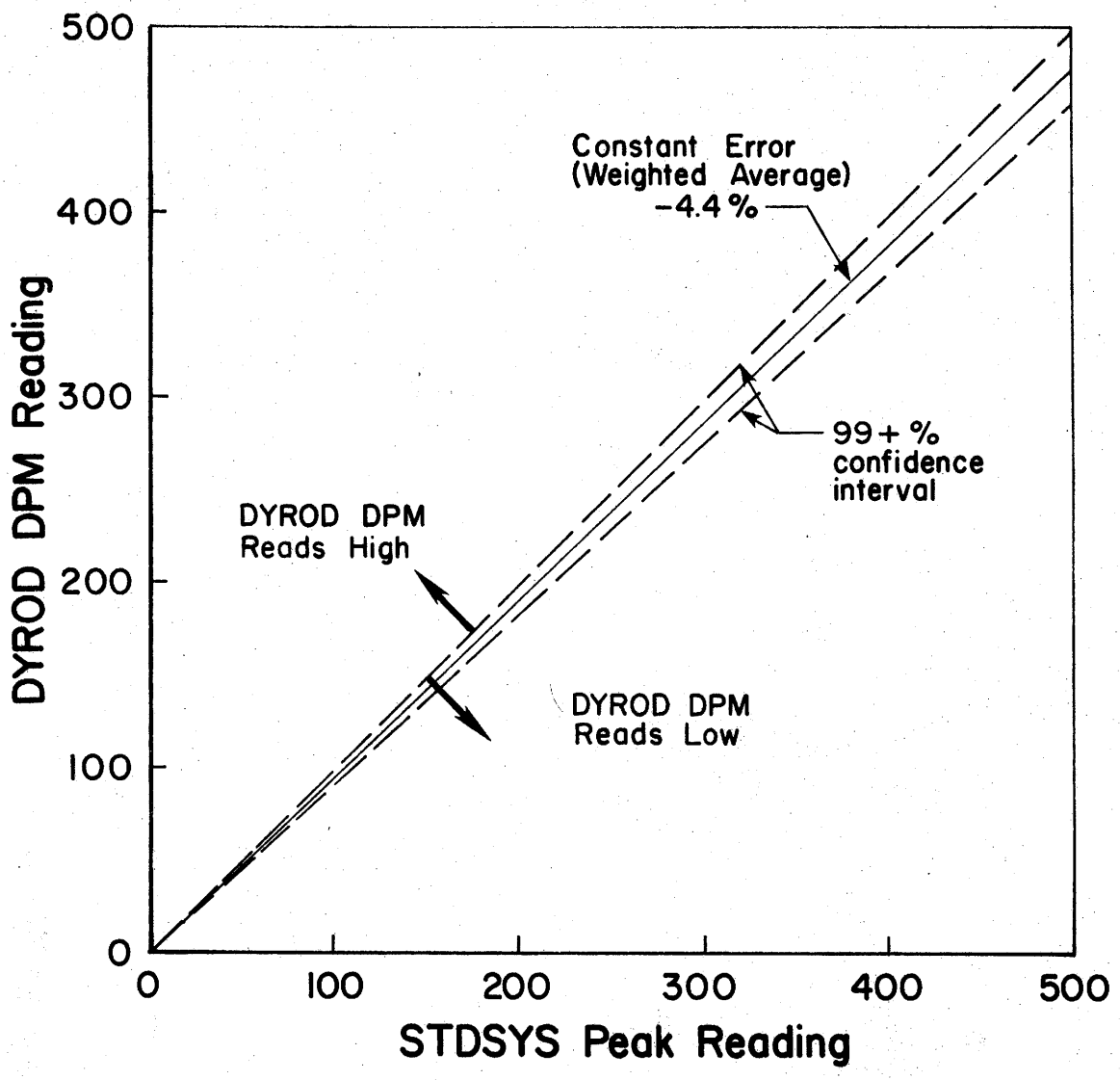

FIG. II - AVERAGE DYROD DPM READING VS. STDSYS READING

Comparison of DYROD GALVO vs. DYROD DPM.-- Analyses of the DYROD GALVO output and the DYROD DPM output with the STDSYS output, individually, have already been presented. It was desirable to also compare the two output modes of the DYROD to get a feel for the variance in output modes of just the DYROD. The problem is not as straightforward as it may at first seem. The Δ% relationship between the two DYROD output modes is not a simple algebraic one where calculated Δ%'s can simply be combined. Since the Δ% calculated for the DPM vs. STDSYS comparison was based on only a portion (less than half) of the data records used for the GALVO:STDSYS comparison, the weighted average percent differences from the two analyses are not really directly comparable. For that reason, they cannot be used to directly calculate a percent difference between the DYROD GALVO and DYROD DPM. Also, there were some additional data available for comparing the GALVO and DPM, data for which there was no counterpart from the STDSYS.

Again, in evaluating the DYROD, this time from the GALVO versus DPM viewpoint, it was desirable to work on a strain basis. The use of strain for comparison eliminates the arbitrary, different, and usually unknown E term from the computations. Also the use of a strain basis, for evaluation the measurement systems, does not alter, limit, or invalidate the conclusions reached. Force (which the DPM displays directly) and stress are nothing more than a constant times the strain. That constant cancels out in the computation of system output mode percent difference, as follows:

$$\frac{K\,(\text{GALVO strain}) - K\,(\text{STDSYS strain})}{K\,(\text{STDSYS strain})} \times 100 \qquad (10)$$

$$= \frac{\text{GALVO strain} - \text{STDSYS strain}}{\text{STDSYS strain}} \times 100$$

$$= \Delta\%$$

where K = 1/E, 1/AE, or 1. Since the constants drop out, the final determination of "weighted average percent difference" is valid for any set of consistent units. Choosing units of strain for evaluating

the DYROD and STDSYS actually enhanced the conclusions reached. Use of strain allowed more data to be evaluated from a number of different tests where E's and A's were different. Stress and force were not directly comparable between the various tests since they were influenced by the differing material moduli (E) and geometries (A).

Data from the Model Pile, Pile Stub and Pendulum, and Gouchy Creek tests were analyzed in the comparison of DYROD GALVO and DPM output modes. The records were reduced in the manner described in previous sections. The comparable indicated strains are listed in Tables IV-1 through IV-4. Summary plots of the data are shown in Fig. IV-10 and IV-11.

The percent difference ($\Delta\%$) between the GALVO scaled peak strain and the DPM converted peak strain was computed for each record by the following equation:

$$\Delta\% = \frac{\text{GALVO strain - DPM strain}}{\text{DPM strain}} \times 100 \qquad (11)$$

The $\Delta\%$'s were then plotted versus DPM strain to check for any trend with increasing DPM strain readings as shown in Fig. IV-12. Considerable scatter was apparent but a meaningful trend was not. A "normality" check of the data proved favorable and again it was decided that the data and relationship between GALVO and DPM could be best represented by means and standard deviations. From those, a weighted average mean, a combined (pooled) variance, and a standard deviation were computed. The results are presented in Table 8.

The final determination of the weighted average mean indicated a percent difference of -0.88, meaning that on the average, the DYROD GALVO output was 0.88% lower than the DYROD DPM. That relationship is plotted in Fig. 12 along with the 99+% confidence envelope.

Normality check.-- A "Normality check" was performed on most of the percent difference data used in the previous sections concerning comparisons of various measurement system output modes. When plots of percent difference in indicated strain exhibited no appreciable

TABLE 8.-- FINAL DETERMINATION OF
WEIGHTED AVERAGE PERCENT DIFFERENCE
OF DYROD GALVO FROM DPM

Sampling	Mean (%)	Std. Dev.	Number of Data Points
Model Pile Test Data	-0.34	0.99	9
Pile Stub & Pendulum Test	-4.44	1.36	3
Gouchy Creek Test Data	+0.723	0.92	37
Weight Average Mean	-0.88		
Combined (Pooled) Variance	0.93		
Std. Deviation	0.97		

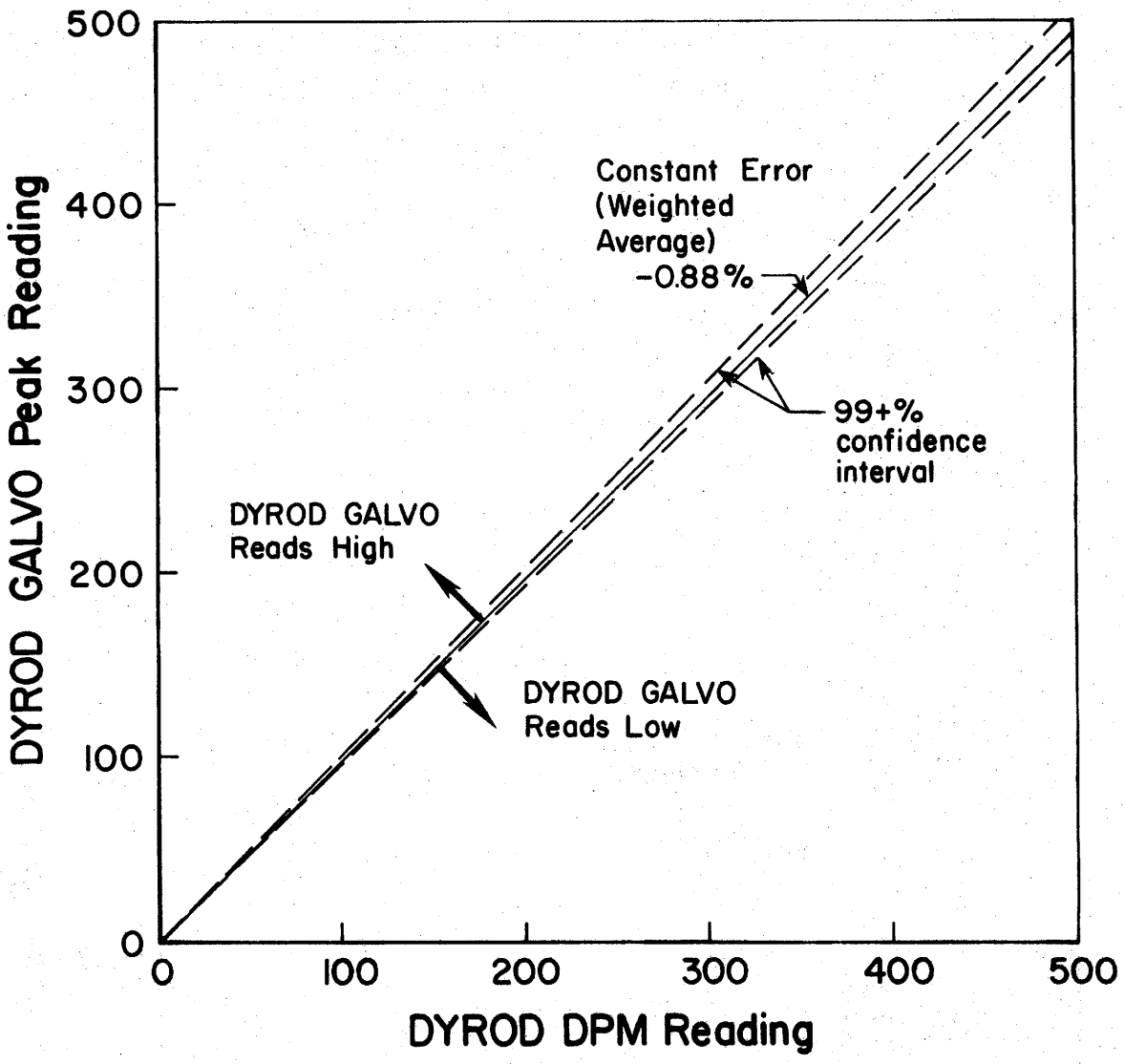

FIG. 12.- AVERAGE GALVO READING VS. DPM READING

trends with increasing amount of strain, it was felt that an average or mean percent difference should be used to describe the system evaluation test data.

It was suspected that the data would follow a standard normal distribution using a sampling with a sufficiently large number of elements (N). Even a small N sampling would be expected to follow a standard normal distribution, if the population from which it was taken was normally distributed. The events measured; the measurements obtained, and reduced; and the errors therein were considered to be natural, random, and independent sampling. Since no evidence to the contrary appeared, it seemed a fair assumption to expect normality in the percent difference data. The expectation of normality was further reinforced by the lack of trends and the large scatter apparent in the data when any one system output was plotted against another.

The normality check was performed in the following manner. Within each sampling of the percent difference data, the percent differences were ranked in order of increasing magnitude. The largest percent difference was given a rank no. = 1, the second largest, 2, and so on. The data were treated as ungrouped data. It was plotted on arithmetic normal probability graph paper, plotting the percent difference in indicated strain against its computed normal cumulative frequency. The normal cumulative frequency was computed for each data point as follows (14):

$$\text{cumulative normal frequency (\%)} = \frac{100\,(i) - 50}{n} \qquad (12)$$

where i = sequence (rank) number in the list of increasing magnitude, and n = total number of data points in the sampling being plotted. Either cumulative less-than or cumulative more-than could be computed and plotted and would have been equally useful. On normal arithmetic probability paper, the S-shaped normal distribution ogive becomes a straight line. A normal distribution line was then drawn through the data. The normal cumulative frequency plots of percent difference in

indicated strain for the various system output samplings are presented in Fig. IV-13 through IV-16.

The data did not generally exhibit any meaningful abnormalities. There were some larger and some smaller deviations from the normal distribution line than would have been expected normally, particularly towards the "tails" of the curves. The differences between those more erratic data points and the normal curve were not considered significant, however. The magnitude of those deviations was smaller than the stated proposed accuracy of either measurement system.

With the general normality of the data confirmed, it was then reasonable to continue with the system output mode analyses and compute meaningful standard means to represent the percent difference data. This allowed the computation of a single statistic, the normal weighted average mean, to describe a constant relationship between the various measurement system outputs, as has been shown in Figs. 10, 11, and 12.

Scaling error.-- The Visicorder oscillograph provided the output medium for the DYROD GALVO and the STDSYS. It was necessary to measure or scale off the amount of trace deflection on the Visicorder records, to obtain the strain value indicated thereon. The trace deflection measurements were then multiplied by a calibration factor to obtain the magnitude of the indicated strain. This manual technique of reducing the output data by scaling off of the recording paper was an inaccurate procedure to some degree, probably limited the precision of the data obtained from those two output modes, and accounted for much of the data scatter.

Repeated measurements indicated that the measuring or scaling error was probably a fixed 0.01 in. (1/4 mm) at the very maximum, about 1/2 interval on an Engineer's 50-scale. The scaling error would have been additive to the measurement system equipment errors, in determining a net error in indicated strain. The percent error, contributed to the strain data by the scaling method of obtaining data, can be computed if the respective calibration factors are known in micro-strain/inch trace deflection. Average calibration factors

were computed for each type of test in which the DYROD GALVO and/or STDSYS were used. Fig. 13 presents the various % error contributed by the scaling method (maximum possible) for various values of indicated strain data. The larger the calibration factor in μ-strain/inch, the greater the significance of a possible 0.01 in. (1/4 mm) fixed scaling error at any given strain. The pile stub and pendulum test data had the smallest calibration factors, since cal. trace deflections were very large for that test. Because the calibration factor was small, the 0.01 in. (1/4 mm) possible scaling error had a smaller impact for the pile stub and pendulum test data. The scaling error increases hyperbolically with decreasing values of strain. Conversely, large value data points are affected much less by possible scaling errors.

DYROD temperature stability.-- Tentative specifications for the DYROD measurement system indicated a probable temperature operating range of $32^{o}F$ to $158^{o}F$ (Table 1). The DYROD was developed to be used as field instrumentation. Considering the breadth of geographic locations included within State Department of Highways and Public Transportation jurisdiction, it seems probable that eventually the DYROD will be expected to withstand the extremes of northern cold and southern heat, during its use in the field. Also, recalling the STDSYS instrumentation over-heating problems during the Gouchy Creek test, it was realized that the instruments just left sitting out in the sun may become extremely hot. For those reasons, a temperature stability test was developed to test the instrument and document its behavior.

The aluminum model pile was again used, along with 100 ft (30.5 m) of Belden #8723 interconnect cable. The DYROD and interconnect cable were placed in controlled environment rooms set continuously at the test temperatures. The DYROD and cable were placed in each temperature room 23 hours before testing to allow the instrument and cable to come to equilibrium at each temperature. A technician went into the temperature room to record the DYROD DPM readings during each test.

A very short piece of leadwire through a wall opening was used to connect the DYROD and interconnect cable in the temperature room with

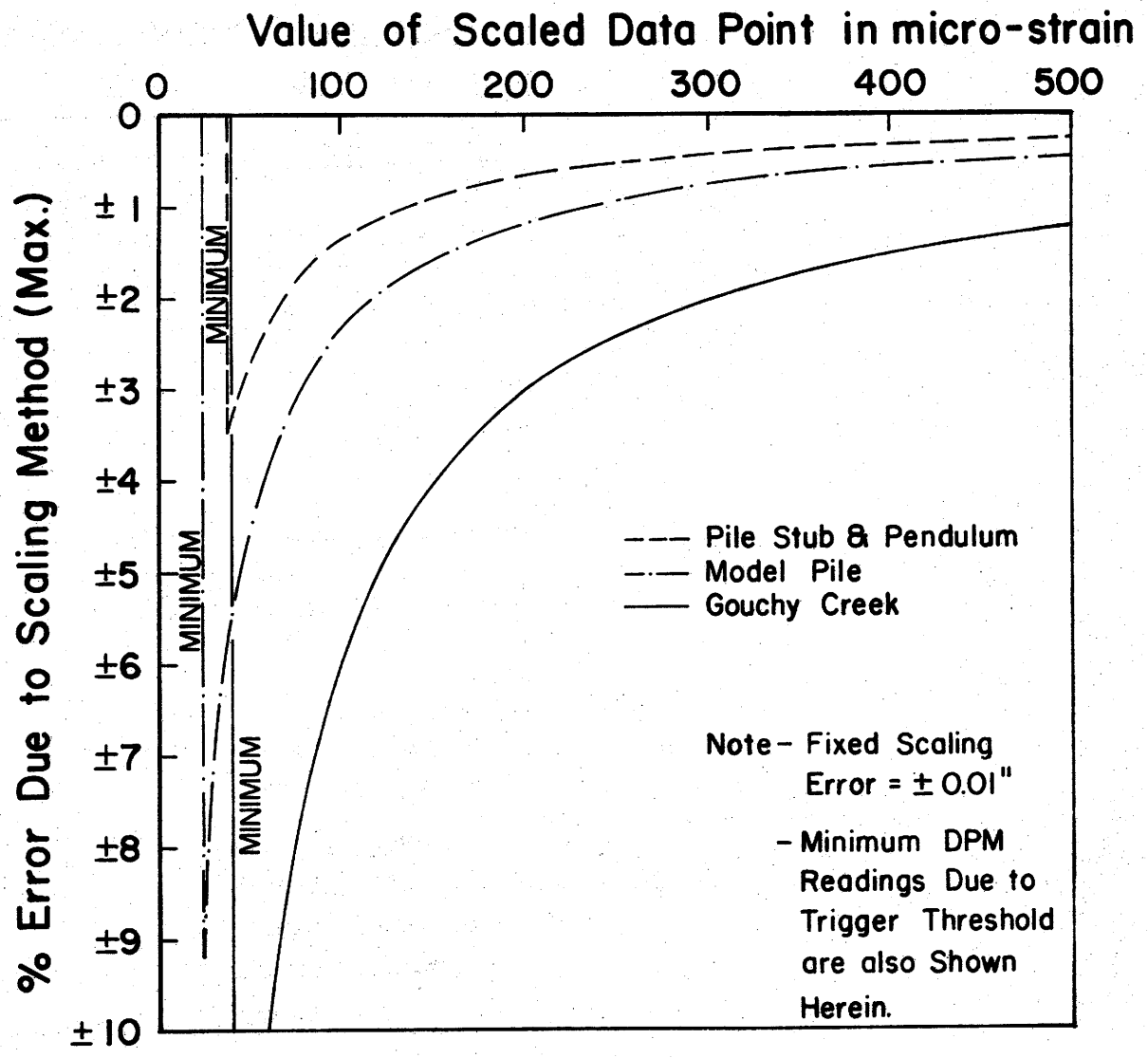

FIG. 13 - SCALING ERROR - MAXIMUM PROBABLE

the model pile outside at room temperature. A constant weight was dropped from a constant height to load the model pile. A wood cushion was also used. The DYROD DPM was set to read every third signal to screen out unwanted subsequent hammer rebounding signals. Five samplings of 30 blows each were obtained and individual averages and standard deviations were computed. The same procedure was followed for subsequent tests of the DYROD at the various other test temperatures.

The results of this first set of DYROD temperature stability tests substantiated the stability of the DYROD throughout its lower temperature operating range. Over 750 blows were applied to the pile during the course of the tests. During this first series of tests the DYROD output remained unaffected by temperatures below 103°F.

In the second series of tests, an exact, reproducible, simulated, 100 micro-strain resistance was electronically induced across one arm of the wheatstone bridge on the model pile. The results from the second series of temperature tests are shown in Fig. 14. The tests indicated a slight increase in indicated strain with increasing temperature, but the increase was less than ±1%. The increase corresponded to the published rate of increase in resistivity with temperature for the 100 feet of interconnect cable, for which no correction is necessary. The DYROD may thus be considered to be stable with respect to and unaffected by temperature within the specified operating range.

Some additional observations were made during the first temperature stability testing. The internal battery was thought to rapidly discharge at higher temperatures, and the edgewise panel meter never indicated a discharged condition. For that reason all tests were run using external AC power. Also, it was noted that at temperatures below 35°F (2°C), at least 11-12 minutes warm-up time should be allowed. The warm-up time was necessary to allow the gain adjustments of the DPM represented calibration signal to bottom out and stabilize. A drop from 784 to 768 was encountered in the first 11 minutes of testing at 2°F (-17°C). Capacitive and resistive rebalancing and

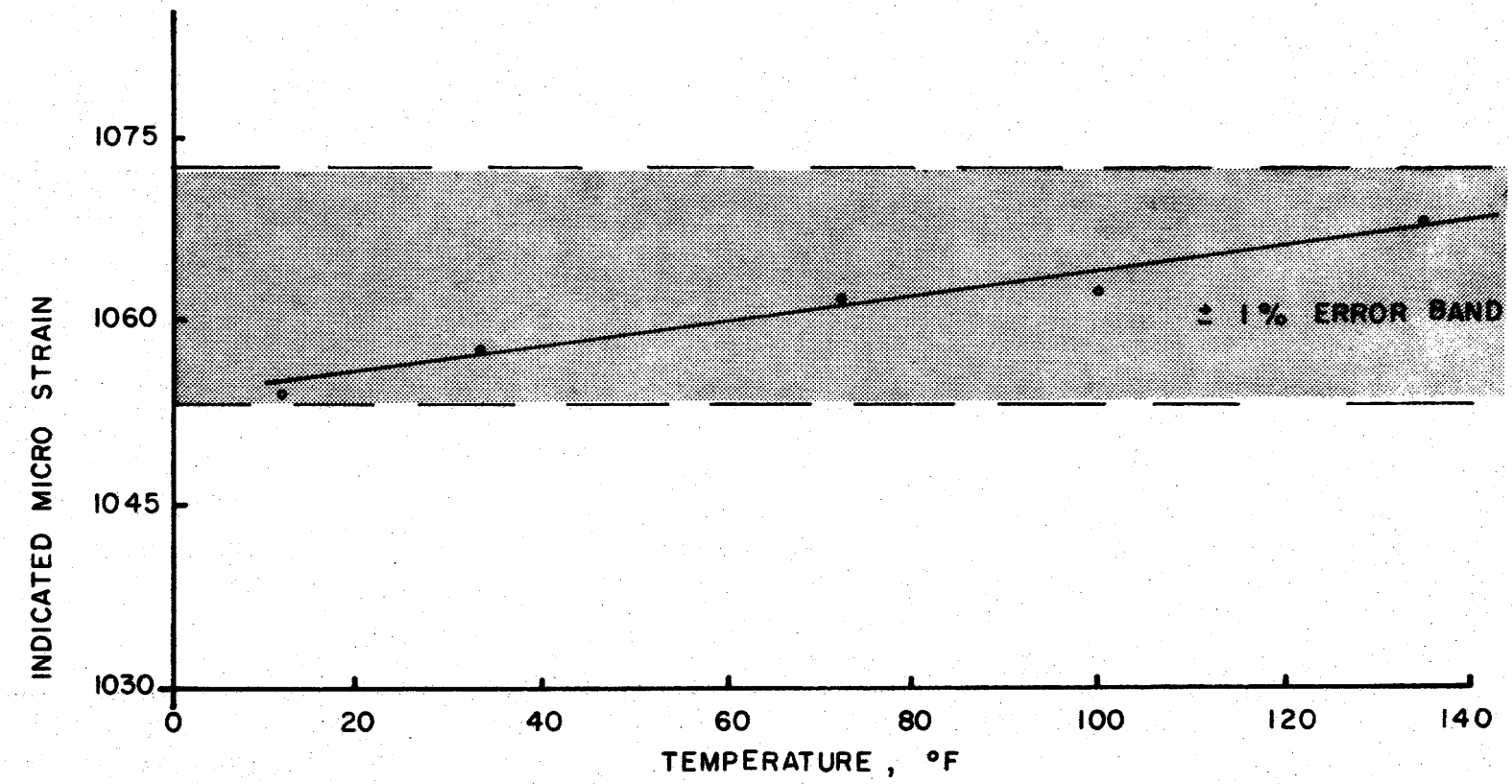

FIG. 14. - INDICATED ERROR OVER TEMPERATURE RANGE

gain readjustment were not necessary when switching from internal battery to external AC at the colder temperatures. Rebalancing and readjustment were necessary however, at higher temperatures, when switching sources of power.

During the tests the internal $\pm$ 15 volt power converter in the DYROD was found to be defective. The DYROD failed to operate in the internal power mode at the highest temperature tested, although it did operate satisfactorily when connected to a source of 117 VAC power. The power converter was removed, tested individually, and found to not meet manufacturer's specifications. This unit was replaced with a new unit.

USE OF PEAK FORCE MEASUREMENT SYSTEM DATA

Wave Equation Technique for Simulation of a Pile Driving Operation.

General.-- As mentioned earlier, work with the wave equation method of analysis has been performed for the past fifteen years, and a considerable number of papers have been published on the subject. More than a few of the authors of those reports have already presented clear and thorough descriptions of the wave equation method of analysis, including principles, assumptions, and analogous explanations. For that reason, only a brief description of the inherent hammer-pile-soil idealization will be presented herein, as reader familiarization and a presentation of parameters to be used later. A successful and clear description of the wave equation method of analysis has been presented by Lowery (9); the reader is referred to that reference for clarification and/or additional explanation of the wave equation technique.

The pile.-- The foundation pile is idealized as a series of massless springs connecting discrete pieces of weight W, of the pile. A pictorial presentation of the pile idealization is shown in Fig. 15a. Associated with the springs connecting the segments or pieces are spring constants, K. The spring constant is an indicator of the "stiffness" of the pile segment.

Internal damping or hysteresis in the pile under cyclic loading is accounted for by adding a spring-loaded dashpot between each piece of pile. The hysteresis (material damping value, B) is zero for short piles and concrete piles. The coefficient of restitution, e, of the pile material is equal to 1, for 100% restitution. If the pile can transmit tensile forces, then the limiting force indicator, GAMMA, between pile segments, is set equal to -1.

The soil.-- The soil is idealized as a linear spring and sliding block in parallel with a dashpot. Soil idealization is depicted in Fig. 15b. A spring and dashpot are associated with each pile segment to simulate the effects of side friction on the pile. An additional spring and dashpot are attached to the bottom segment of the pile

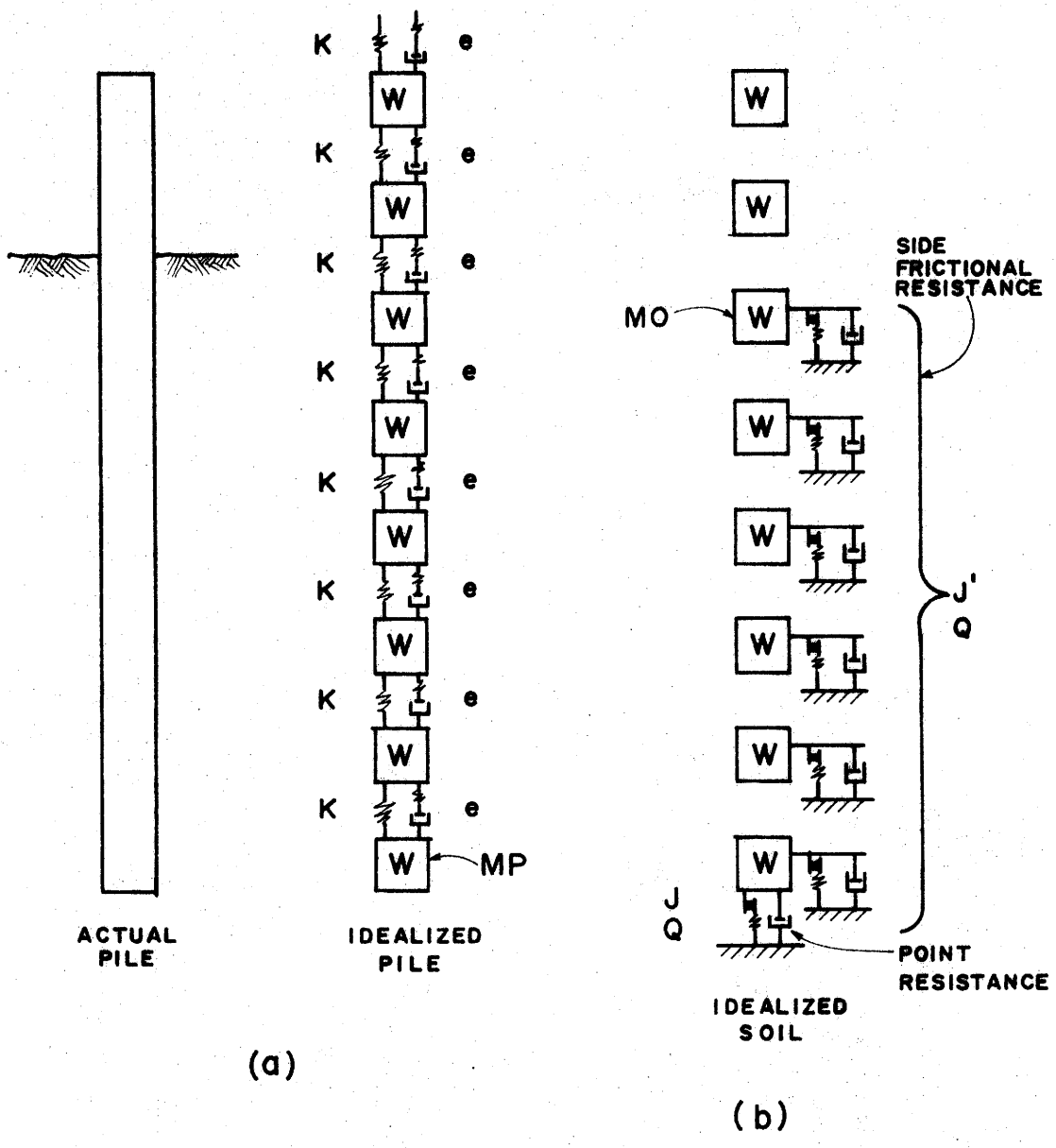

FIG. 15. - PILE AND SOIL SIMULATION.

to simulate the end-bearing effects of the soil on the pile tip. The soil spring constants, K', are computed in the computer program using the "quake" or maximum elastic deformation, Q, of the soil at the maximum elastic force, RU, associated with that Q. A Q equal to 0.1 in. (2.5 mm) has been found applicable for most soils.

The dashpot in parallel with the soil spring has been included to account for dynamic loading effects on the soil. The resistance provided by the damper is assumed to be proportional to the velocity of the associated pile segment. The total static and dynamic resistance of the spring plus the dashpot is a function of displacement, D, of segment W; the plastic displacement of the soil, D'; the spring stiffness of the soil spring, K'; the velocity of the pile segment, V; the soil quake, Q; and the damping constant, J, of the soil dashpot. Values of J depend upon whether the soil is cohesive or granular and are different for the side friction type dashpot versus end-bearing type dashpot. The sliding block simulates the continued static straining of the soil without further increase in resistive force offered by the soil to the pile. The state-of-the-art with respect to soil idealization has been presented by Coyle et al. (5).

The hammer and cushion.-- Drop, steam, and diesel hammers may be simulated and analyzed in the wave equation method of analysis. A typical diesel hammer idealization is shown in Fig. 16. The hammer ram may be broken into a number of segments with associated springs and dashpots similar to the pile simulation, or the ram may be treated as a single weight with one spring and dashpot. A fair portion of the numbers used to simulate hammer rams are still based upon manufacturer's recommendations and have various degrees of validity. The ram has at least one W, and one K associated with it. Ram velocity, VELMI, at impact must be computed or measured, and supplied as program input.

If an anvil, helmet, impact block, or pile cap is used in the pile driving operation, they too are simulated by weights, springs and dashpots. Pile caps, however, are assumed to have infinite

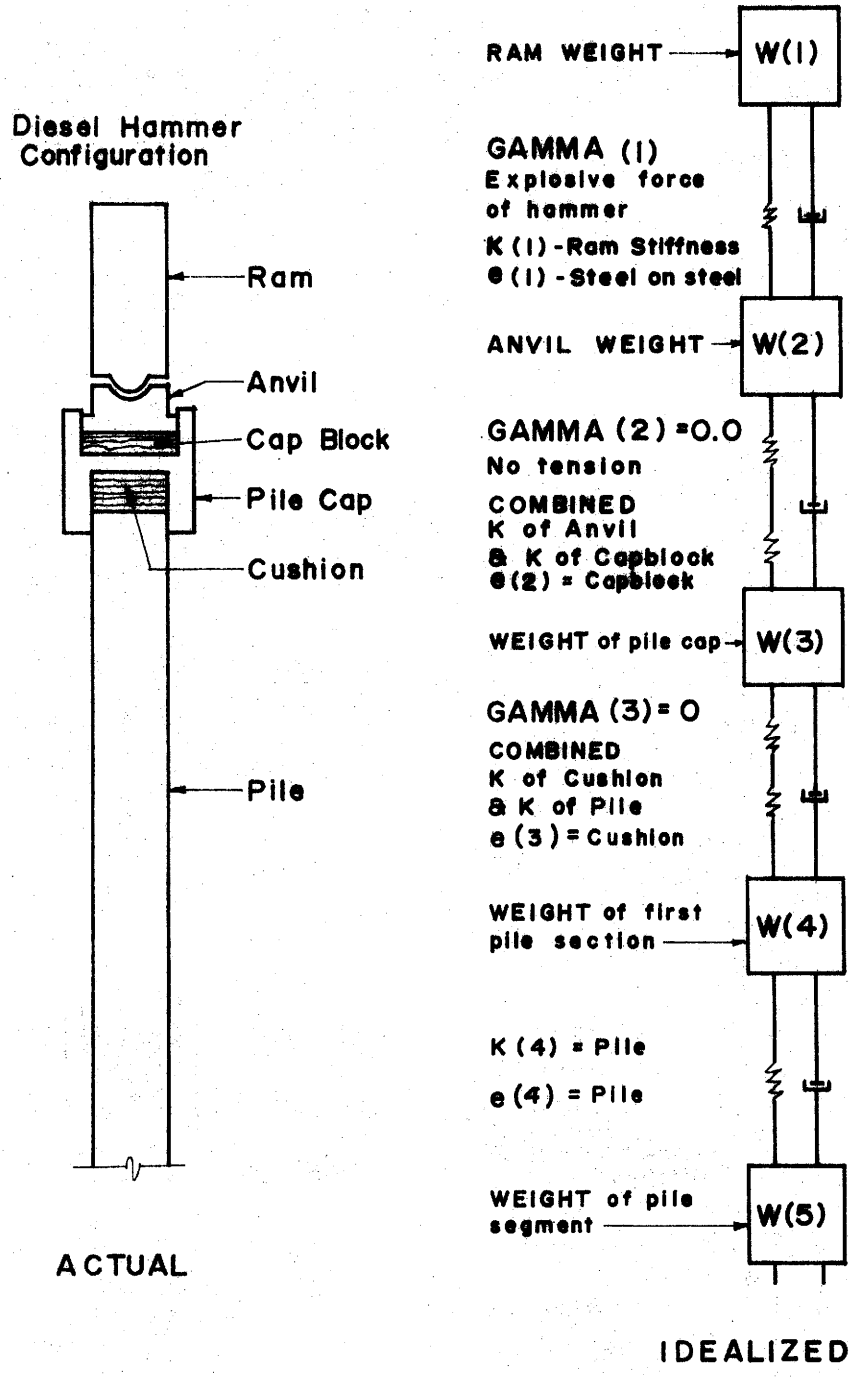

FIG. 16.- HAMMER SIMULATION.

stiffness; hence the K beneath the pile cap is actually only the stiffness of the cushion. Springs associated with the hammer assembly are located beneath the segments (W's) to which they apply. This is just the opposite of the pile simulation springs.

Where capblocks and cushions are used, they are considered weightless. Their K's are combined with other element stiffnesses, and their e's predominate. Such a combination is always necessary at the pile top.

Typical values of K and e for describing pile driving equipment are presented in the utilization manual (9). Those values may be improved as new data become available. GAMMA should be zero where components are not connected and hence cannot transmit tensile forces, and should be equal to the rated explosive force beneath the ram for diesel hammers. A state-of-the-art report concerning pile driving analysis has been written by Lowery et al. (10).

The solution.-- The solution technique used in the wave equation method of analysis in an idealized pile driving problem is as follows:

1. The velocity of the ram segment is set equal to its velocity at impact and all other segment velocities and displacements are set equal to zero, initially. (Gravity effects however may be accounted for, initially.)

2. A short time interval is allowed to elapse, during which time the ram velocity is assumed to be uniform. A new position of the ram is computed at the end of the first time interval. (The displacements of all other system segments are still zero since they had a zero original velocity.)

3. Because of the ram movement in the first interval, the spring beneath it was compressed. Using the ram displacement and spring constant K, the amount of force in the spring may be computed.

4. The force in the spring however acts on both the ram above and next segment below. The force in the spring tends to slow the ram above and simultaneously give a velocity to the segment below. All other segment velocities and displacements are still zero.

5. A second time interval is allowed to elapse.

6. The velocities of the ram and segment below are assumed uniform during the second time interval, so that their new displacements at the end of the second time interval may be calculated. The new displacements induce additional compression of springs above and below. The new force in those springs may be again calculated.

7. The above sequence is allowed to continue until maximum stresses and displacements have been found.

The solution is for one blow of the hammer for the pile at a specific embedment, "seeing" a specific resistance. By assuming the single blow penetration to be typical for a whole foot of driving, a blows-per-foot can be computed. If the analysis is conducted for a number of resistances, a driving resistance versus blow count curve may be developed.

Proposed Standard Method of Analysis Using Measured Peak Force Data.

Summary of procedure. -- The proposed standard method of analysis using measured peak force data may be briefly summarized as a three step process as follows:

1. Necessary input data for a normal run of the wave equation program are collected and an initial run is made.

2. The peak force at the top of the pile, indicated by the initial run, is compared with the peak force measured in the field. A lower ram velocity is chosen if the initial run showed a peak force higher than was actually measured, and the wave equation program is run once more.

3. When the program peak force matches the measured peak force, the corresponding program input data is used to develop a complete resistance vs. blows per inch graph (RUT) from the program, instead of just a single peak force output as obtained in 1 and 2. Knowing the final pile penetration in blows per inch, assuming driving resistance is indicative of bearing capacity, it is possible to enter the generated graph with the final blow count and get the indicated resistance at the time of driving.

If it is desired to perform the analysis before actual pile

driving and then be able to use the results on the job-site, the following procedure is recommended.

1. Necessary input data for a normal run of the wave equation program are collected. A number of runs of the program are made using a number of ram impact velocities that will cover the range of what will probably be encountered at the job-site. Static resistance (RUT) curves are obtained for each of those typical ram velocities chosen.

2. The ram impact velocities are also plotted against the peak forces predicted by the wave equation program, and this graph is then taken to the job-site along with the static resistance curves.

3. The actual peak force during driving is measured at the job-site. Knowing the actual peak force, the graph is used to read the ram impact velocity that corresponds to that peak force as predicted by the wave equation program.

4. Having read off the indicated ram impact velocity, the corresponding RUT curve is used to read the static bearing capacity indicated by the blow count at that moment.

Possible limitations.-- Two features of the proposed standard method of analysis using measured peak force data should be emphasized. First, the accuracy, meaningfulness and usefulness of this method is dependent upon the accuracy of the data input to the wave equation program. The more "best guess" input data used to describe the hammer-pile-soil system, the greater will be the probability of error in using the output of the method. Conversely the more actually-measured or determined parameters that are available from the contractor, field inspector, equipment manufacturers, etc., then the more valid will be the use of the method.

The second characteristic has to do with performing the analysis prior to the actual pile driving. Unless the person running the analysis has some degree of assurance of what equipment the contractor will be using, there will constantly be a risk of the analysis being rendered useless if the contractor changes equipment from what was assumed in the initial analysis.

The input data required to implement the standard method are the same as that presently used by SDHPT personnel in their current wave equation analyses. The required input data for running the wave equation computer program including recommended hammer and cushion simulation values are presented in the program utilization manual (9).

The procedure for the standard method of analysis using measured peak force data is simple and straightforward, and as such, should provide a useful tool for obtaining more meaningful analysis of pile foundations. As indicated by Coyle et al. (5), use of unaltered hammer simulation, considering the present state-of-the art, is the least accurate approach to wave equation analysis of piles. Adjusted hammer-pile-soil simulation using measured peak force provides a superior approach and probably will prove to be the most economical and generally adequate standard method of analysis. It has been suggested that simulation of measured complete force-time curves provides even more accurate analysis but that technique has proved difficult, time-consuming and expensive. Complete force-time simulation is a necessary and valuable research tool but has not been suitable in the past for production (non-instrumented) pile driving where the DYROD is expected to be used.

Sample Problem Using Standard Method of Analysis - Gouchy Creek Data.

General.-- The evaluation test of the DYROD and STDSYS peak force measuring systems at Gouchy Creek provided pile driving data from a typical production pile driving job. The piles were analyzed by the standard method of analysis using measured peak force data for three reasons. The Gouchy Creek data analysis provided a good sample problem with which to demonstrate the procedures and calculations involved in the standard method of analysis. It also provided an opportunity to check the possible accuracy of the method. Finally, it exemplified some of the typical problems that may be encountered in the regular implementation of the method.

At Gouchy Creek several problems were encountered including the inability to determine what equipment the contractor intended to use in driving the piles, what the exact method of installation was going

to be, and what the nature of the soil was and how it might be simulated in the wave equation program. Because of those unknown factors, it was not possible to perform an analysis prior to the actual driving. An analysis was performed after the fact according to the first procedure presented in the previous section.

Input data.-- Some of the required input data was obtained prior to, during, and after the actual pile driving. Some of the data could not be provided at all and currently recommended simulation values were assumed to fill in the gaps. The required input data will be presented in the order in which it is coded for keypunching.

The time interval was computed by the computer program to be 1/7721 seconds. For convenience in plotting results and maintenance of accuracy, a value of 1/8000 was used for all subsequent computer runs. The number of time intervals was eventually reduced from 500 to 300 to save computer time with no loss in accuracy. The pile was idealized as 35 feet in length and was divided into 7 five-foot segments. The ram, anvil, and pile cap were individual segments in the idealization yielding a total of 10 segments for the whole system.

A six foot bounce height of the ram had been observed. The initial velocity of the ram for a first try was computed as recommended (9) for single-acting (open-ended) diesel hammers. The distance from the anvil to the ports, c, could not be measured at the jobsite and the contractor could not provide that information, so 1.08 ft was used as recommended in Table A2 of the Utilization Manual (9). A ram velocity of 17.8 ft/sec was computed for the initial run.

Coefficients of restitution were recommended as 0.8 for springs 1 and 2, and 0.5 from Table A (9) for spring 3. Spring 3 represents the e for the cushion. The cushion was reported to be 7 pieces of 3/4 in. plywood (type - "old concrete form wood") which was assumed to be fir. All other coefficients of restitution were assumed to be 1.0. The limiting force between pile segments, GAMMA, was set equal to -1.0 by the program, implying ability to transmit tension. Material damping, BEEM, was assumed equal to zero for these short

concrete piles.

The static pile capacity was computed as approximately 150 tons by the Engineering News Record formula by the field inspector at Gouchy Creek based upon the final 20-blow penetration, and was used as a first guess for the total static soil resistance acting on the pile, RUT. A 95% point loading was assumed given a soil resistance beneath the pile point RUP of 285 kips initially.

The pile was assumed to be embedded 30 ft. Soil quake, Q, was assumed to be 0.1 in. and since no recommended soil damping factors have been developed for hard shale, a side J = 0.2 and point J = 0.15 were used. The point J value of 0.15 was chosen because of the known high point load at Gouchy Creek. Such a value has been found to be appropriate for simulating high point loadings from an actual case in dense sand. Since such an over-sized hole had been pre-drilled at Gouchy Creek, the average side J of 0.2 for clays, chosen for Gouchy Creek, actually had little or no significant effect on the solution of the sample problem.

Hammer and component weights and stiffnesses were used as recommended in Table A(2) of the Utilization Manual (9). Current recommendations are that the ram stiffness values, K(1), in this table should be reduced by a factor of 2 to 5. A K(1) of 16,000 kips/in. was used rather than the listed 31,500. The recommended anvil stiffness of 18,600 kips/in. was used for K(2) in the case where no capblock was assumed. A capblock could not be observed during actual driving and no information was obtained about it at that time. Subsequently, contractor representatives guessed that perhaps 3 in. of plywood had been used. TTI personnel recommended that 1 in. be assumed, believing that the wood would have been beaten down during driving. The stiffness was then computed using 1 in. depth, 14 in. x 14 in. area, and a modulus of elasticity of 35×10^3 psi, yielding a K = 6860. This K was then combined with the K for the anvil to get a combined K(2) for the cases tried assuming a capblock was present. A computed cushion stiffness of 1300 kips/in. was combined with the first pile segment to obtain a combined K(3).

Better agreement was obtained between the shapes of the program force time and the actually measured force time, assuming 17.8 ft/sec. for ram velocity, if the pile was not pre-loaded with the rated explosive force of the diesel hammer. Gravity effects were accounted for. Pile penetrations and implied blow counts were computed using maximum displacement minus quake, DMAX-Q. The data were coded, keypunched, and the "no capblock" case run first. (It may be recalled that it was not known whether a capblock was actually present or not during the actual pile driving at Gouchy Creek.) The input data are summarized in Table 9.

Adjustment of hammer simulation using measured peak force.-- The force-time output, computed by the wave equation using the input data given in Table 9 at the top of the pile, is plotted in Fig. 17. The computer indicated a peak force of 479 kips. Blow #80 on pile B-17 was chosen as a typical blow with a measured peak force of only 304 kips. It was apparent that the impact velocity of the ram, VELMI, needed to be reduced. A graph of velocity of ram versus peak force is shown in Fig. 18. The graph indicated that a ram velocity as low as 10 ft/sec. might be needed to bring the computed peak force down to 300 kips.

The program was rerun with a VELMI of 10 ft/sec. and 10.2 ft/sec. The latter indicated a peak force of 302 kips which was close enough to the actually measured peak force of 304 kips.

Static Resistance.-- After the peak forces had been matched between the wave equation program output and the actually measured value, the 10.2 ft/sec. data were used to generate a graph of RUT vs. blows per in. The graph is shown in Fig. 19. The equivalent blow count for the last 20 blows of driving was 80 blows per in. Entering the graph at 80 blows per in., yields a static capacity for that pile of about 342 kips, at the time of driving, assuming no capblock was present.

The same procedure was then followed assuming a 1 in. capblock to see what effect that might have. The bearing graph assuming 1 in. capblock is also shown in Fig. 19.

TABLE 9

SUMMARY OF STANDARD METHOD OF ANALYSIS INPUT DATA FOR GOUCHY CREEK PILES

Item	Abbrev.	Value
Critical time interval ÷ 2	$1/\Delta t$	8000
Number of intervals	NSTOP	Varied
Print frequency	INPRINT	1
Total number of segments	MP	10
Element number of first pile segment	MH	4
Number of ram segments	NR	1
Initial velocity of the ram	VELMI, V_R	17.8 ft/sec
Conversion factor to kips	AREA	1000
Coefficient of restitution	e, EEM1	0.8
	e, EEM2	0.8
	e, EEM3	0.5
Explosive force	GAMMA 1	93.7 kips
Limiting force no tension	GAMMA 2	0
Limiting force no tension	GAMMA 3	0
Internal damping	B, BEEM	0
Total soil resistance	RUT	300 kips
Point soil resistance	RUP	285 kips
First pile segment on which soil acts	MO	5
Soil quake	Q	0.1 in.
Soil damping factor, side	SIDE J, J'	0.2 sec/ft
Soil damping factor, point	POINT J, J	0.15 sec/ft
Ram weight	W, WAM (1)	2.75 kips
Anvil weight	WAM (2)	0.816 kips
Pile cap weight	WAM (3)	1.300 kips
Concrete pile segment weights	WAM (4)-(10)	1.02 kips
Stiffness of ram	K(1), XKAM	16,000 kips/in.
Stiffness of anvil	K(2)	18,600 kips/in.
Stiffness of anvil + capblock	K(2)	5010 kips/in.
Stiffness of pile	K	20,250 kips/in.
Stiffness of pile + cushion	K(3)	1230 kips/in.

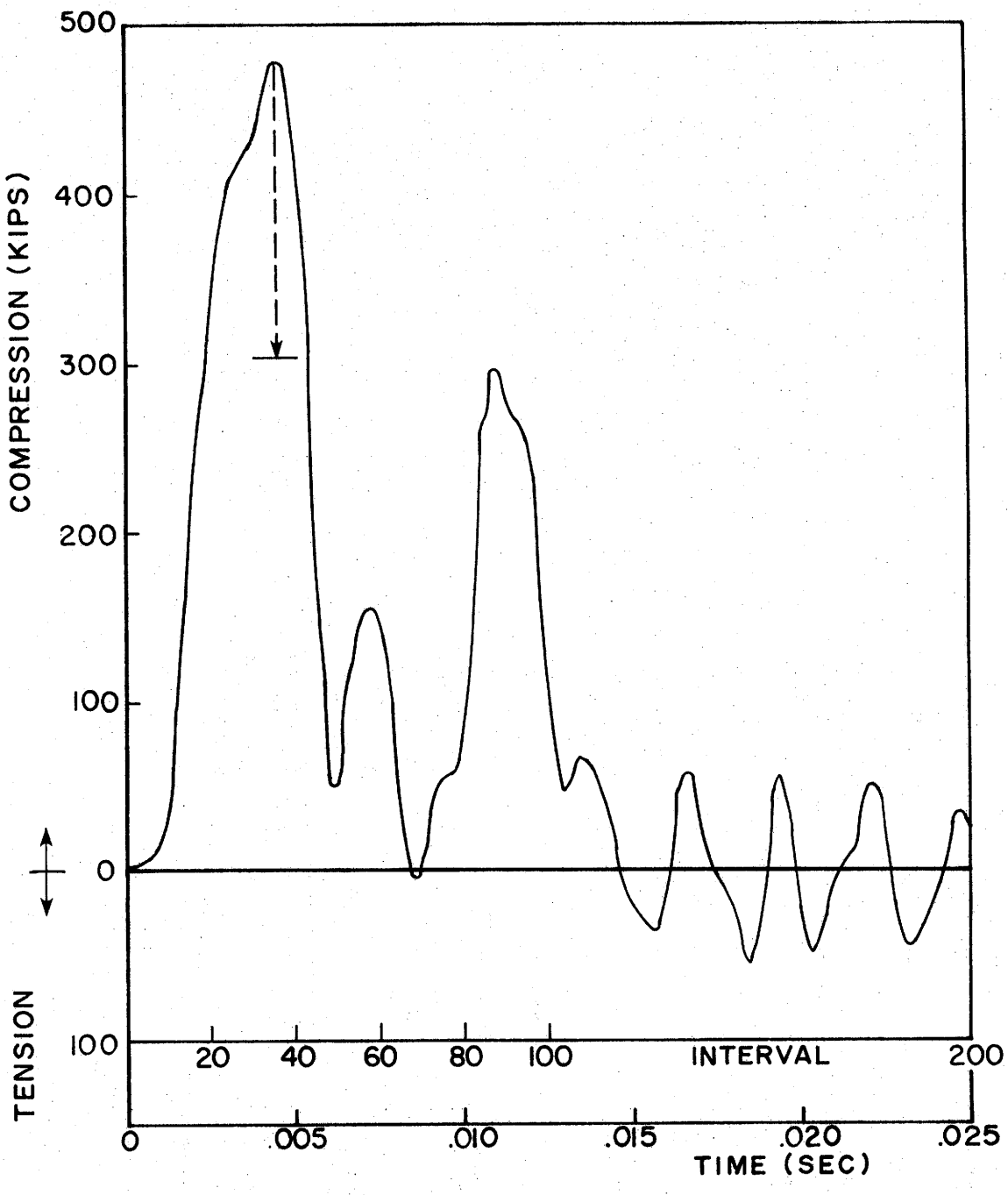

FIG. 17. - FORCE - TIME FOR VELMI = 17.8 FT/SEC ASSUMING NO CAPBLOCK.

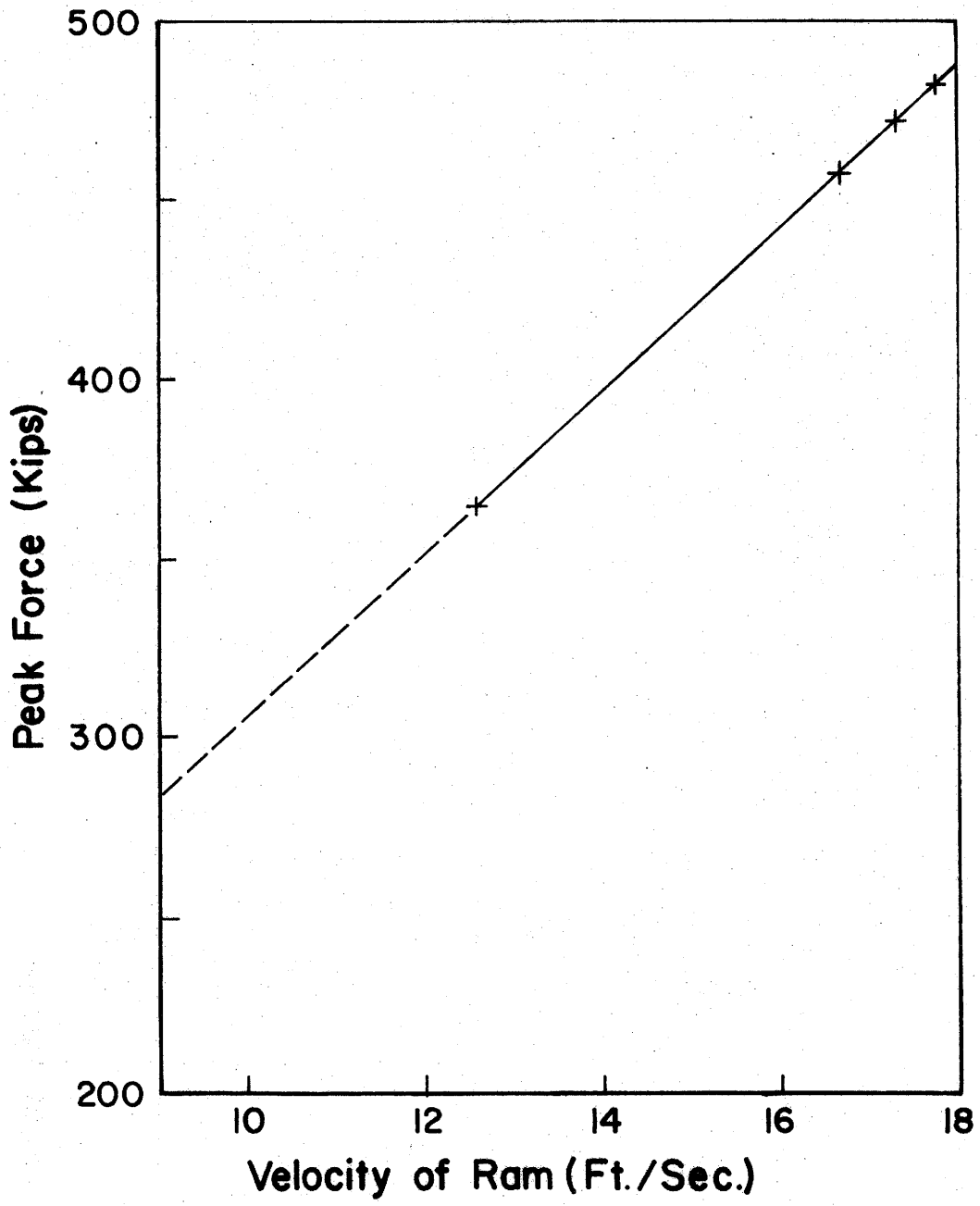

FIG. 18.- RAM VELOCITY VS. COMPUTED PEAK FORCE IN THE TOP OF A PILE

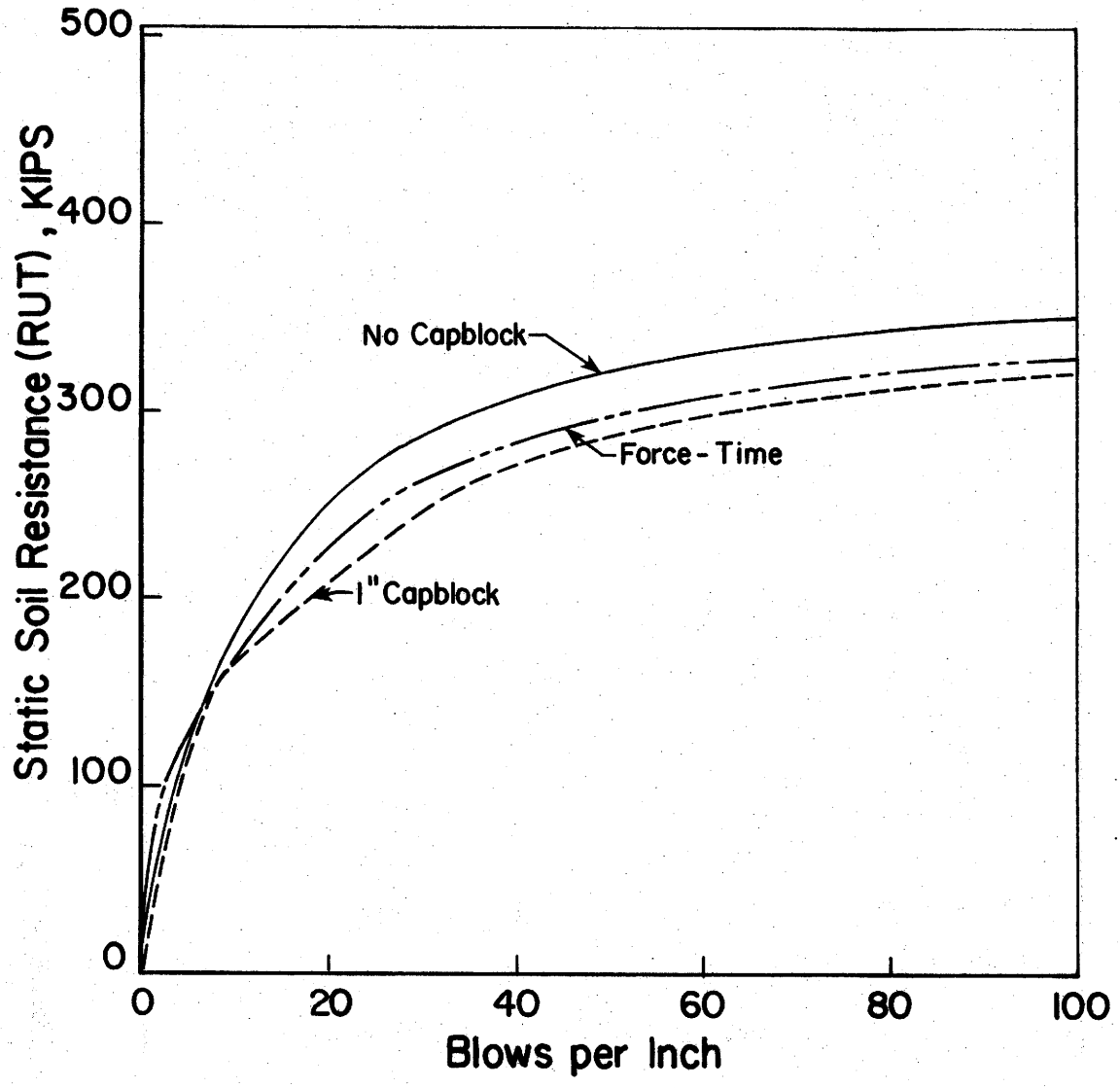

FIG. 19 - BEARING GRAPH FOR PILE B-17

Accuracy of the method.-- A load test was not performed at Gouchy Creek so there was no absolute way to check the accuracy of the predicted bearing capacity obtained using the standard method of analysis. Complete measured force-time was available however for the top of the pile and is presented in Appendix VI. The actual measured force-time was input to the wave equation program and a bearing graph was obtained. This force-time bearing graph is also shown in Fig. 19.

Comparison of the three curves in Fig. 19 indicates that the standard method of analysis using measured peak force data yields bearing curves that are in good agreement with the curve obtained using the actual force-time as input. The "no capblock" assumption yielded a predicted capacity that was 7% higher than the actual force-time curve. The 1" capblock assumption yielded a capacity that was 4% lower than the force-time curve. Considering all of the unknowns involved, this would seem to indicate that the standard method of analysis using measured peak force data can give bearing graphs approximating the RUT vs. blows per in. indicated by actual, measured force-time, fairly accurately.

CONCLUSIONS AND RECOMMENDATIONS

Conclusions.

The objectives of this research were to conduct a series of field tests on a new dynamic peak-force read-out device (DYROD) under conditions expected to exist in normal usage, and to develop a procedure for using the apparatus in connection with routine wave equation analysis. As a result of this study, the following conclusions were made:

1. The dynamic peak-force read-out device was shown to be adequate for use by the State Department of Highways and Public Transportation (SDHPT) in connection with their routine wave equation analyses of piles. The tests and work performed with the device amply demonstrated its durability. The facility of using it, under field conditions, instead of the complex and cumbersome equipment previously required, was apparent. Suitability for production pile driving work was especially obvious.
2. Use of the DYROD DPM peak force output in conjunction with the wave equation program in accordance with the proposed standard method of analysis was found to offer a significant improvement in developing static resistance vs. blows per in. curves.
3. Data obtained with the DYROD was consistently within approximately 4% of that obtained with the standard carrier amplifier system previously used in this type of research. This comparison is considered favorable in light of the inaccuracies associated with the individual measurement systems and the individual gage installations, especially those in concrete. The excellent linearity shown in Appendix VII indicates the stated accuracy to be applicable over the whole range of DYROD output capability.
4. The tests with the aluminum force transducer yielded valuable insight and experience into many design aspects for such a

universal transducer which could be used with the DYROD instead of gages embedded in a test pile.

5. The DYROD was found to be stable climatically and was found to have a lower temperature operating limit on the order of 0°F.
6. Rapid and significant hammer rebounds occurred on the laboratory model pile tests. The DYROD could be set by using the thumbwheel switches to skip one or more signals (blows) to screen out the unwanted lower rebound readings and to prevent loss of the desired peak force value from initial impact.
7. The balancing and gain adjustment knobs and locking mechanisms were found to be susceptible to breakage or loosening.
8. The DYROD was found to be equally well suited for use with various types of transducers including bonded wire resistance strain gages and embedded resistance strain gages.

Recommendations.

A dynamic peak-force read-out device (DYROD) has been tested and a standard method of analysis using measured peak-force data has been developed. During the course of this study, problems have appeared which warrant further research and development, and the following recommendations are offered:

With respect to DYROD -

1. The DYROD should be temperature tested again to insure that the new replacement power supply operates within the desired specified temperature range. During normal usage of the DYROD in cold conditions, an initial warm-up time of 11 minutes should be allowed. During normal use, especially in hot temperatures, a regular check should be made on gain calibration to detect and correct any drifting tendency.
2. A force transducer should be developed for use with the DYROD and should be re-usable, portable, durable, easily connected and easily calibrated. This would be the final step in rendering the DYROD usable for all SDHPT production

pile driving jobs.

3. A standard form for recording data from the DYROD should be developed. Such a standard form would insure that pertinent supplementary information is obtained at the time of driving.
4. A description or a reference to a published description of the calibration computations for half-bridge transducers should be appended to the DYROD operations manual. Such a presentation of the available equations, theory and schematics would extend the use of the DYROD.
5. In general, any further studies involving the DYROD and standard method of analysis should include a static load test and re-driving of the pile. The load test and re-driving are absolutely necessary for verifying bearing capacity predictions and chosen soil parameter values.

With respect to the standard method of analysis using measured peak-force data --

6. A standard procedure should be adopted for accurately estimating the magnitude and distribution of RUT to be input into the initial wave equation run in the standard method of analysis.
7. Additional studies should be made to confirm the use of the VELMI for adjusting the computed peak force at the head of the pile. A check should be made to ascertain whether concurrent variation of two parameters, instead of just one, would yield any improvement in the standard method of analysis.
8. Additional comparisons should be made using actually measured force-time data to establish what magnitude of improved accuracies can be expected using the DYROD and standard method for other typical SDHPT combinations of the hammer-pile-soil system.
9. A standard procedure should be initiated to inform SDHPT field inspectors of the type and gravity of input information needed in using the DYROD and standard method on production

pile driving jobs. A procedure should also be initiated wherein contractors will be required to submit all necessary, certified, input information concerning the driving equipment used, etc., on standard submittal forms.

With respect to the wave equation phase of the standard method of analysis --

10. Additional studies should be performed to improve the simulation of diesel hammers. This will necessitate extensive information about the pile driving equipment used on an actual job where complete records of force-time have been recorded at the pile head.
11. Additional studies should be performed of actual pile driving to develop some recommended soil quake, Q, and damping, J, values for point bearing piles on hard strata in general and hard shales in particular.

pile driving jobs. A procedure should also be initiated wherein contractors will be required to submit all necessary, certified, input information concerning the driving equipment used, etc., on standard submittal forms.

With respect to the wave equation phase of the standard method of analysis --

10. Additional studies should be performed to improve the simulation of diesel hammers. This will necessitate extensive information about the pile driving equipment used on an actual job where complete records of force-time have been recorded at the pile head.
11. Additional studies should be performed of actual pile driving to develop some recommended soil quake, Q, and damping, J, values for point bearing piles on hard strata in general and hard shales in particular.

APPENDIX I. - REFERENCES

REFERENCES

1. "BA-4, Signal Conditioner with Amplifier," Bulletin 80, Vishay Instruments, Malvern, Penn., 1974.

2. Bartoskewitz, R.E. and Coyle, H.M., "Wave Equation Prediction of Pile Bearing Capacity Compared with Field Load Test Results," Research Report 125-5, Texas Transportation Institute, Texas A&M University, College Station, Texas, Dec., 1970.

3. Bowles, J.E., Foundation Analysis and Design, McGraw-Hill Book Co., Inc., New York, N.Y., 1968.

4. Chellis, R.D., Pile Foundations, 2nd ed., McGraw-Hill Book Co., Inc., New York, N.Y., 1961.

5. Coyle, H.M., Bartoskewitz, R.E. and Berger, W.J., "Bearing Capacity Prediction By Wave Equation Analysis - State of the Art", Research Report 125-8F, Texas Transportation Institute, Texas A&M University, College Station, Texas, August, 1973.

6. Foye, R., Jr., et al., "Wave Equation Analyses of Full-Scale Test Piles Using Measured Field Data," Research Report 125-7, Texas Transportation Institute, Texas A&M University, College Station, Texas, August, 1972.

7. "Instructions For Carrier and Linear/Integrate Amplifier Model 119," Technical Manual, Honeywell, Denver Division, Denver, Colorado, January, 1966. (This manual also describes the power supply device.)

8. "Instructions For Visicorder Oscillograph Model 1508," Technical Manual, Honeywell, Denver Division, Denver, Colorado, April, 1965.

9. Lowery, L.L., Wave Equation Computer Program Utilization Manual, Department of Civil Engineering, Texas A&M University, College Station, Texas, January, 1974,(Available from author only.)

10. Lowery, L.L., Jr., et al., "Pile Driving Analysis - State of the Art," Research Report 33-13(F) , Texas Transportation Institute, Texas A&M University, College Station, Texas, January, 1969.

11. Lowery, L.L., Hirsch, T.J., and Samson, C.H., Jr., "Pile Driving Analysis - Simulation of Hammers, Cushions, Piles and Soil," Research Report 33-9, Texas Transportation Institute, Texas A&M University, College Station, Texas, August, 1967.

12. Milberger, L.J. and Zimmer, R.A., "Operating Instructions For Dynamic Pile Force Readout, Model 2174 (draft)," Research Report 174-1(F), Texas Transportation Institute, Texas A&M University, College Station, Texas, August, 1974.

13. Miller, F.E. and Doeringsfeld, H.A., Mechanics of Material, 2nd ed., International Textbook Company, Scranton, Penn., 1965, p. 49.

14. Miller, I. and Freund, J.E., Probability and Statistics for Engineers, Prentice-Hall, Inc., Engelwood Cliffs, N.J., 1965, pp. 69-74, 105-114, 254-258.

15. Smith, E.A.L., "Pile-Driving Analysis By the Wave Equation," Transactions, American Society of Civil Engineers, Paper No. 3306, Vol. 127, 1962.

16. "Standard Method of Test for Static Modulus of Elasticity and Poisson's Ratio of Concrete in Compression," Standard C-469-65(1970), Part 10, 1973 Annual Book of ASTM Standards, American Society for Testing and Materials, Philadelphia, Penn., November, 1973.

17. Timoshenko, S.P., and Young, D.H., Elements of Strength of Materials, 5th ed., Van Nostrand and Company, Inc., Princeton, N.J., 1968, pp. 10-13.

18. Van Reenen, D.A., Coyle, H.M. and Bartoskewitz, R.E., "Investigation of Soil Damping on Full-Scale Test Piles," Research Report 125-6, Texas Transportation Institute, Texas A&M University, College Station, Texas, August, 1971.

19. Wang, C.K. and Solomon, C.G., Reinforced Concrete Design, International Textbook Company, Scranton, Penn., 1965, pp. 36-37.

APPENDIX II. - NOTATION

NOTATION

The following symbols are used in this paper:

- A = cross-sectional area
- AI = amplifier impedance in ohms
- B = material damping constant
- c = distance from anvil to ports
- D = displacement of a segment
- D' = plastic displacement of soil
- E = Young's modulus of elasticity
- E_{AVG} = average modulus of elasticity
- e = coefficient of restitution
- GF = gage factor (sensitivity factor)
- H = average ram bounce height
- h = jump height of open-ended diesel ram
- i = sequence (rank) number
- J = damping constant of a soil dashpot
- K = spring constant representing stiffness
- K = any constant number (eqn. 10)
- K' = soil spring constant
- L = length
- N = number of elements
- N_{eff} = number of effective longitudinal strain gages
- n = total number of data points in a sampling
- P = pile driving hammer ram weight (eqn. 1)
- P = force in pile (eqn. 2)
- Q = quake, maximum elastic deformation of soil
- R = manufacturer's stated strain gage resistance
- R_l = leadwire resistance in ohms
- R_{cal} = value of shunt calibration resistor in ohms
- RU = maximum elastic force in the soil
- S = permanent set of the pile point

V = velocity of a pile segment

W = weight

$\Delta\%$ = percent difference between two system outputs

ε = strain in the pile

ξ = strain

μ = Poisson's ratio

σ = stress

APPENDIX III. - CORRELATION OF DRIVING RATES AND PEAK FORCE

CORRELATION OF DRIVING RATES AND PEAK FORCE

The Visicorder oscillograph was used to record continuous signals of force with time at the top of piles B-16 and B-17 at Gouchy Creek. The direct-writing Visicorder oscillograph records a continuous tracing on light sensitive paper using a mercury vapor lamp. The recording, mercury light spot is deflected in proportion to changes in input signal. Two signals on separate channels were input during the Gouchy Creek test, one from the DYROD GALVO and one from the STDSYS, and two simultaneous tracings were then recorded. The time delay between the two signals was too small to be detected on the tracings usually, being on the order of only 0.22 milliseconds for sensing gages spaced 3 feet (91 cm) apart for a 13,800 ft/sec (4200 m/sec) compressive force wave in the piles.

The Visicorder recording paper drive was set to drive the recording paper at a speed of 80 inches (200 cm) per second. Timing lines were printed across the recording paper at 0.01 second intervals or about every 0.8 inch (2 cm). The compressive force wave signals were only 0.03 - 0.04 seconds long, and since the diesel hammer was operating at a rate of roughly 50 blows/minute, there were about six feet of recording paper with no trace deflections between blows. Thus for purposes of convenience in working with and later storing the records, the force wave portions were numbered and cut out of the 100 ft (30 m) rolls of recording paper. At that time, accurate measurements were made of the time between the first peaks of successive blows. Those times to blow peak are presented in Table III-1.

The open-ended Delmag D-12 diesel hammer used at Gouchy Creek operated in the following cycle. The hammer ram fell from some top-of-stroke height where it had zero velocity. The ram was allowed to free-fall until it passed intake/exhaust ports near the bottom of the stroke. With the ports thereafter blocked, the ram continued down, compressing the fuel/air mixture beneath it, eventually causing ignition. The resulting explosion would blow

TABLE III-1

GOUCHY CREEK DRIVING RATE DATA

Blow No. (1)	SDTSYS Peak Strain (μ-strain) (2)	Time to Blow Peak (sec) (3)	Equivalent Driving Rate (blows/min) (4)
Pile B-16			
Roll 1			
8	216	-	-
9	254	1.220	49.2
10	234	1.154	52.0
11	257	1.192	50.3
12	245	1.160	51.7
13	252	1.170	51.0
14	250	1.179	50.9
15	265	1.193	50.3
16	258	1.188	50.5
17	265	1.202	49.9
18	265	1.206	49.8
19	265	1.192	50.3
Roll 2			
68	276	-	-
69	269	-	-
70	268	1.170	51.3
71	288	1.205	49.8
72	285	1.199	50.0
73	278	1.191	50.4
74	294	1.211	49.5
75	276	1.190	50.4
76	293	1.220	49.2
77	294	1.218	49.3
78	278	1.184	50.7
79	273	1.198	50.1
80	286	1.202	49.9
Roll 3			
128	289	-	-
129	303	-	-
130	292	1.206	49.8
131	292	1.200	50.0
132	289	1.197	50.1
133	297	1.215	49.4
134	282	1.190	50.4
135	289	1.197	50.1
136	268	1.176	51.0
137	297	1.215	49.4

TABLE III-1 (CONTINUED)

(1)	(2)	(3)	(4)
138	303	1.223	49.1
139	292	1.205	49.8
140	298	1.212	49.5
Roll 4			
1*	304	-	-
2	292	1.218	49.3
3	297	-	-
4	295	1.221	49.1
5	277	1.206	49.8
6	302	1.222	49.1
7	290	1.204	49.8
8	297	1.216	49.3
9	290	1.211	49.5
10	297	1.221	49.1
11	294	1.211	49.5
12	284	1.201	50.0
Pile B-17			
Roll 5			
10	250	-	-
11	242	1.179	50.9
12	240	1.172	51.2
13	246	1.186	50.6
14	263	1.199	50.0
15	268	1.194	50.3
16	252	1.172	51.2
17	242	1.162	51.6
18	254	1.180	50.8
19	260	1.174	51.1
20	255	1.182	50.8
Roll 6			
75	267	-	-
76	264	-	-
77	262	1.182	50.8
78	256	1.171	51.2
79	255	1.176	51.0
80	250	1.164	51.5
81	256	1.174	51.1
82	263	1.189	50.5
83	255	1.178	50.9
84	255	1.151	52.1
85	261	1.167	51.4
86	255	1.165	51.5
87	257	1.168	51.4
Roll 7			
126	264	-	-
127	261	-	-

*No correlation with blow count possible.

TABLE III-1 (CONTINUED)

(1)	(2)	(3)	(4)
128	252	1.141	52.6
129	247	1.141	52.6
130	262	1.164	51.5
131	267	1.174	51.1
132	270	1.182	50.8
133	266	1.168	51.4
134	252	1.146	52.4
135	255	1.154	52.0
136	262	1.154	52.0
137	256	1.163	51.6
138	255	1.149	52.2
139	267	1.173	51.2
Roll 8			
1 *	241	-	-
2	257	-	-
3	262	1.191	50.4
4	261	1.199	50.0
5	258	1.189	50.5
6	266	1.196	50.2
7	255	1.185	50.6
8	278	1.204	49.8
9	260	1.184	50.7
10	250	1.172	51.2
11	242	1.162	51.6
12	252	1.173	51.2
13	257	1.180	50.8
14	267	1.195	50.2

* No correlation with blow count possible.

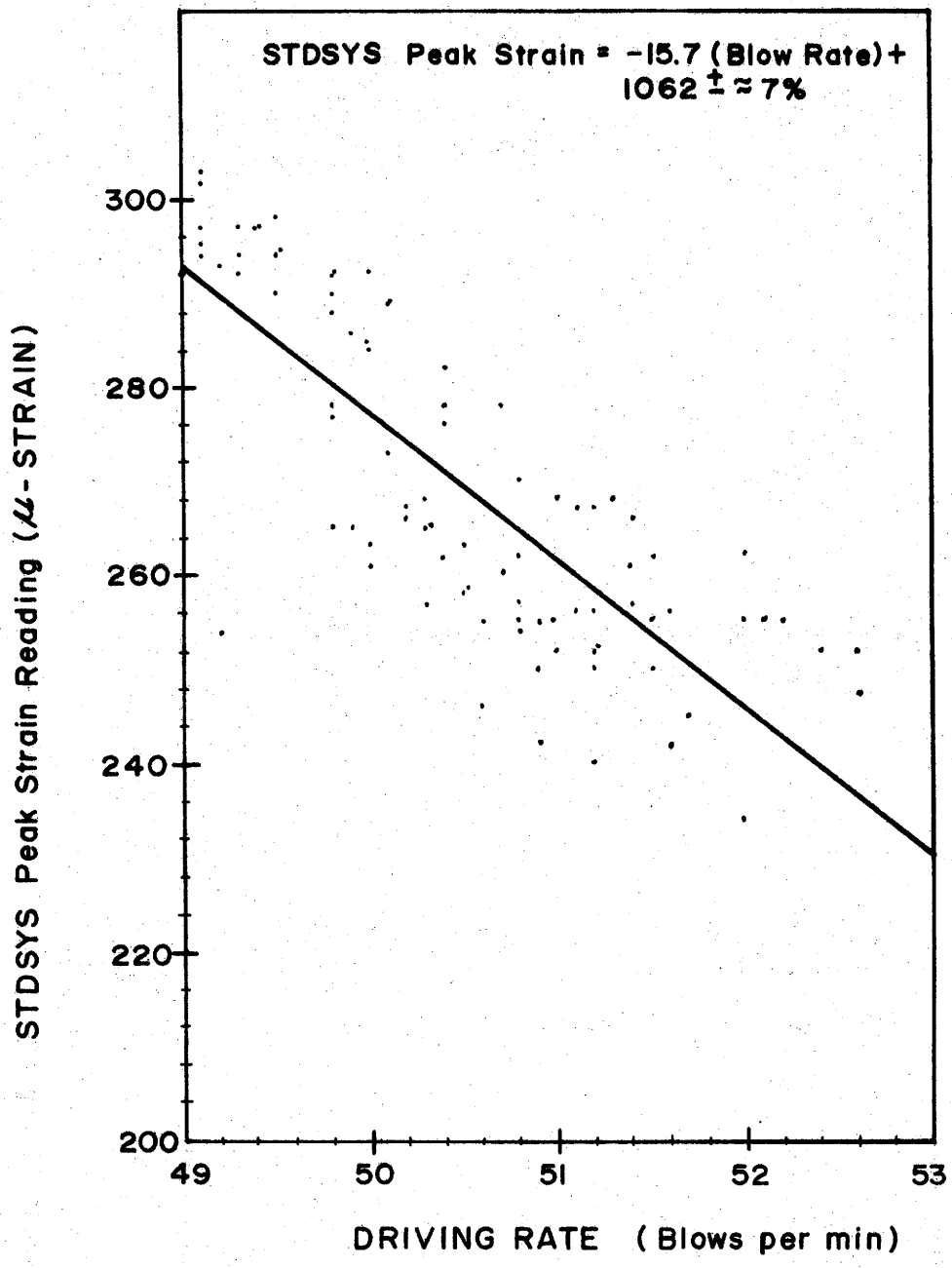

FIG. III - 1. - STRAIN INDUCED IN PILE vs. HAMMER DRIVING RATE.

the ram back up to its top-of-stroke height to start the cycle again.

One complete cycle of the hammer thus required one trip down and a return trip back up for its ram. The amount of force required to blow the ram back up the travel height and the amount of driving force generated by the ram during its trip down are forces probably directly related to that travel height. These forces and that travel height are also related to the time required to traverse that travel height twice per cycle, or in other words, the blow rate. It was thus suspected that the blow rate or driving rate might be useful as an additional indicator of driving force, or hammer efficiency perhaps.

To check the relationship between driving force and blow rate, the previously mentioned, measured, time-between-blows from the Visicorder records were inverted, to obtain implied blow rates. Those blow rates or driving rates were then plotted against STDSYS indicated peak strain in Fig. III-1. A relationship was evident but the data was too scattered to be of use in checking the indicated strain computations made earlier for the measurement systems' evaluations.

APPENDIX IV. TABULAR AND GRAPHICAL PRESENTATION OF DATA USED IN EVALUATING MEASUREMENT SYSTEMS INCLUDING PERCENT DIFFERENCES

TABLE IV-1 - MODEL PILE TEST DATA

Test No.	DYROD DPM		DYROD GALVO			STDSYS		
	Read lb. (uncorrected)	Computed micro-strain (corrected)	Calibration Trace Defl. in.	Defl. From Hammer Blow in.	Implied Strain micro-strain	Calibration Trace Defl. in.	Defl. From Hammer Blow in.	Implied Strain
Box 1								
Roll 1	---	---	1.674	1.674	385	1.670	1.765	409
1	870	399	"	1.744	401	"	1.796	417
1	---	---	"	1.606	369	"	1.662	386
Roll 2	---	---	1.662	1.036	239	1.663	1.050	245
2	534	245	"	1.040	240	"	1.066	248
2	---	---	"	0.156	36	"	0.162	38
Roll 3	691	317	1.667	1.380	317	1.642	1.400	330
3	---	---	"	1.364	314	"	1.394	329
3	---	---	"	0.294	68	"	0.280	66
3	---	---	"	0.100	23	"	0.102	24
Roll 4	235	108	1.668	0.464	107	1.640	0.488	115
4	---	---	"	0.140	32	"	0.166	39
Roll 5	497	228	1.665	0.988	228	1.640	1.002	236
5	---	---	"	0.280	65	"	0.242	57
Box 2								
Roll 1	None	---	1.660	0.200	46	1.862	0.200	47
1	↓	---	"	0.312	72	"	0.302	70
1	Slow	---	"	0.416	96	"	0.392	91
1	Push	---	"	0.320	74	"	0.358	83
1	Test	---	"	0.328	76	"	0.320	74
1	↓	---	"	0.378	88	"	0.370	86
Roll 2	533	245	1.663	1.058	244	1.869	1.062	246
Roll 3	---	---	1.659	1.242	288	1.885	1.326	305
3	910	418	"	1.782	413	"	1.818	418
Roll 4	591	271	1.663	1.168	270	1.883	1.270	292
Roll 5	159	73	1.662	0.322	74	1.885	0.320	74

TABLE IV-2.

PILE STUB & PENDULUM TEST DATA

Test No.[2]	DYROD DPM		DYROD GALVO		
	Reading (kips) Uncorrected	Computed (micro-strain) Corrected[1]	Calibration Trace Defl. (in.)	Defl. From Hammer Blow (in.)	Implied Strain (micro-strain)
Sheet 5	56.7	44.7	1.305	0.320	42.8
Sheet 6	108	85	1.290	0.598	80
Sheet 7	120	94	1.299	0.680	91

1. A correction factor of 224/222 had to be applied to the readings (units of force) obtained from the DPM. Only one lead-wire was erroneously accounted for in computing the equivalent value of the calibration signal. See Table 5, note 6.

2. Data is taken from the Nov. 20, 1974 test records.

TABLE IV-3. - GOUCHY CREEK TEST DATA - PILE B-16

Record No.		DYROD DPM		DYROD GALVO			STDSYS		
Roll	Blow	Peak Force Read Kips	Computed Strain μ-strain	Calibration Trace Defl. in.	Hammer Blow Trace Defl. in.	Computed Strain μ-strain	Calibration Trace Defl. in.	Hammer Blow Trace Defl. in.	Computed Strain μ-strain
(1)	(2)	(3)	(4)	(5)	(6)	(7)	(8)	(9)	(10)
--	--[1]	--	--	--	--	--	--	--	--
1	8	184	209	2.10	0.366	211	1.84	0.326	216
1	9	--	--		0.432	248		0.384	254
1	10	199	226		0.396	228		0.354	234
1	11	--	--		0.436	251		0.388	257
1	12	205	232		0.406	234		0.370	245
1	13	--	--		0.420	242		0.380	252
1	14	212	240		0.422	243		0.378	250
1	15	--	--		0.446	257		0.400	265
1	16	218	247		0.436	251		0.390	258
1	17	--	--		0.450	259		0.400	265
1	18	228	258		0.460	265		0.400	265
1	19	--	--		0.440	253		0.400	265
--[2]	20	228	258	--	--	--	--	--	--
2	68	231	262	2.10	0.446	257	1.84	0.416	276
2	69	--	--		0.440	253		0.406	269
2	70	--[3]	--		0.440	253		0.404	268
2	71	--	--		0.486	280		0.434	288
2	72	238	270		0.476	274		0.430	285
2	73	--	--		0.480	276		0.420	278
2	74	248	281		0.496	286		0.444	294
2	75	--	--		0.468	269		0.416	276
2	76	247	280		0.490	282		0.442	293
2	77	--	--		0.494	284		0.444	294
2	78	231	262		0.460	265		0.420	278
2	79	--	--		0.460	265		0.412	273
2	80	241	273		0.478	275		0.432	286

TABLE IV-3. - CONTINUED

(1)	(2)	(3)	(4)	(5)	(6)	(7)	(8)	(9)	(10)
--	126	249	282	--	--	--	--	--	--
3	128	238	270	2.10	0.480	276	1.84	0.436	289
3	129	--	--		0.502	289		0.458	303
3	130	245	278		0.480	276		0.440	292
3	131	--	--		0.484	279		0.440	292
3	132	240	272		0.478	275		0.436	289
3	133	--	--		0.500	288		0.448	297
3	134	237	269		0.470	271		0.426	282
3	135	--	--		0.478	275		0.436	289
3	136	232	263		0.454	261		0.404	268
3	137	--	--		0.494	284		0.448	297
3	138	253	287		0.498	287		0.458	303
3	139	--	--		0.484	279		0.440	292
3	140	250	283		0.490	282		0.450	298
--	142	231	262	--	--	--	--	--	--
4	--[4]	--	--	2.10	0.498	287	1.84	0.459	304
4	--	--	--		0.486	280		0.440	292
4	--	--	--		0.500	288		0.448	297
4	--	--	--		0.498	287		0.446	295
4	--	--	--		0.478	275		0.418	277
4	--	--	--		0.500	288		0.456	302
4	--	--	--		0.492	283		0.438	290
4	--	--	--		0.490	282		0.448	297
4	--	--	--		0.484	279		0.438	290
4	--	--	--		0.496	286		0.448	297
4	--	--	--		0.486	280		0.444	294
4	--	--	--		0.480	276		0.428	284

[1] Pile hit 6 blows to check cals.; DYROD DPM set to read every other blow.
[2] See Fig.IV-1 & IV-2 for presentation of additional DPM readings obtained.
[3] Missed DPM reading.
[4] Correspondence, between roll 4 of Visicorder readings and DPM readings, could not be established.

TABLE IV-4. --GOUCHY CREEK TEST DATA - PILE B-17

Record No.		DYROD DPM		DYROD GALVO			STDSYS		
Roll	Blow	Peak Force Read Kips	Computed Strain μ-strain	Calibration Trace Defl. in.	Hammer Blow Trace Defl. in.	Computed Strain μ-strain	Calibration Trace Defl. in.	Hammer Blow Trace Defl. in.	Computed Strain μ-strain
(1)	(2)	(3)	(4)	(5)	(6)	(7)	(8)	(9)	(10)
--	9	181	205	--	--	--	--	--	--
5	10	--	--	2.10	0.402	232	2.01	0.412	250
5	11	--	--		0.407	234		0.399	242
5	12	201	228		0.400	230		0.396	240
5	13	--	--		0.414	238		0.406	246
5	14	--	--		0.440	253		0.434	263
5	15	230	261		0.454	261		0.442	268
5	16	--	--		0.420	242		0.416	252
5	17	--	--		0.412	237		0.400	242
5	18	213	241		0.420	242		0.418	254
5	19	--	--		0.434	250		0.428	260
5	20	--	--		0.420	242		0.420	255
--	21	222	252	--	--	--	--	--	--
6	75	220	249	2.10	0.432	249	2.01	0.440	267
6	76	--	--		0.436	251		0.436	264
6	77	--	--		0.420	242		0.432	262
6	78	210	238		0.418	241		0.422	256
6	79	--	--		0.428	246		0.420	255
6	80	--	--		0.416	240		0.412	250
6	81	214	243		0.424	244		0.422	256
6	82	--	--		0.432	249		0.434	263
6	83	--	--		0.436	251		0.420	255
6	84	214	243		0.420	242		0.420	255
6	85	--	--		0.434	250		0.430	261
6	86	--	--		0.420	242		0.420	255
6	87	219	248		0.435	250		0.424	257

TABLE IV-4. --CONTINUED

(1)	(2)	(3)	(4)	(5)	(6)	(7)	(8)	(9)	(10)
7	126	222	252	2.10	0.438	252	2.01	0.436	264
7	127	--	--		0.434	250		0.430	261
7	128	--	--		0.408	235		0.416	252
7	129	207	235		0.410	236		0.408	247
7	130	--	--		0.436	251		0.432	262
7	131	--	--		0.440	253		0.440	267
7	132	224	254		0.448	258		0.446	270
7	133	--	--		0.446	257		0.438	266
7	134	--	--		0.420	242		0.416	252
7	135	211	239		0.420	242		0.420	255
7	136	--	--		0.428	246		0.432	262
7	137	--	--		0.431	248		0.422	256
7	138	213	241		0.420	242		0.420	255
7	139	--	--		0.440	253		0.440	267
8	--[1]	203	230		0.400	230		0.398	241
8	--	--	--		0.426	245		0.424	257
8	--	--	--		0.434	250		0.432	262
8	--	220	249		0.436	251		0.430	261
8	--	--	--		0.430	248		0.426	258
8	--	--	--		0.440	253		0.438	266
8	--	218	247		0.440	253		0.420	255
8	--	--	--		0.460	265		0.458	278
8	--	--	--		0.428	246		0.428	260
8	--	211	239		0.418	241		0.412	250
8	--	--	--		0.400	230		0.400	242
8	--	--	--		0.416	240		0.416	252
8	--	216	245		0.430	248		0.424	257
8	--	--	--		0.440	253		0.440	267

[1] A record of blow count was not kept while Visicorder paper roll was being changed.

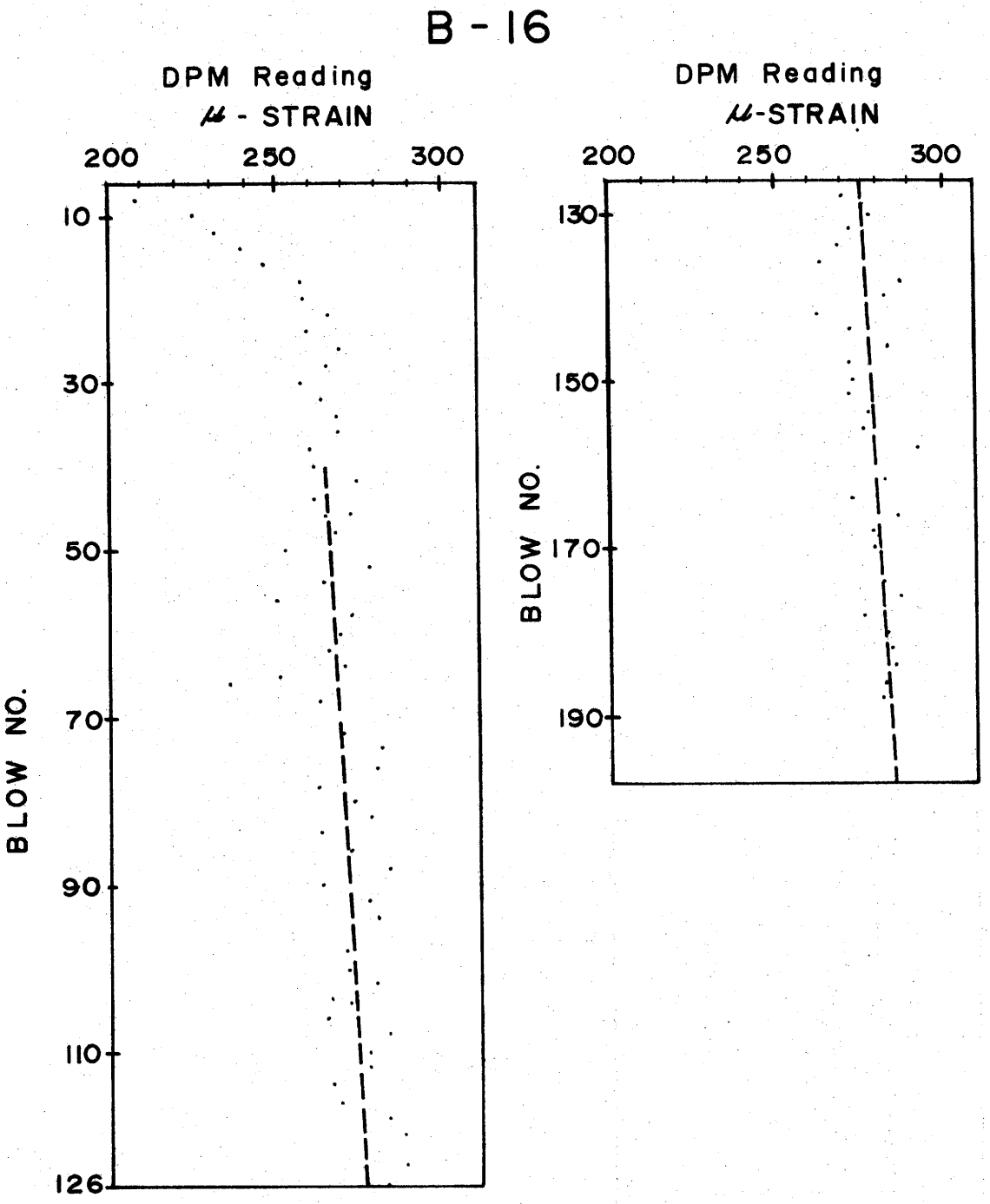

FIG. IV-1.- BLOW NO. vs. DYROD DPM-INDICATED PEAK STRAIN FOR ALL DPM READINGS ON PILE B-16.

B-17

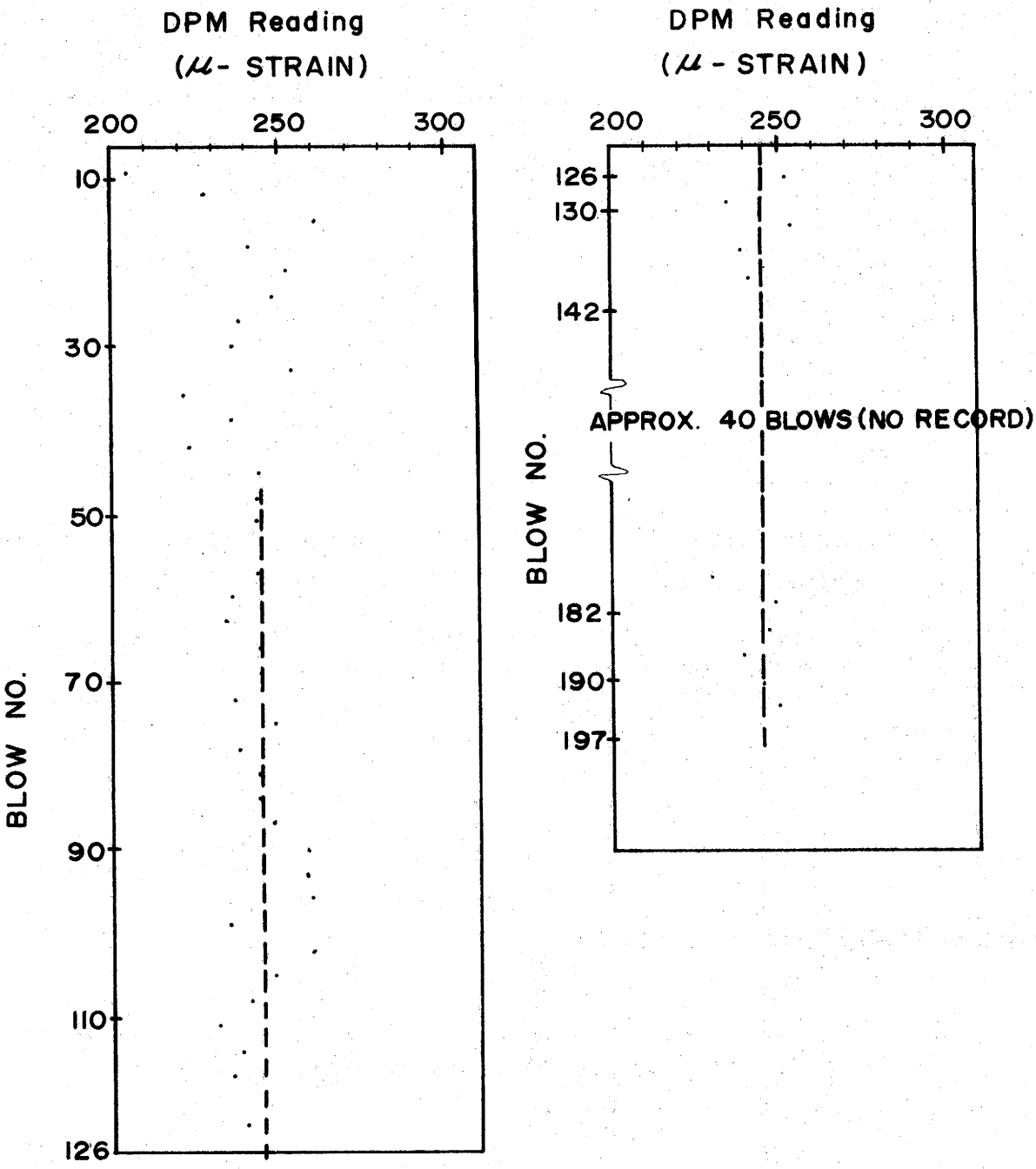

FIG. IV-2. - BLOW NO. vs. DYROD DPM-INDICATED PEAK STRAIN FOR ALL DPM READINGS ON PILE B-17

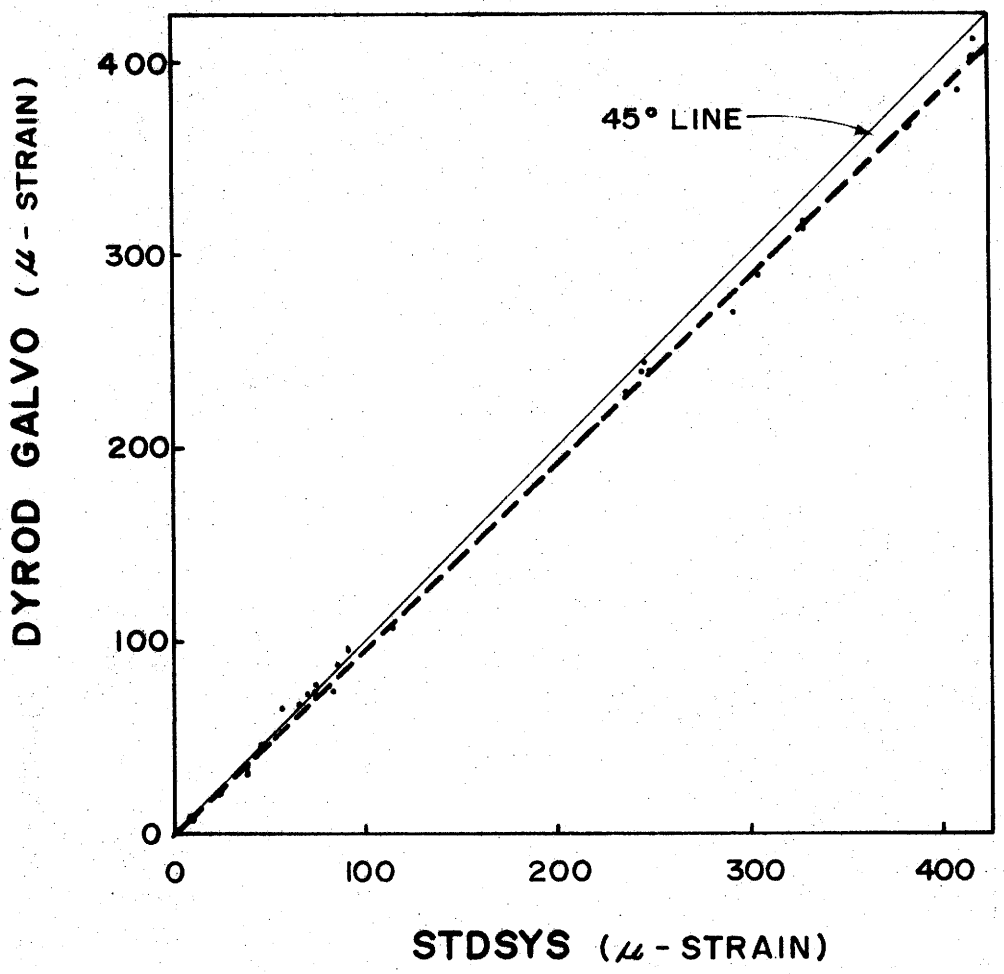

FIG. IV - 3. - MODEL PILE **DYROD GALVO vs. STDSYS.**

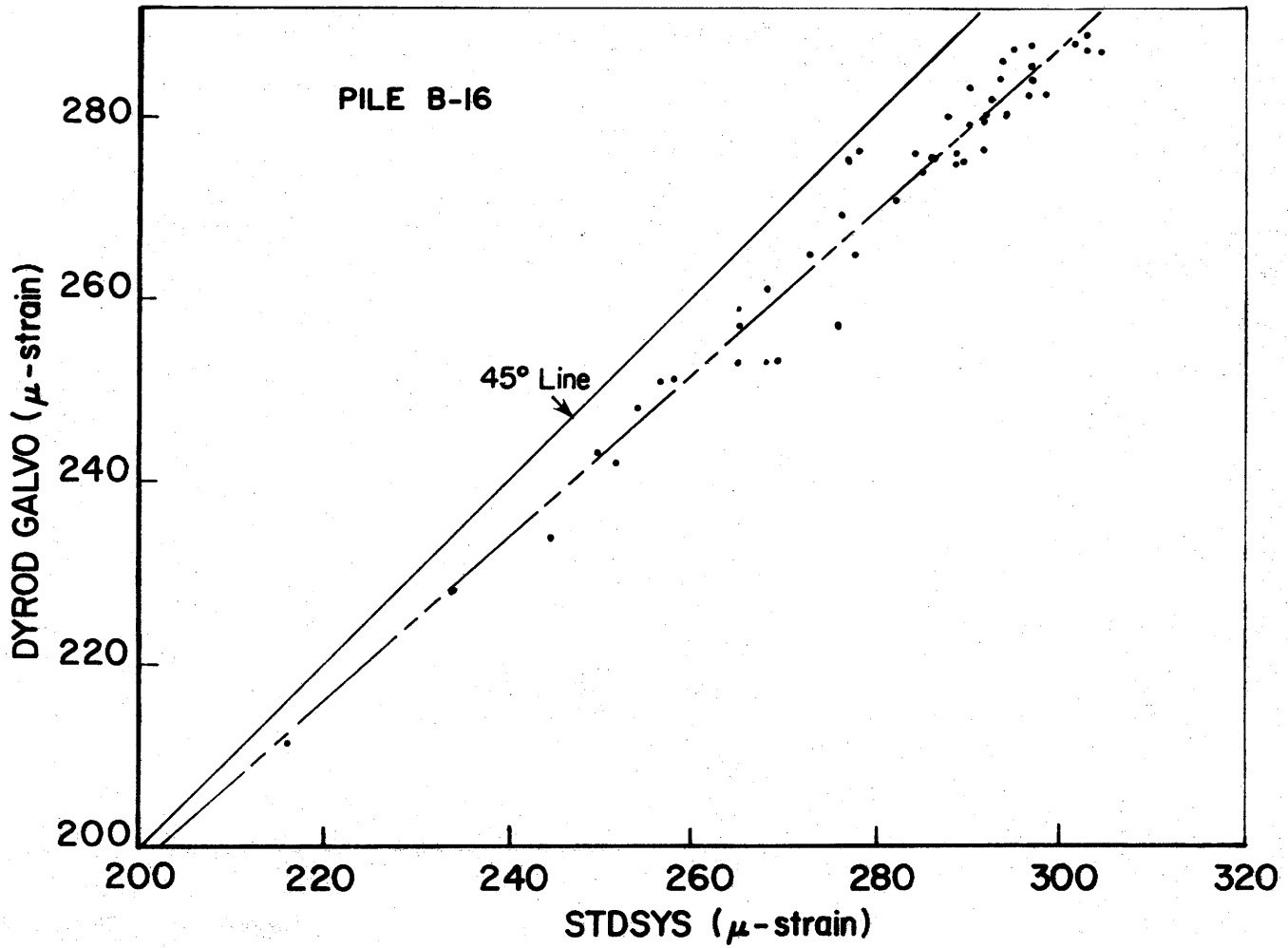

FIG. IV-4. - B-16 DYROD GALVO VS. STDSYS

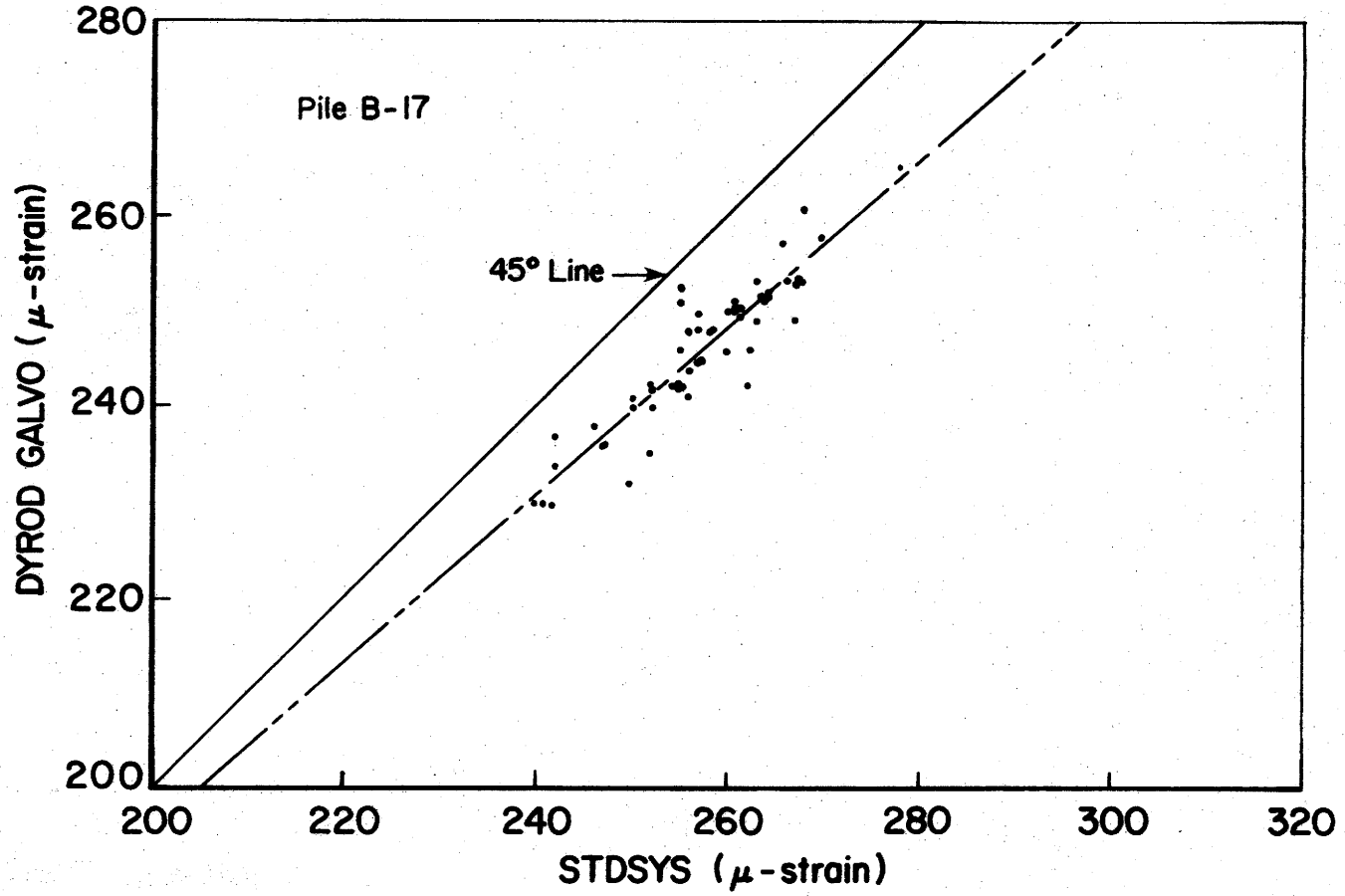

FIG. IV-5. - B-17 DYROD GALVO VS. STDSYS

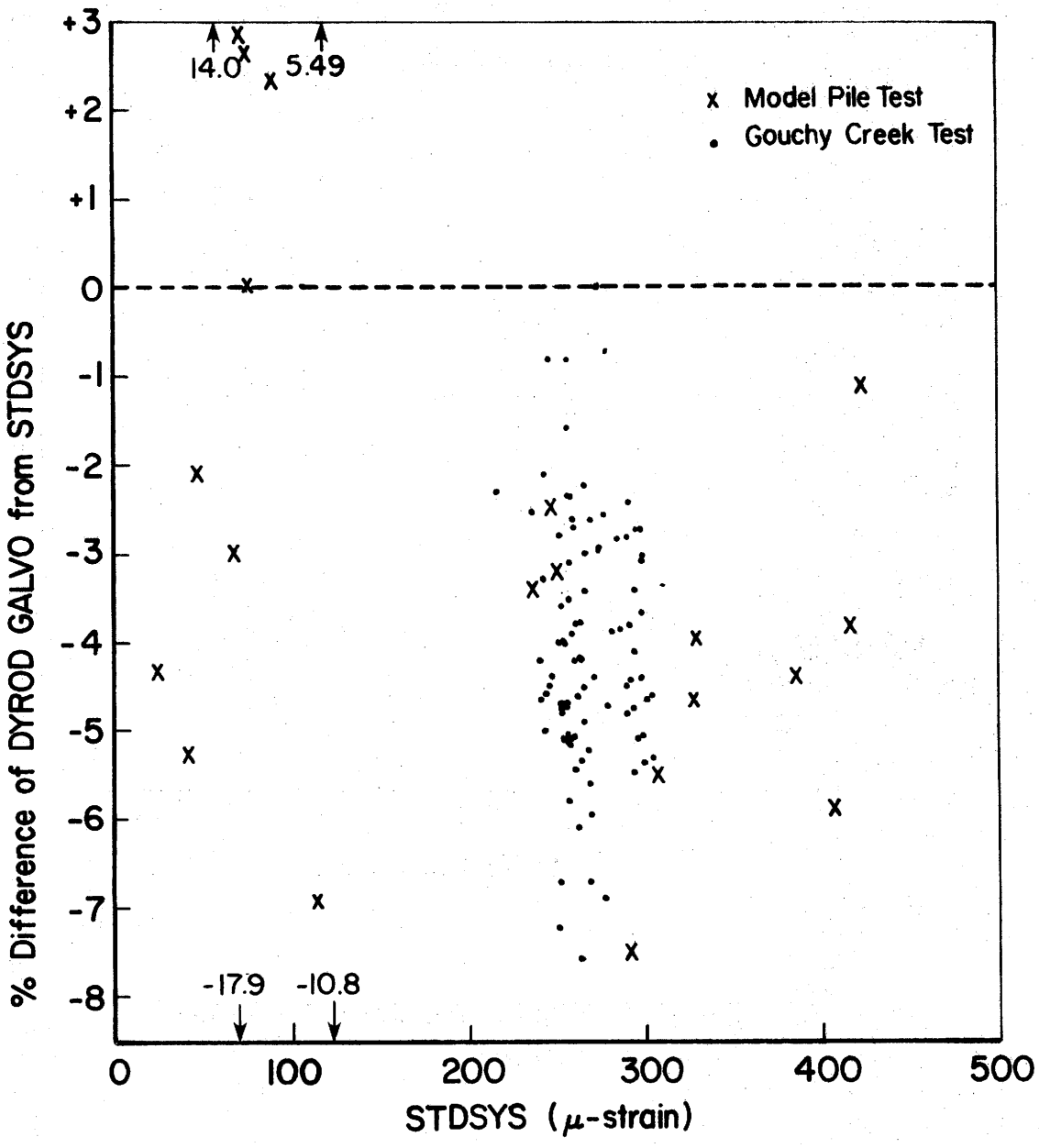

FIG. IV - 6 - PERCENT DIFFERENCE OF GALVO FROM STDSYS INDICATED STRAIN

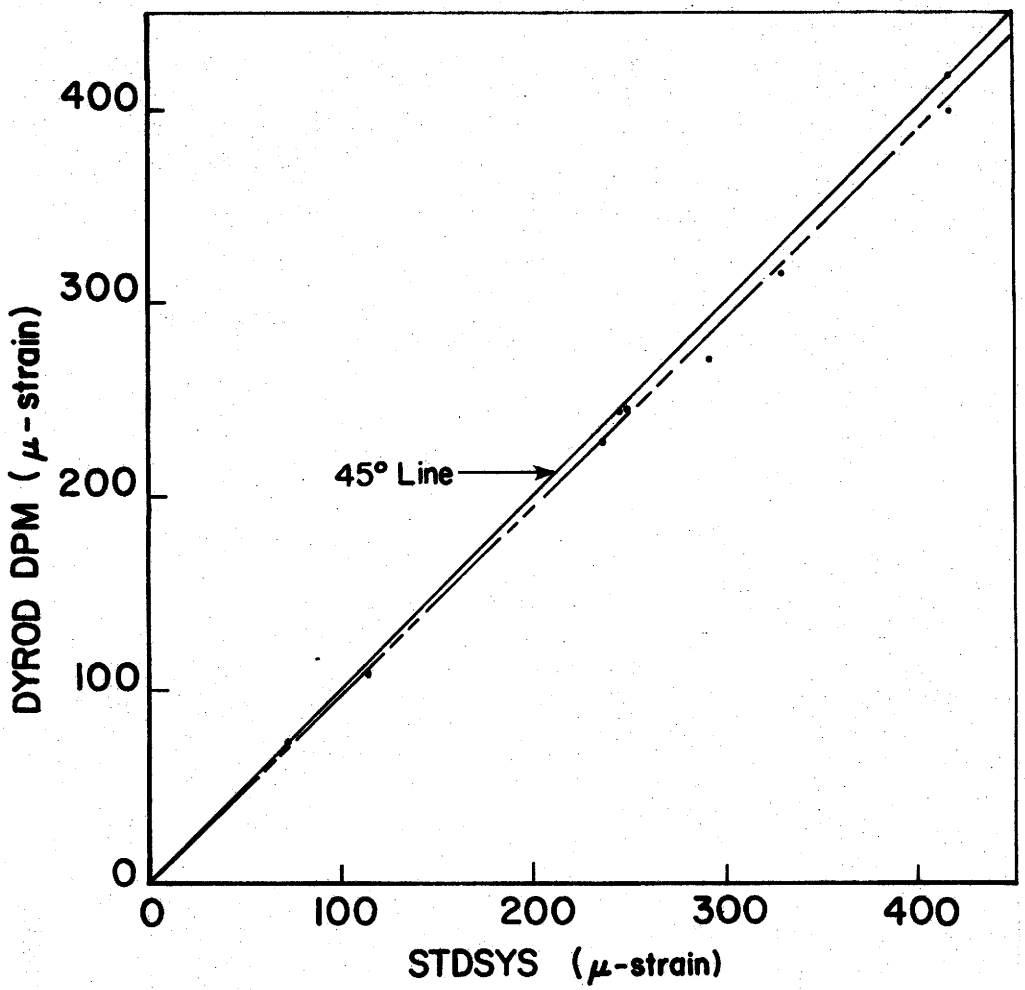

FIG. IV-7 - DYROD DPM VS STDSYS FOR MODEL PILE TEST DATA

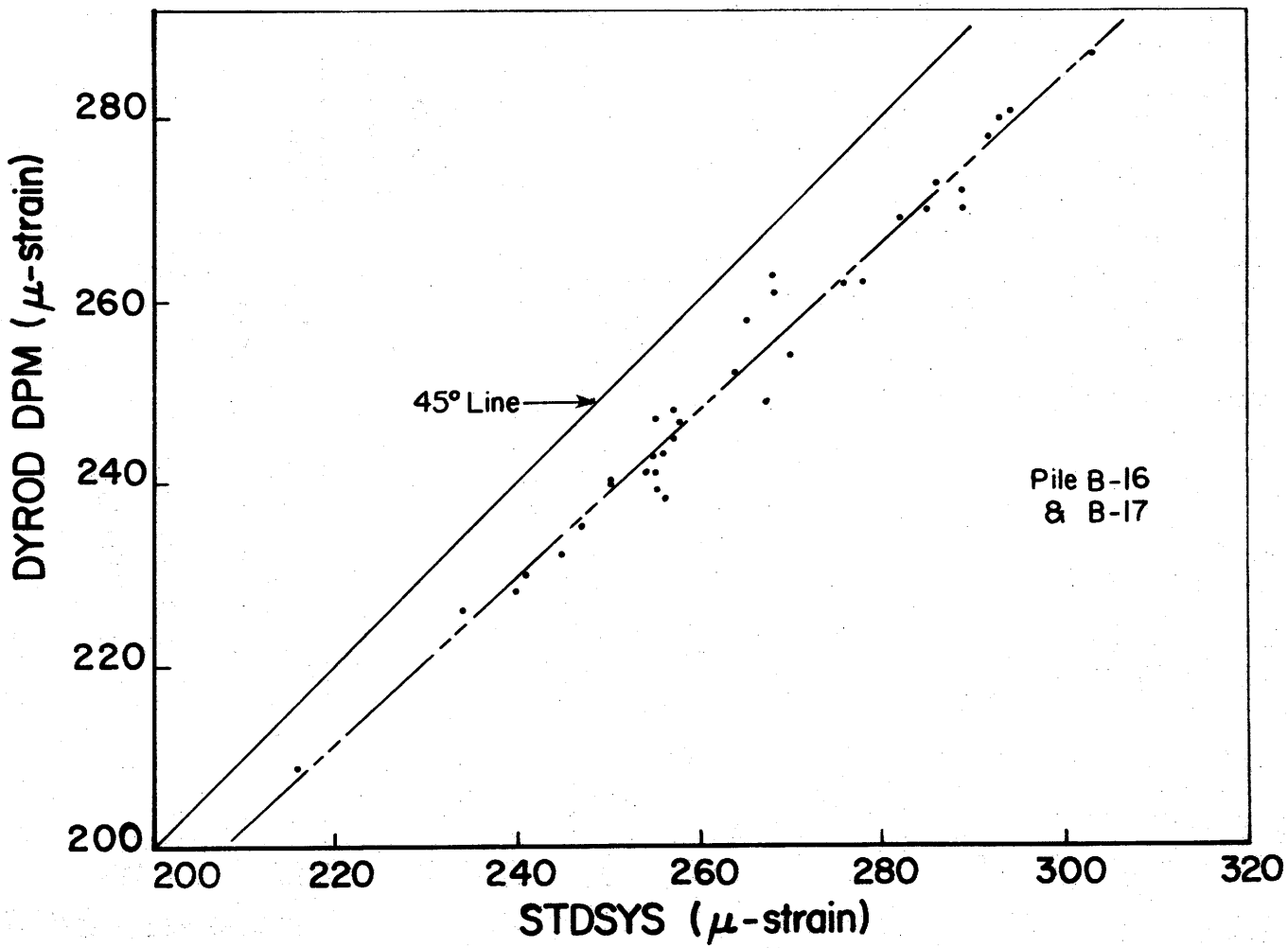

FIG. IV-8 - DYROD DPM VS. STDSYS FOR GOUCHY CREEK TEST

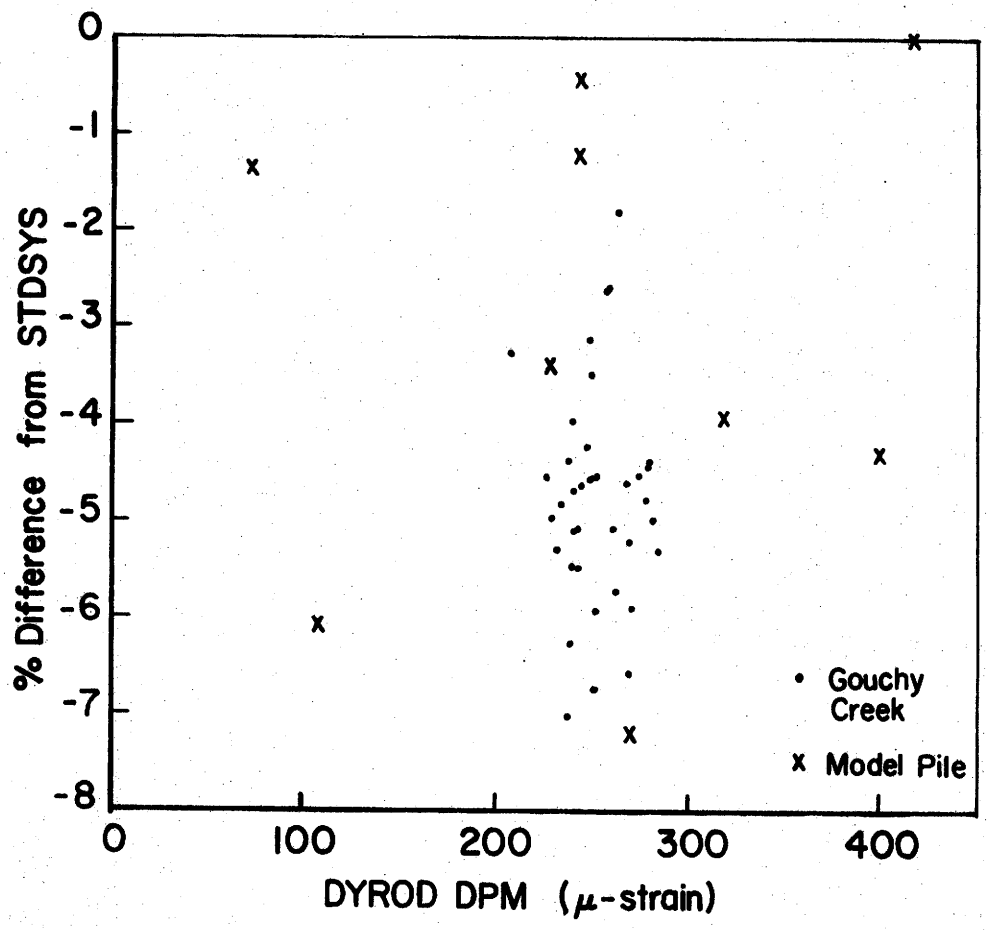

FIG. IV-9 % DIFFERENCE OF DYROD DPM FROM STDSYS

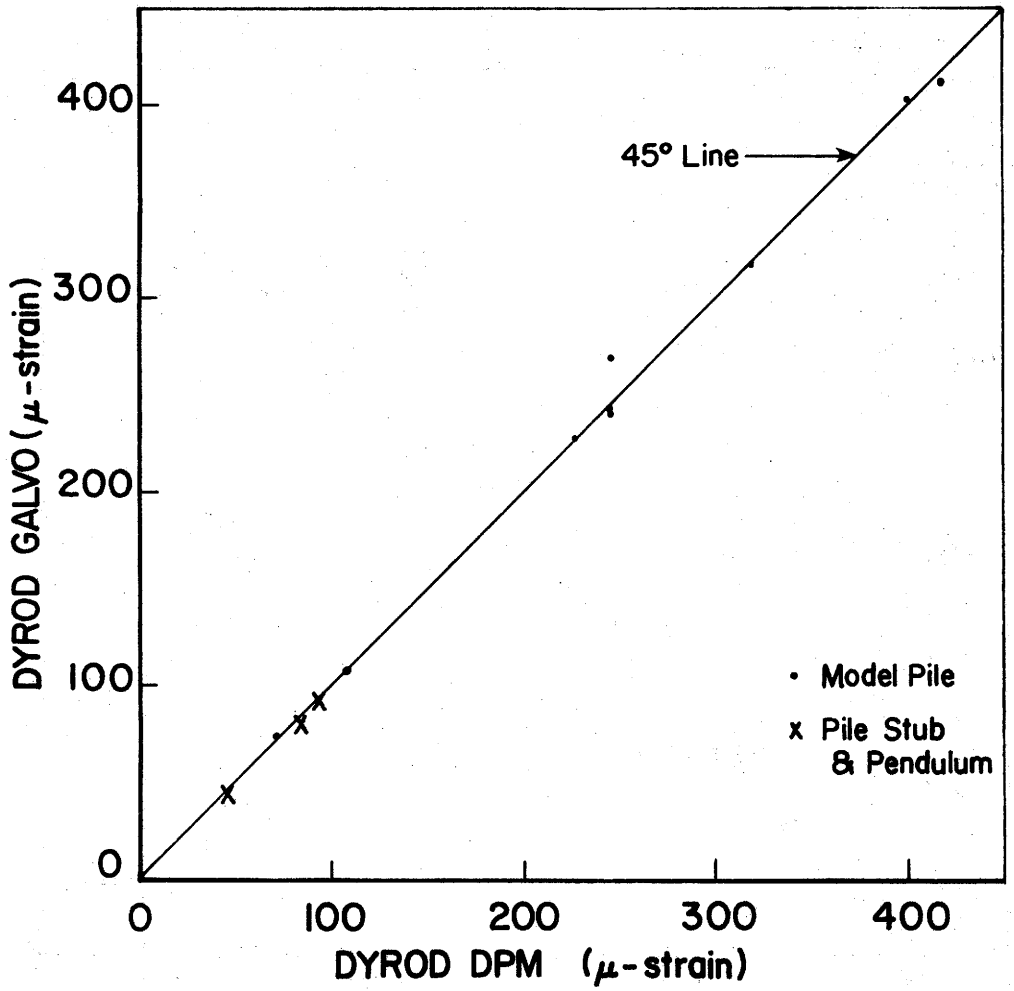

FIG. IV-10- GALVO VS DPM FOR MODEL PILE & PILE STUB AND PENDULUM TESTS

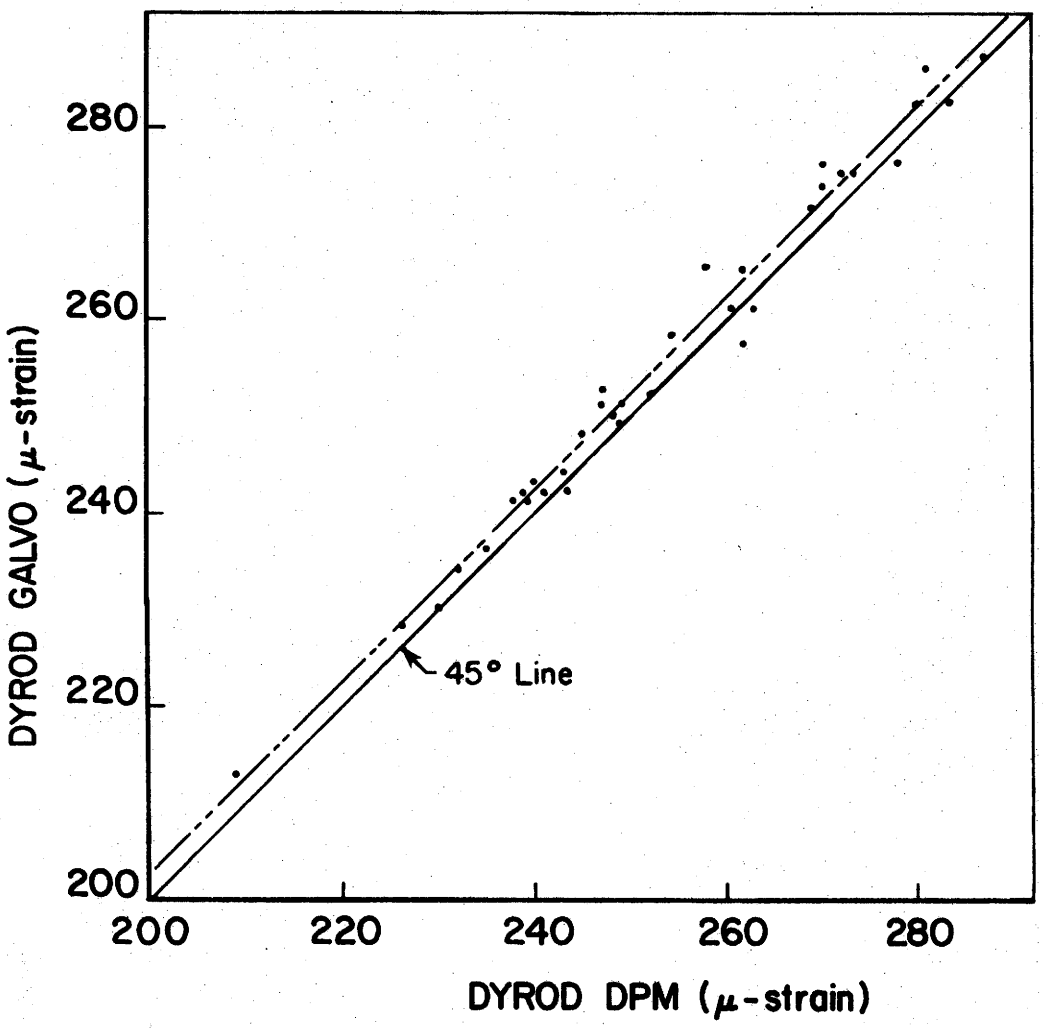

FIG. IV-11.- GALVO VS. DPM FOR GOUCHY CREEK TEST

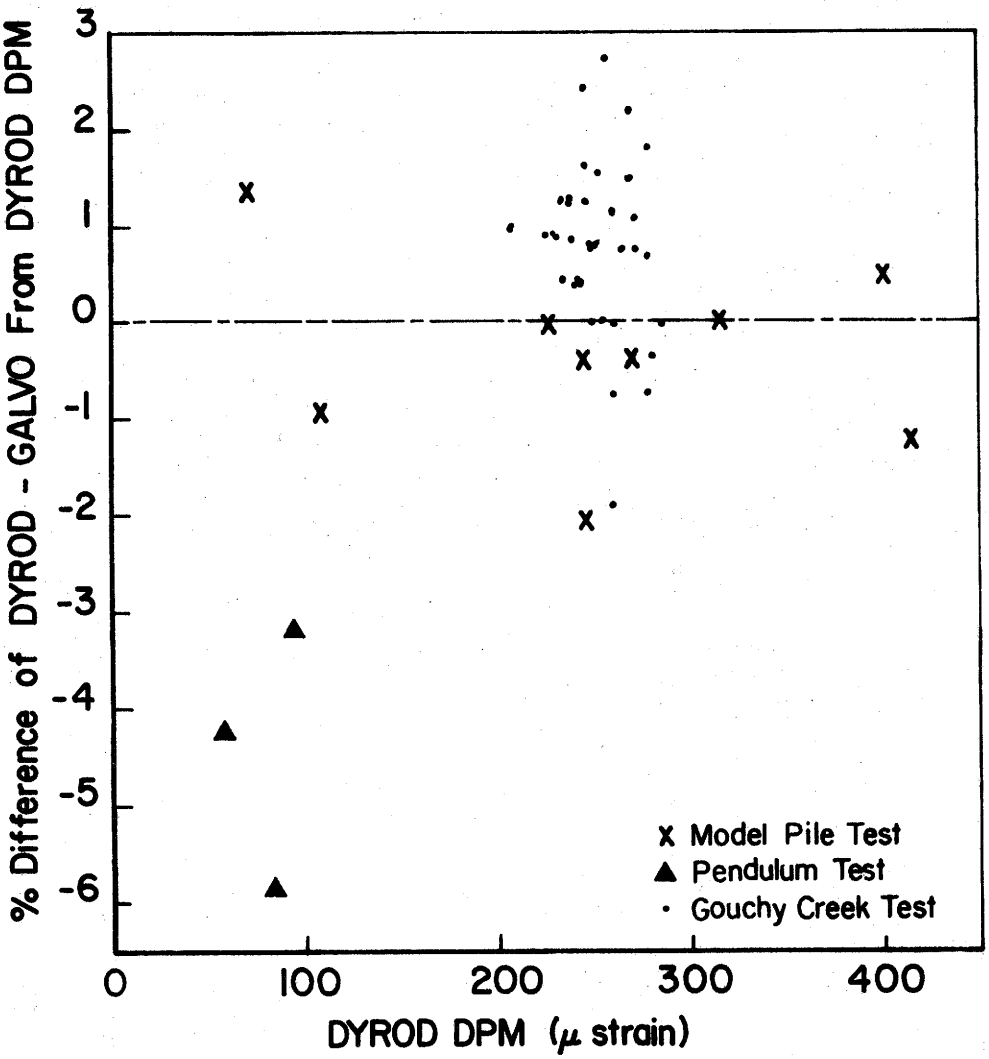

FIG.IV-12.-% DIFFERENCE OF GALVO FROM DPM PEAK STRAIN

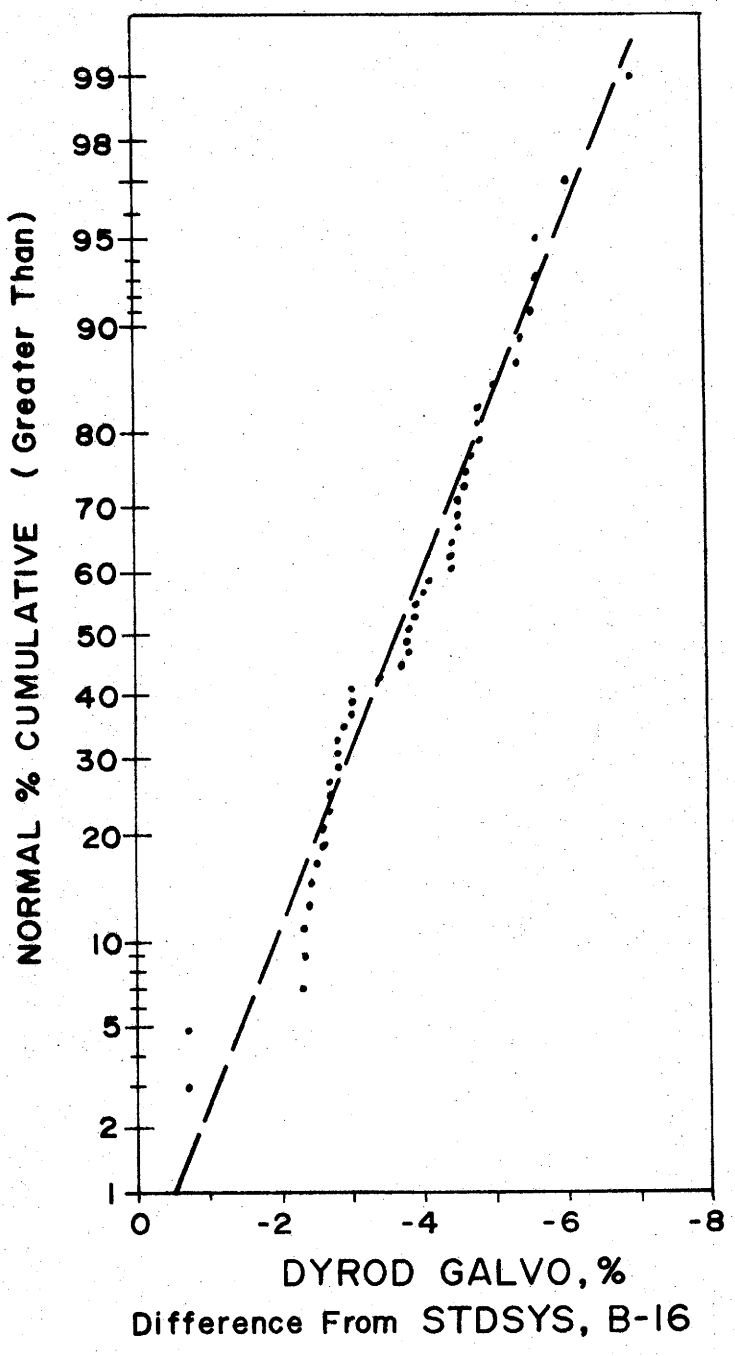

FIG. IV-13.- NORMALITY OF DYROD GALVO vs. STDSYS DATA, B-16

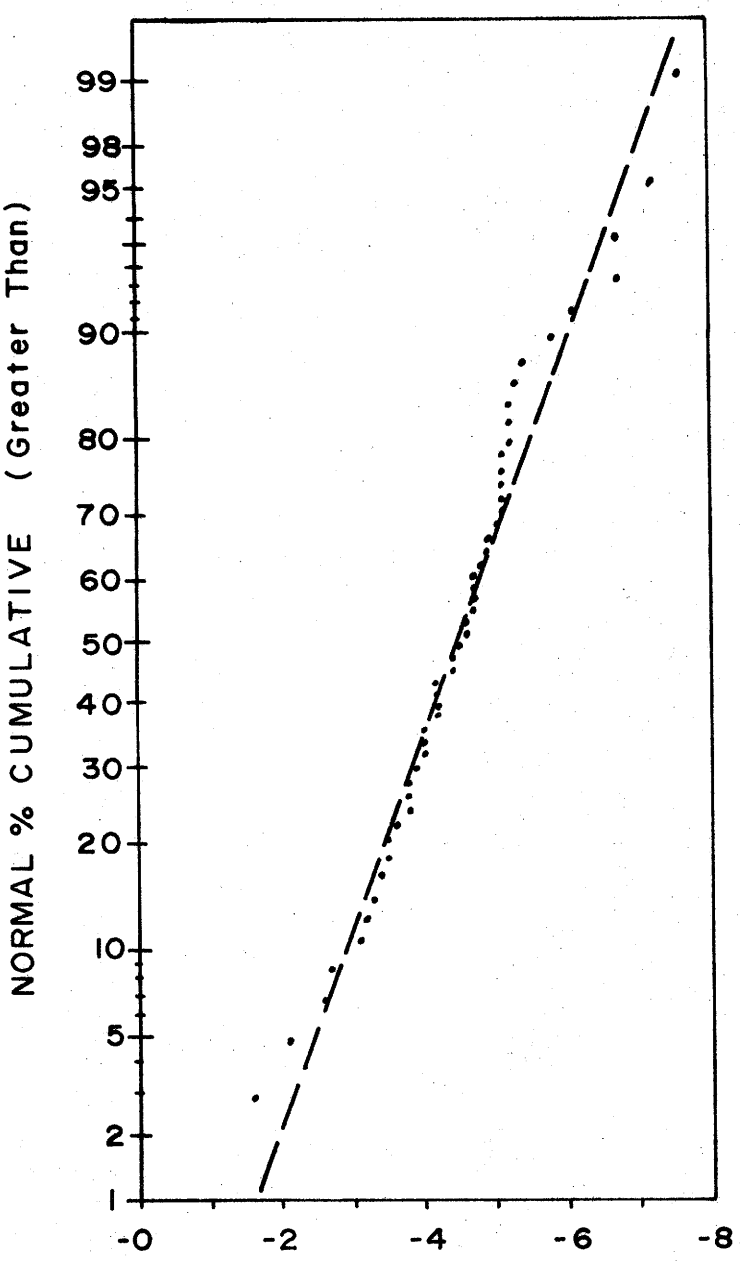

FIG. IV-14.- NORMALITY OF DYROD GALVO vs. STDSYS DATA, B-17.

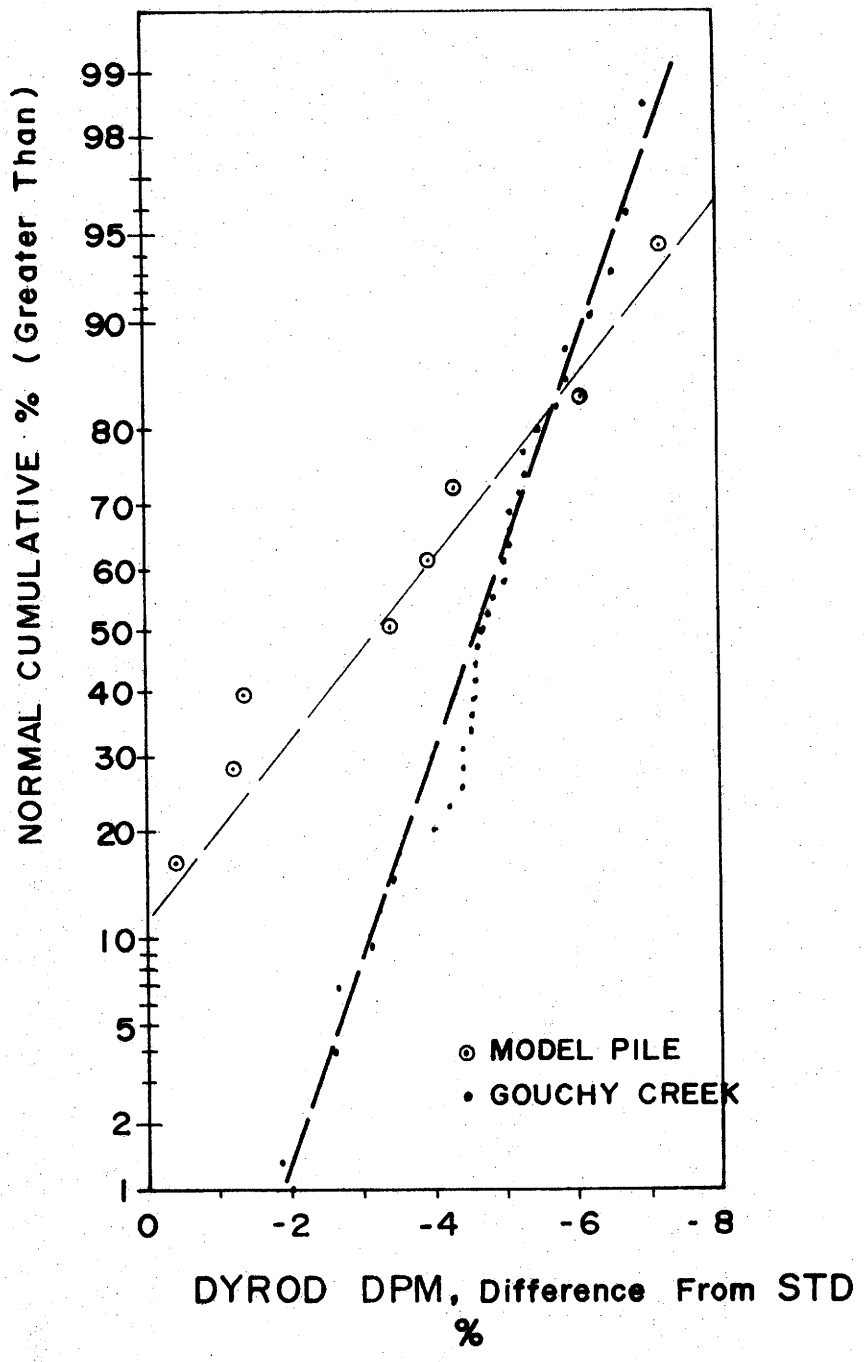

FIG. IV-15. - NORMALITY OF DYROD DPM vs. STDSYS.

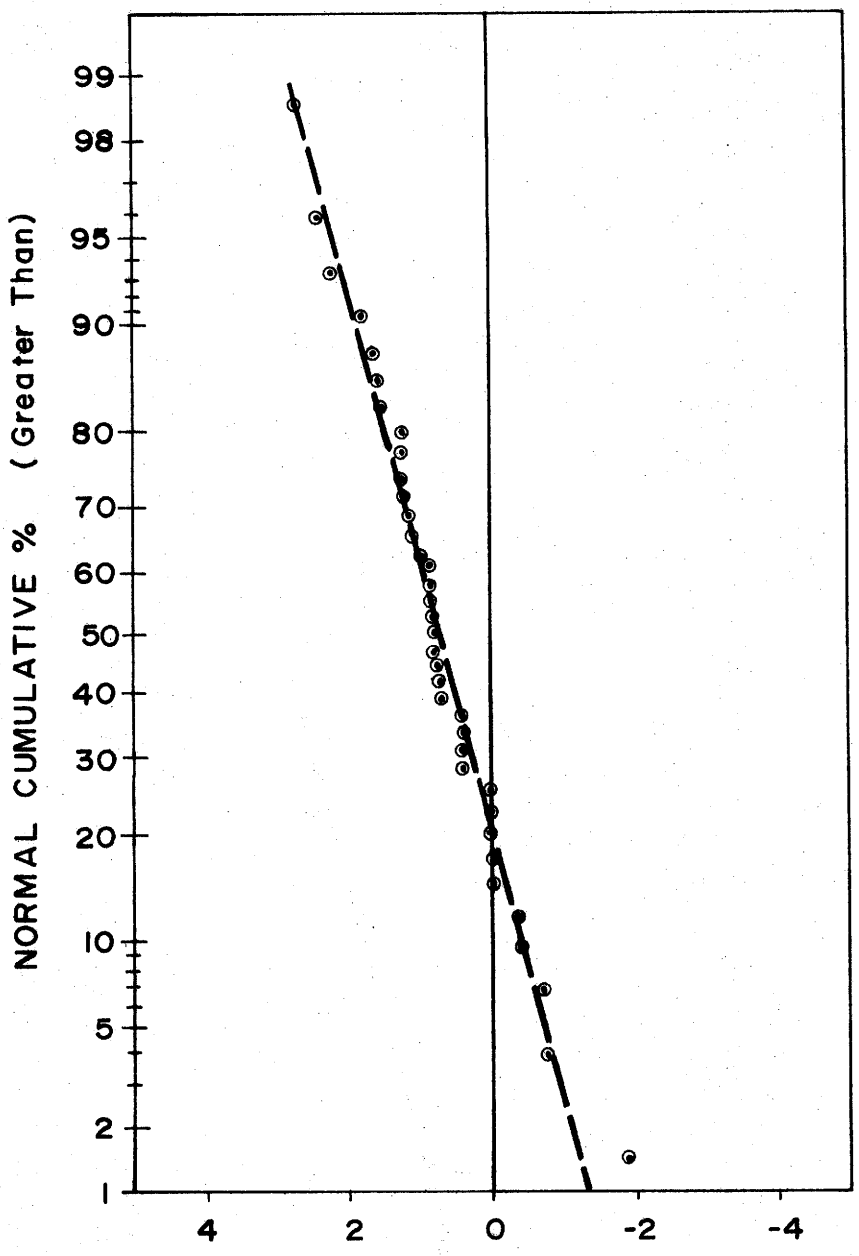

FIG. IV-16 - NORMALITY OF GALVO vs. DPM DATA.

APPENDIX V - TEST OF PERFORATED, ALUMINUM LOAD CELL

TEST OF PERFORATED, ALUMINUM FORCE TRANSDUCER

Description of the Transducer.

During the middle of this study of the dynamic peak force readout device (DYROD), an aluminum force transducer concept was tested. The transducer was suggested for possible use with the DYROD.

The perforated aluminum load cell consisted of a 16-in. (41 cm) square by 1-1/2-in. (3.8 cm) thick block of aluminum. The block of aluminum was drilled with 256 regularly spaced holes, each approximately 3/4-in. (1.9 cm) in diameter. Twelve of the holes were instrumented with bonded foil resistance strain gages of the type indicated in Table 3. Instrumented holes were reamed larger, to about 13/16-in. (2.1 cm) to smooth those holes for gage installation. The gage locations are shown in Fig. V-1. The gage centers were located 3/4-in. (1.9 cm) from the upper and lower surfaces of the aluminum force transducer, on the sidewalls of the holes. The upper half of each gage sensed vertical or axial strain and the lower half of each gage sensed circumferential or tangential strain. The circumferential strain was deemed equal to the diametric strain and related by Poisson's ratio to the axial strain. Troughs, 1/4-in. (6.3 mm) deep and wide, were cut for running-out strain gage leadwires. The perforated aluminum force transducer was covered on the top and bottom with 16x16x1/4 in. solid steel cover plates. The cover plates were held to the aluminum force transducer by countersunk, flathead screws. Any time that the perforated aluminum transducer was tested, eight pieces of 16x16x1/2 in. plywood were used on top of the transducer and two pieces were used beneath it, to simulate normal concrete pile cushioning material.

Description of Transducer Evaluation Tests.

The aluminum force transducer was first tested during the pile stub and pendulum tests. The transducer and wood cushioning were set on the front end of the pile stub and readings recorded for a number of blows. The 12 strain gages were read simultaneously by

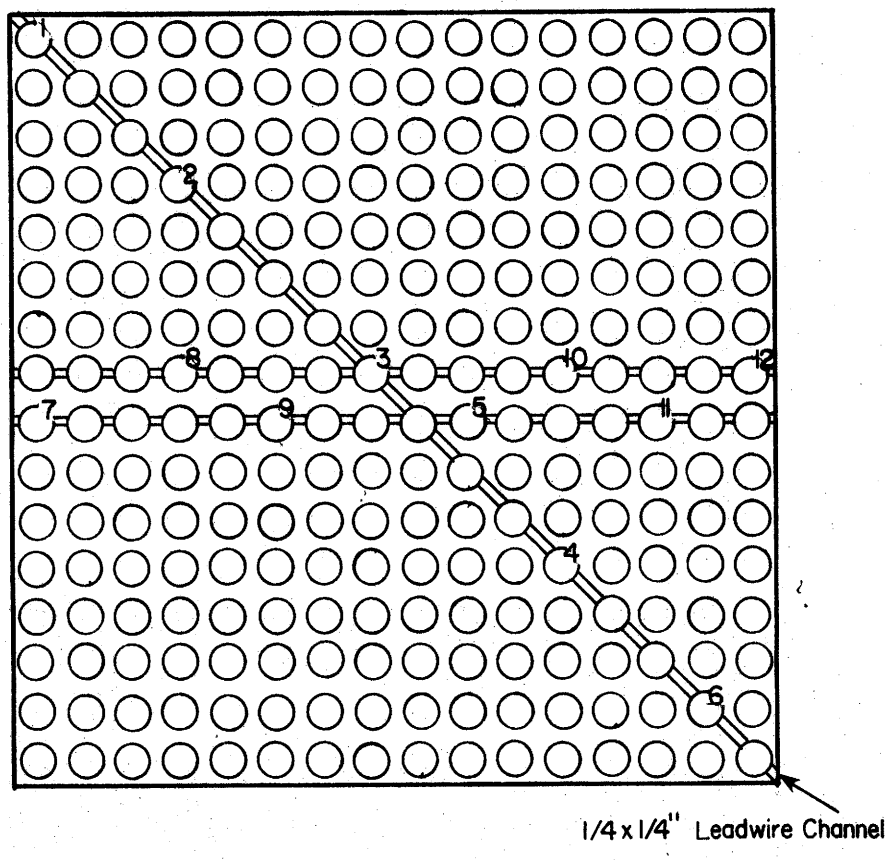

(a) Plan

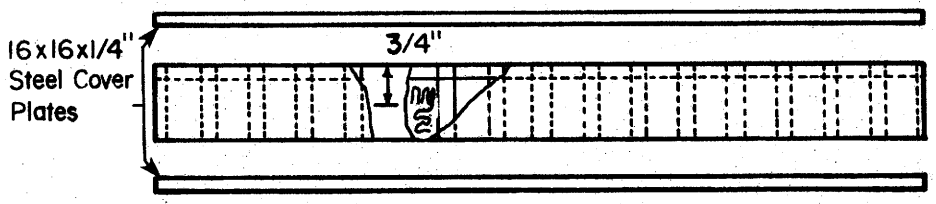

(b) Elevation

FIG. V-1- FORCE TRANSDUCER

the standard carrier amplifier and Visicorder system (STDSYS). The force transmitted to the pile stub was read by the DYROD digital panel meter (DPM) connected to embedded strain gages in the pile stub. An oscilloscope was also connected to the BNC connection on the DYROD for checking purposes. Some dynamic forces would not be transmitted through the 1-in. (2.5 cm) wood cushion to the pile stub and would be reflected back through the aluminum force transducer. It was felt that the difference between the dynamic force sensed by the aluminum transducer and the force sensed in the pile stub, however, would not be significant.

The other evaluation test of the aluminum force transducer was a static one, performed in a Southwark 120,000 lb (534 kN) Loading Machine. Static loads were applied through a ball bearing, loading cap, and 16x16x2-in. steel loading plate to the 8 pieces of plywood on top of the force transducer. The 12 individual strain gages in the transducer were read via an SR-4 Baldwin Switching and Balancing Unit and Budd P-350 Portable Strain Indicator set for a gage factor of 2.03.

Test Results.

Pile stub and pendulum test.-- The Visicorder traces were reduced to values of peak strain by measuring peak trace deflections and multiplying by the corresponding measured and computed calibration factor for each channel, for each blow. The peak strain indicated by each gage was then individually plotted versus applied peak force as detected by the DYROD DPM and pile stub strain gages. Two typical plottings are shown in Fig. V-2.

It was apparent that the gages did not show a pattern when plotted individually and that was expected. No special effort had been made to keep the pendulum from hitting high, low, right, or left, since it was desired to simulate a pile driving hammer. It was assumed that a hammer could hit slightly and occasionally eccentrically. Various potential load distributions have been sketched in Fig. V-3. The relatively few number of data points (gages), however, renders such contouring to be an academic exercise. The

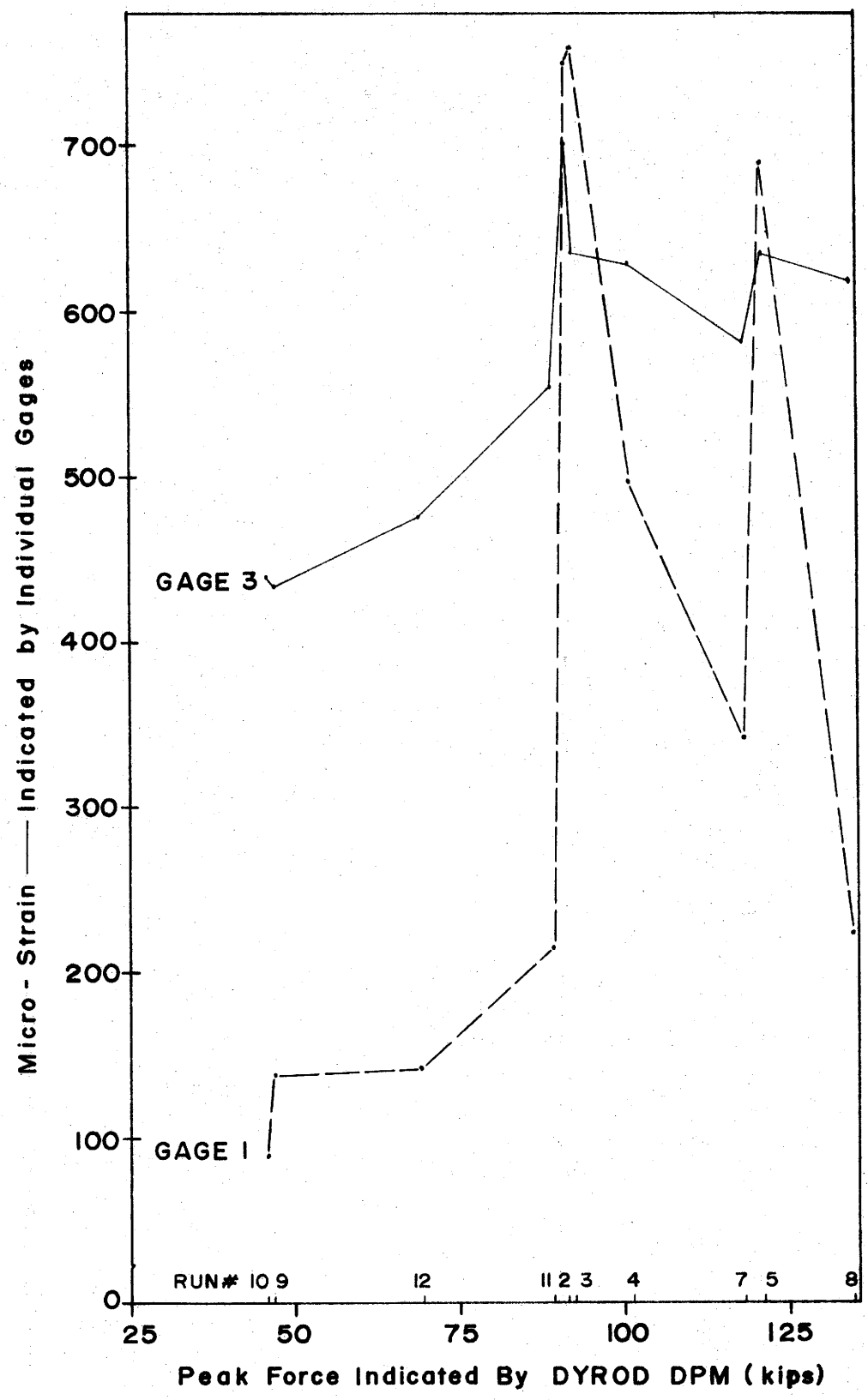

FIG. V - 2. - DATA FROM GAGES 1 & 3.

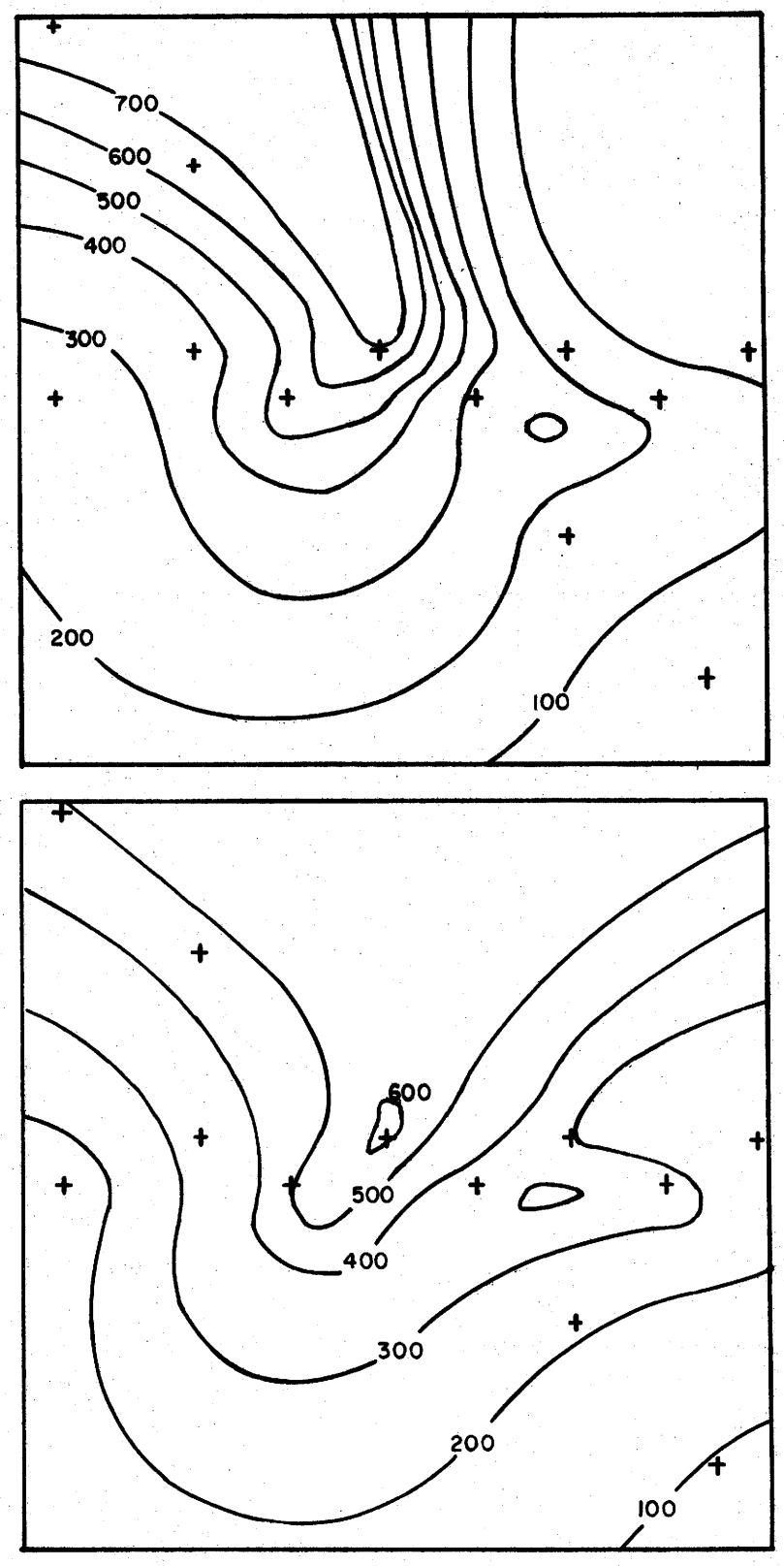

FIG. V-3- LOADING CONTOURS IN MICRO-STRAIN

point to be realized is this. For an infinite variety of loading patterns, it is possible to generate the same force in the pile. By extension it is also possible for an infinite combination of individual strain gage readings. It was thus decided that the strain gages should be dealt with collectively.

Either of two dubious but simplifying assumptions then had to be made. One could assume an infinite stiffness in the materials above and below the transducer and hence a uniform distribution in the transducer, with no concentrations at edges, corners, thin wall sections, etc. Or one could assume that all such stress concentrations would be averaged out in treating the gages collectively. Since gages 2 and 12 did not yield any signals during the test, probably due to some bad leadwire connections, 10-gage-averages of dynamic peak strain were computed for each blow. They are plotted in Fig. V-4. It should be noted that the standard deviations corresponding to those 10-gage-averages ranged from 25% to 74% of the value of those averages.

Static test.-- Notwithstanding the fact that proportionality or linearity may exist in a material under quick dynamic loading and not under slow static loading, it was the purpose of the static test to check for a degree of consistency of behavior among the gages used to instrument the aluminum force transducer.

The loading machine was loaded to 80,000 lbs (356 kN) in increments of 10,000 lbs (44.5 kN) and corresponding readings of the strain gages were obtained. The loads had to be held to enable switching and reading of gages one at a time. The resulting gage readings are plotted individually in Fig. V-5 and V-6. A 12-gage-average is also shown along with a theoretical curve corresponding to an assumed E of 10×10^6 psi ($69 \times 10^6 kN/m^2$) for aluminum. The theoretical and 12-gage-average curves are also shown on Fig. V-4, though no dynamic-static relationship is implied.

The individual gages showed erratic and inconsistent behavior and as a whole, behaved non-linearly, appearing eventually to begin approaching a limit as an average. The protective coating on gage #3

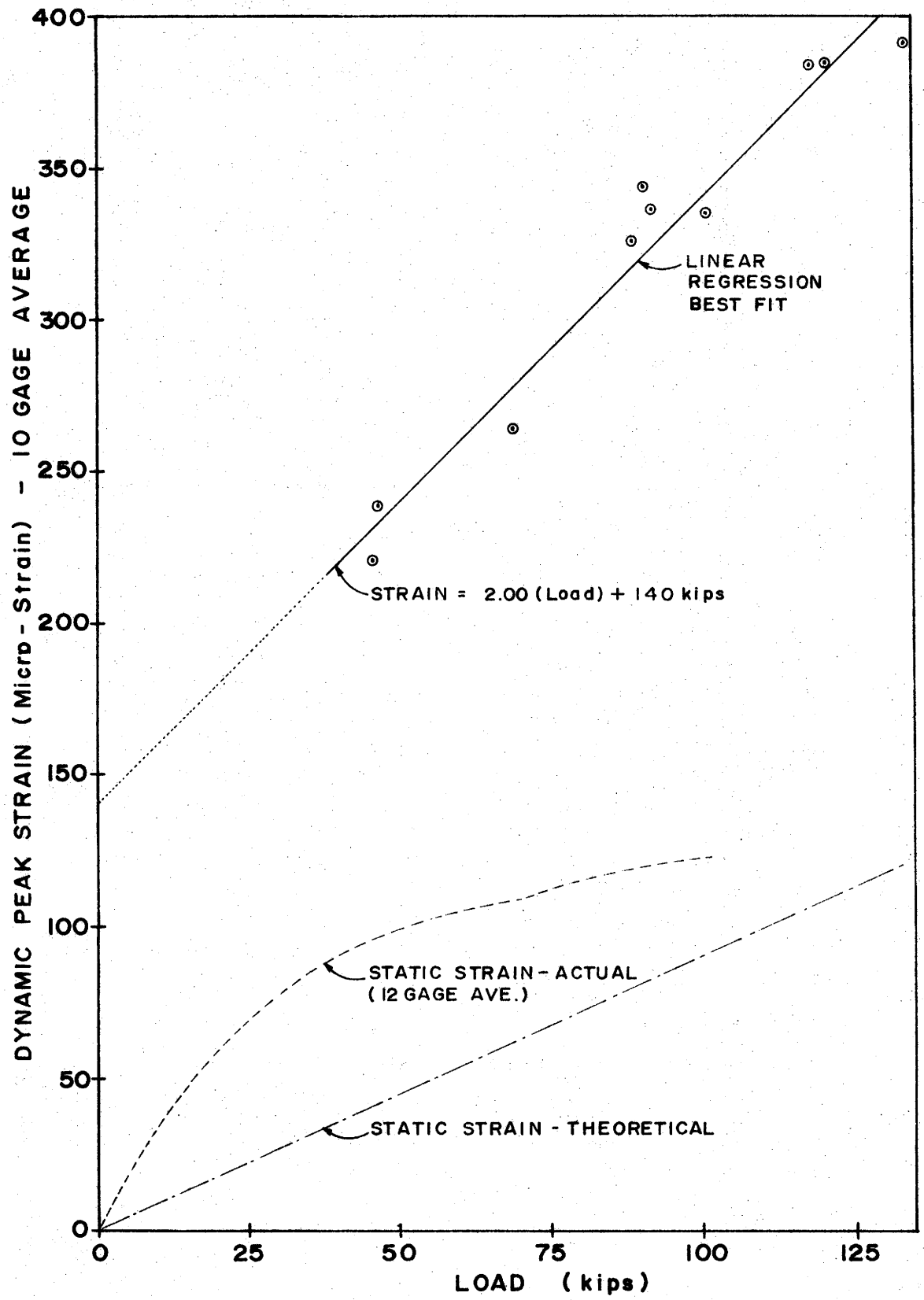

FIG. V-4. AVERAGE STRAIN vs. LOAD.

was loosened at the end of static testing.

If additional testing is to be performed on the perforated aluminum force transducer or any other self-contained, portable, and reusable transducer for use with the DYROD, it is strongly recommended that dynamic testing in a Gilmore machine be performed. Only by this means can a dynamic modulus of elasticity and calibration curve be accurately obtained. A range of usable loading frequencies should also be used.

was loosened at the end of static testing.

If additional testing is to be performed on the perforated aluminum force transducer or any other self-contained, portable, and reusable transducer for use with the DYROD, it is strongly recommended that dynamic testing in a Gilmore machine be performed. Only by this means can a dynamic modulus of elasticity and calibration curve be accurately obtained. A range of usable loading frequencies should also be used.

APPENDIX VI. ACTUALLY MEASURED FORCE-TIME DATA AND PARAMETER VARIATION STUDIES

ACTUALLY MEASURED FORCE-TIME DATA AND PARAMETER VARIATION STUDIES

Actual Force-Time Data.

Continuous records of force in the pile with time were recorded at the Gouchy Creek test on the Visicorder oscillograph. All of those records were compared and very little difference was noted in the recorded wave magnitudes and shapes. Five curves of blows during driving of pile B-17 were representative of all the Visicorder data. There was that much similarity. STDSYS trace curves were chosen since that system produced slightly sharper traces than the DYROD perhaps because of slight differences in galvanometer damping. Those five representative curves are shown in Fig. VI-1. The differences between the curves are only small differences in the shape and timing of the backslope of the third peaks. Such differences are not significant in the hammer-pile-soil simulation techniques at this time. The curves have been reproduced at their original size.

Blow #80 during the driving of pile B-17 has been digitized and used in the sample problem of the proposed standard method of analysis using measured peak force data for comparison of bearing graphs. The digitized and replotted STDSYS trace for blow #80 is shown in Fig. VI-2. As usual with these curves, time zero is an arbitrary starting point.

Force-Time Simulation and Parameter Variations.

The most accurate method of analysis using the wave equation probably lies in simulation of the actual, complete force-time curve by varying parameters until good reproduction is obtained.

The techniques of parameter variation and force-time simulation are the means by which improved values for key parameters are obtained. Such improved parameter values then become the standard and recommended values for simulating the more common hammers, cushions, capblocks and other pile driving equipment.

Parameter variation is also used in the proposed standard method

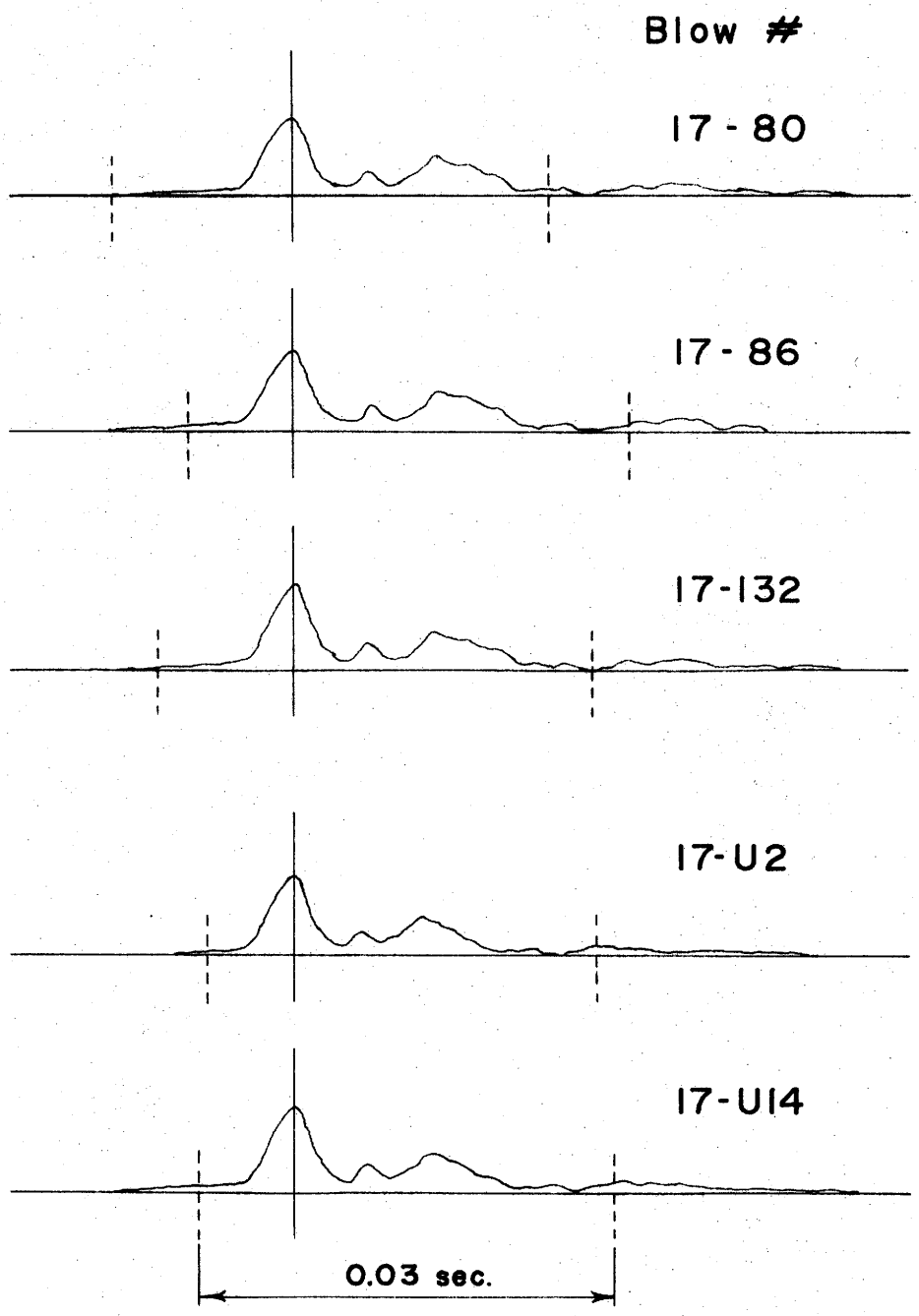

FIG. VI-1. - ACTUAL FORCE - TIME TRACES.

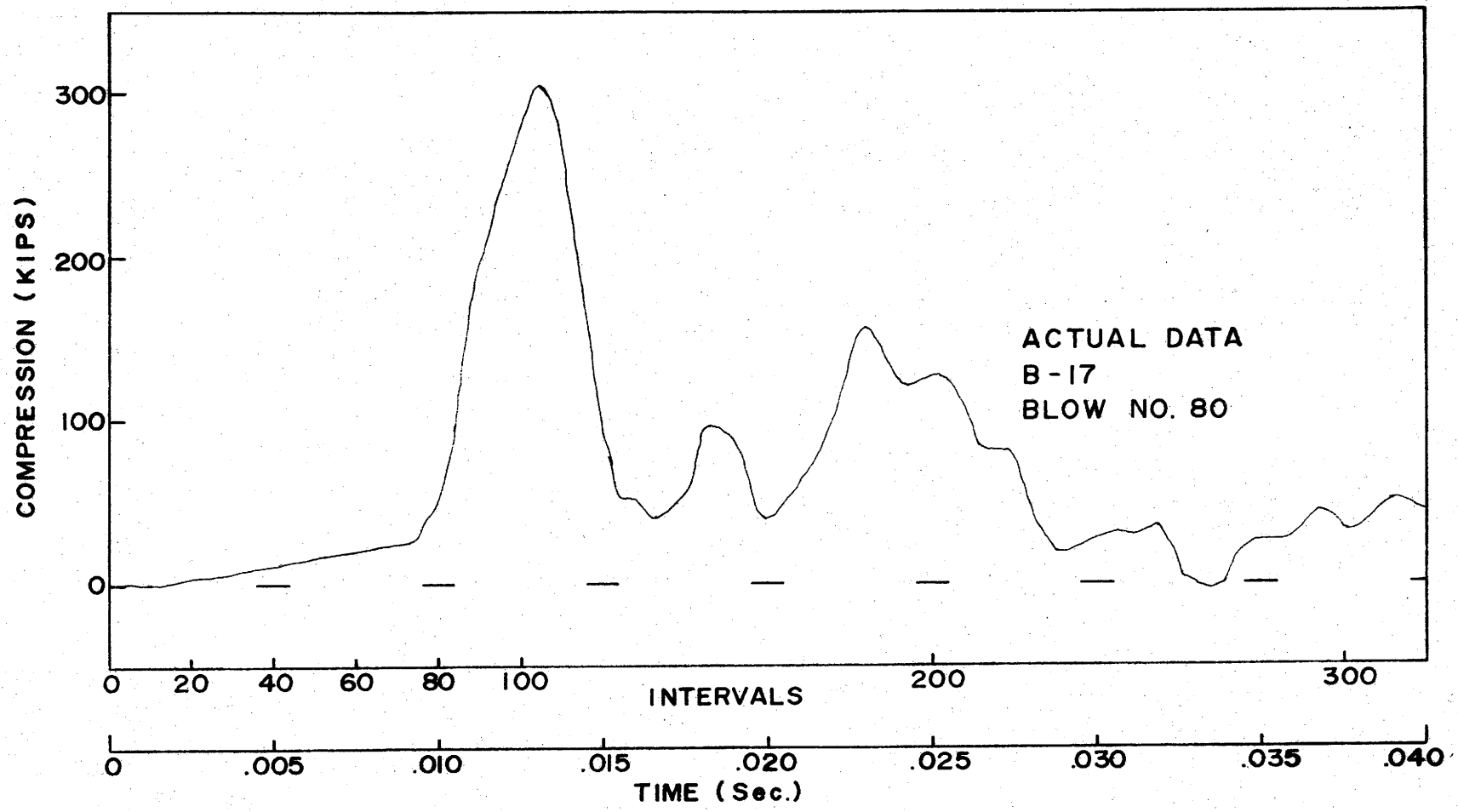

FIG. VI-2. - ACTUAL FORCE-TIME FOR BLOW 17-80.

of analysis using measured peak force data. In that method only VELMI, initial ram velocity, is varied and only to match peak forces, not complete force-time curves.

Some parameter variation studies were made on the Gouchy Creek data. However, project termination coupled with a considerable lack of measured information about the actual pile driving equipment used, precluded completion of parameter variation studies to improve hammer simulation. Such efforts are seriously needed however for diesel hammer simulation in particular. Fig. VI-3 gives ample evidence of that. The bearing graph, using unadjusted, currently recommended hammer-pile-soil simulation input data into the wave equation program, yields ultimate resistances that are slightly-less-than twice as large as those resistances indicated by the actual measured force-time data bearing graph. This area is where additional work needs to be done. Any time actual force-time is measured and a load test will be performed, detailed information about the equipment and materials used should be obtained and multiple, concurrent parameter variation studies performed to obtain better numbers for ordinary simulation of diesel hammers in pile driving. A load test was not available for checking the Gouchy Creek bearing graphs.

The limited, single parameter variation studies made on the Gouchy Creek data were initiated to determine what parameter should be varied in the standard method of analysis using measured peak force data. The VELMI was chosen as most straightforward and according to recent offshore industry findings, would have the least effect of undesirably altering the shape of the computed force-time curve for changes in the value of that parameter.

It was originally planned to vary stiffness parameters instead of VELMI but studies on hammer-pile-soil configurations very similar to Gouchy Creek showed the stiffness to be undesirable choices. Data shown in Fig. VI-4 for ram stiffness, K(1), indicates that large reductions in recommended K(1) values could not be meaningfully used to reduce computer program indicated peak forces at the top of

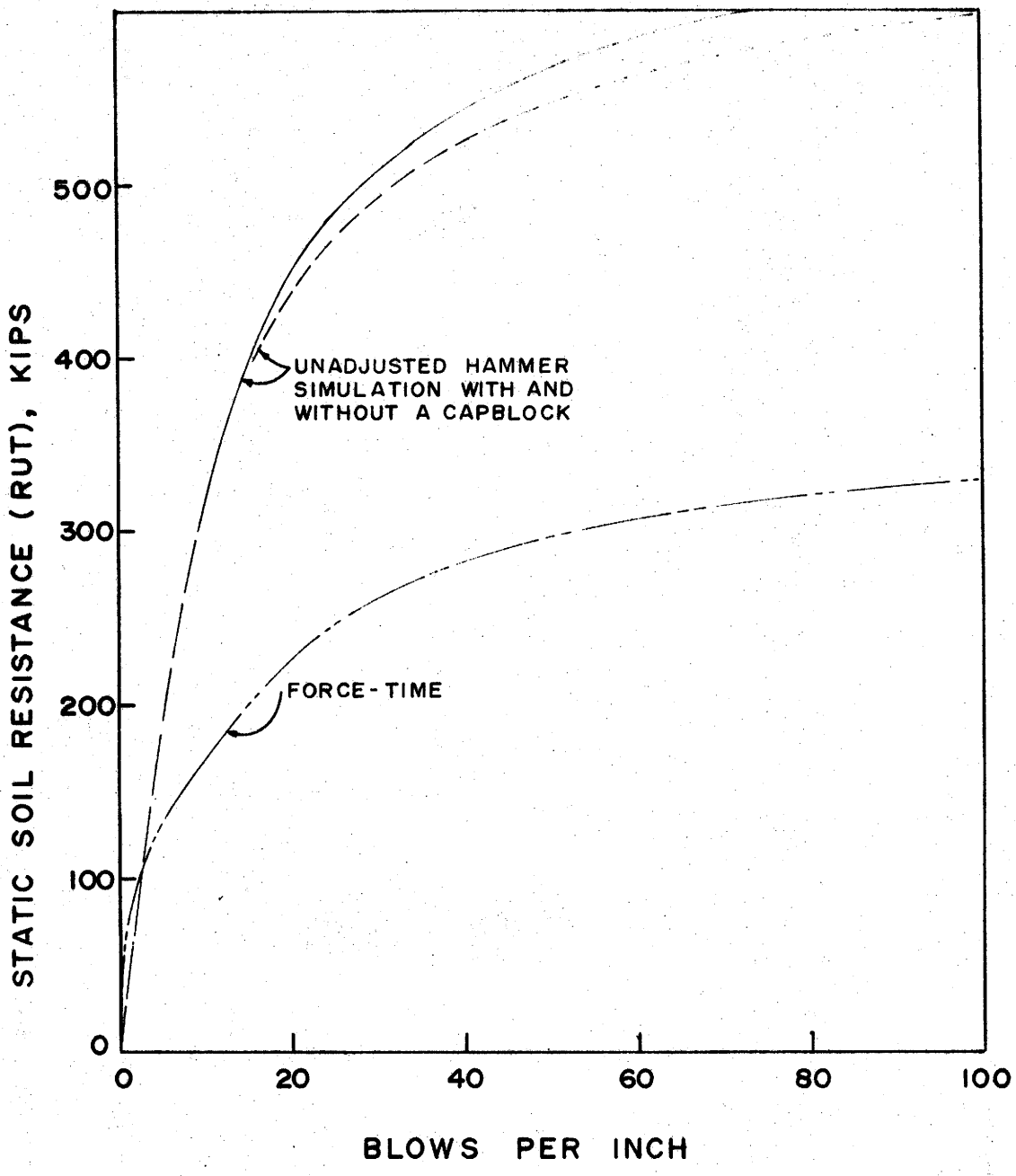

FIG. VI.-3.-BEARING GRAPH OF UNADJUSTED HAMMER SIMULATION.

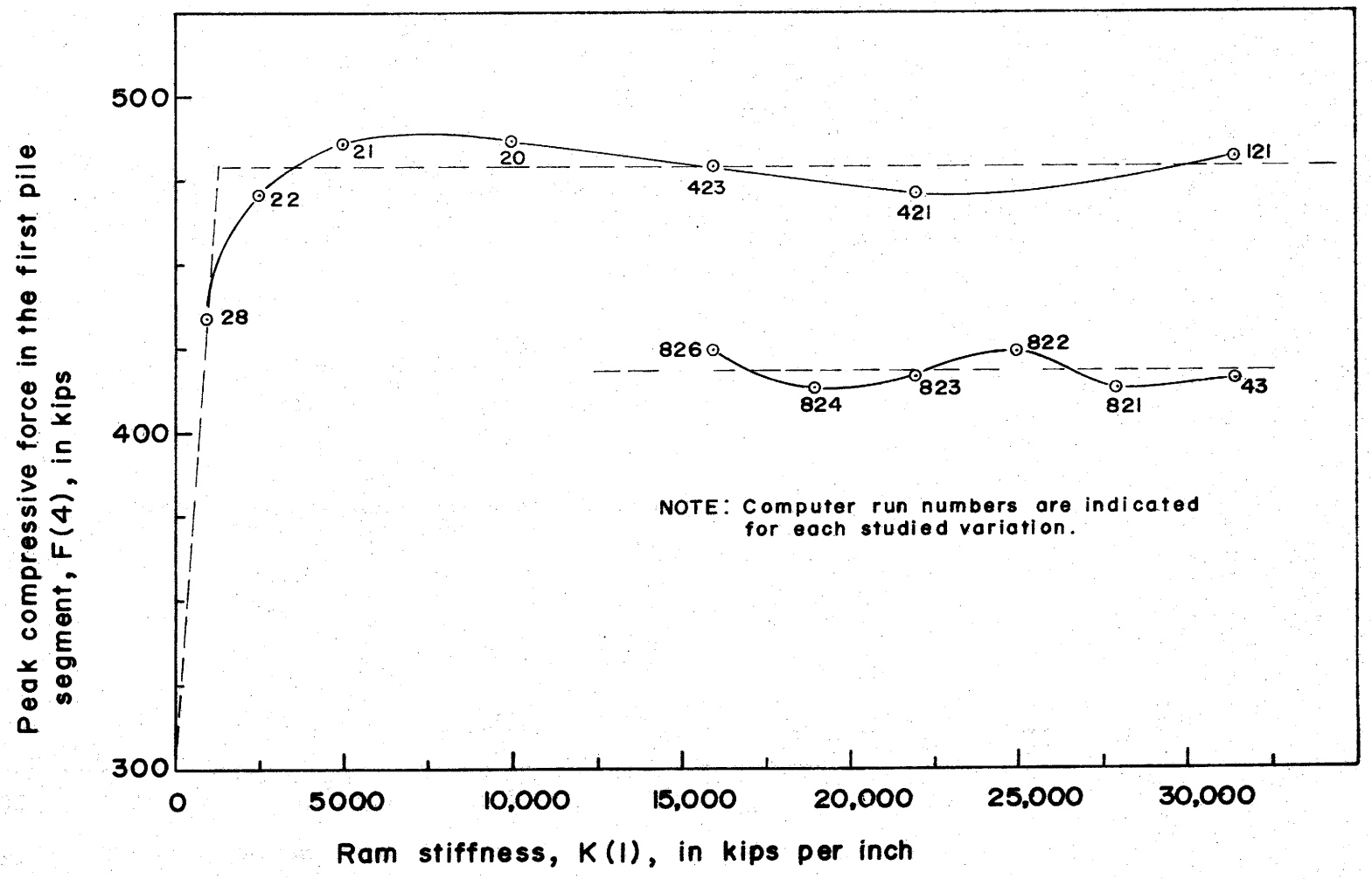

FIG. VI-4.- VARIATION OF K(1).

the pile. Values seemed to oscillate over a large range of the ram stiffness values used.

Variation of combined stiffness, K(3), was also studied for configurations similar to the Gouchy Creek hammer-pile-soil system. The variations are shown in Fig. VI-5. The stiffness K(3) is a combined stiffness composed of a stiffness for the cushion and a stiffness for the first pile segment. The K(3) variations showed a much more significant and immediate effect on peak force. The VELMI was chosen over K(3), however, because recent findings in the offshore industry indicated that variations in K(3) cause pronounced and now predictable alterations of the shape of the computed force-time curve. For that reason the VELMI was chosen as the parameter to be varied in the standard method of analysis. It was later determined however that even the VELMI changes severely altered the shape of the force time curve for the particular case of the short point-bearing, concrete piles at Gouchy Creek, but since the bearing graphs turned out so well, this was not deemed to be a problem.

A very few, minor variations of the anvil and capblock stiffness, K(3), and coefficients of restitution, e, were also varied but were found to have insignificant effects.

It is strongly felt that such a large reduction in VELMI for the Gouchy Creek data would not have been necessary to correct the wave equation program peak force, if better hammer simulation numbers had been available for use in the initial computer run. This is probably going to be a continuing problem with the use of the hammer-pile-soil simulation in the wave equation method of analysis particularly for diesel hammer applications.

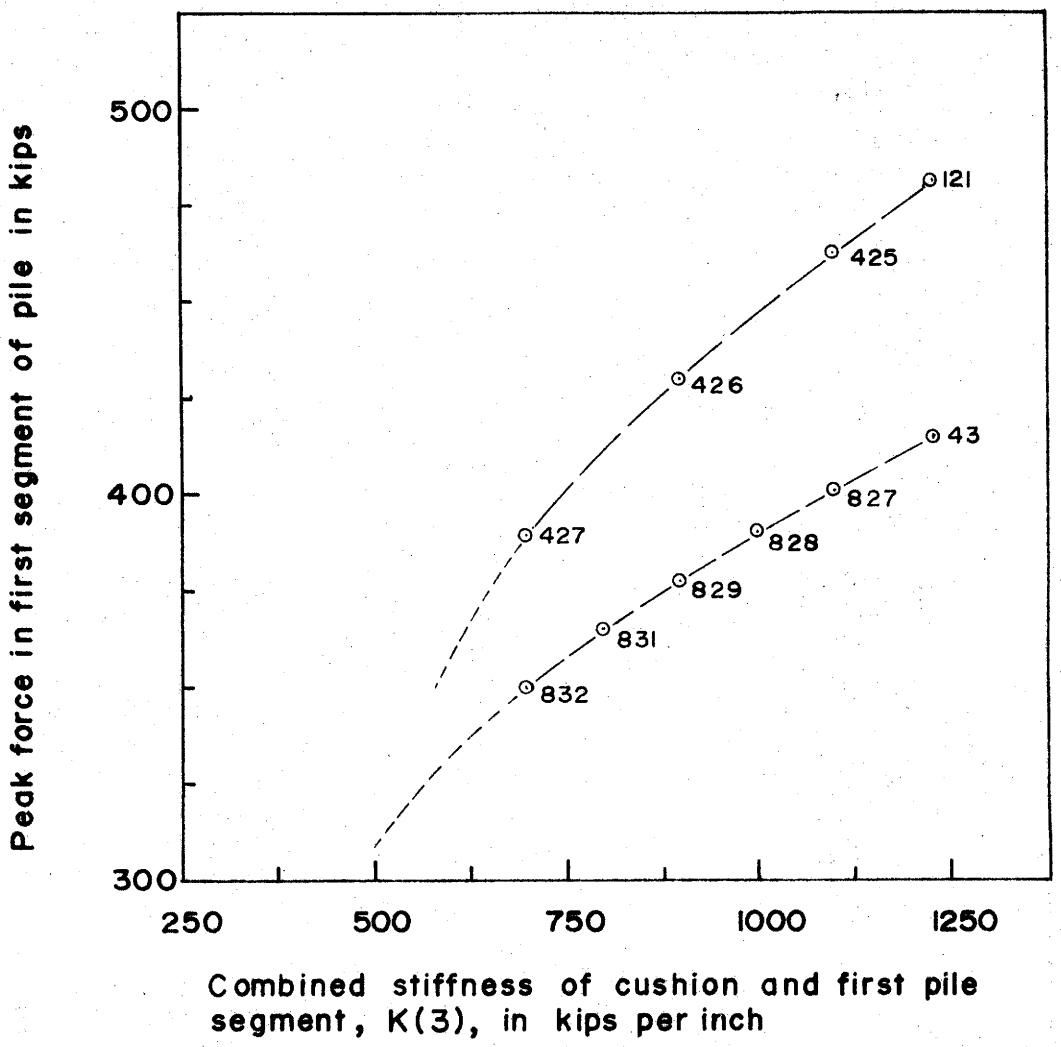

FIG. VI - 5. - VARIATION OF K(3).

APPENDIX VII. - LINEARITY AND CALIBRATION RESISTORS

LINEARITY AND CALIBRATION RESISTORS

DYROD Output Linearity

The output of the DYROD DPM and the GALVO binding posts were checked to be certain that the desired linearity was present. This test was accomplished by connecting a transducer bridge to the DYROD, balancing it, then adjusting the DYROD gain so that calibration resistor position 3 yielded a reading on the DPM of 1000 when the calibrate button was depressed. DPM readings corresponding to positions 4 through 10 were likewise observed. The stated value for the several calibration resistors was converted to equivalent microstrain using the following relationship. (12)

$$M_s = \frac{120}{2\ (\text{Cal R} + 120)}$$

The resultant plot of these values vs. their corresponding DPM is shown in Fig. VII-1.

Calibration Resistor Check

When the peak force measurement systems evaluation test data had been analyzed and the DYROD was found to average 4% lower readings when compared to the STDSYS, it was decided that the internal calibration resistors of the DYROD should be checked. The resistance of the calibration resistors were checked by connecting the DYROD to an instrumented cantilever beam. A known

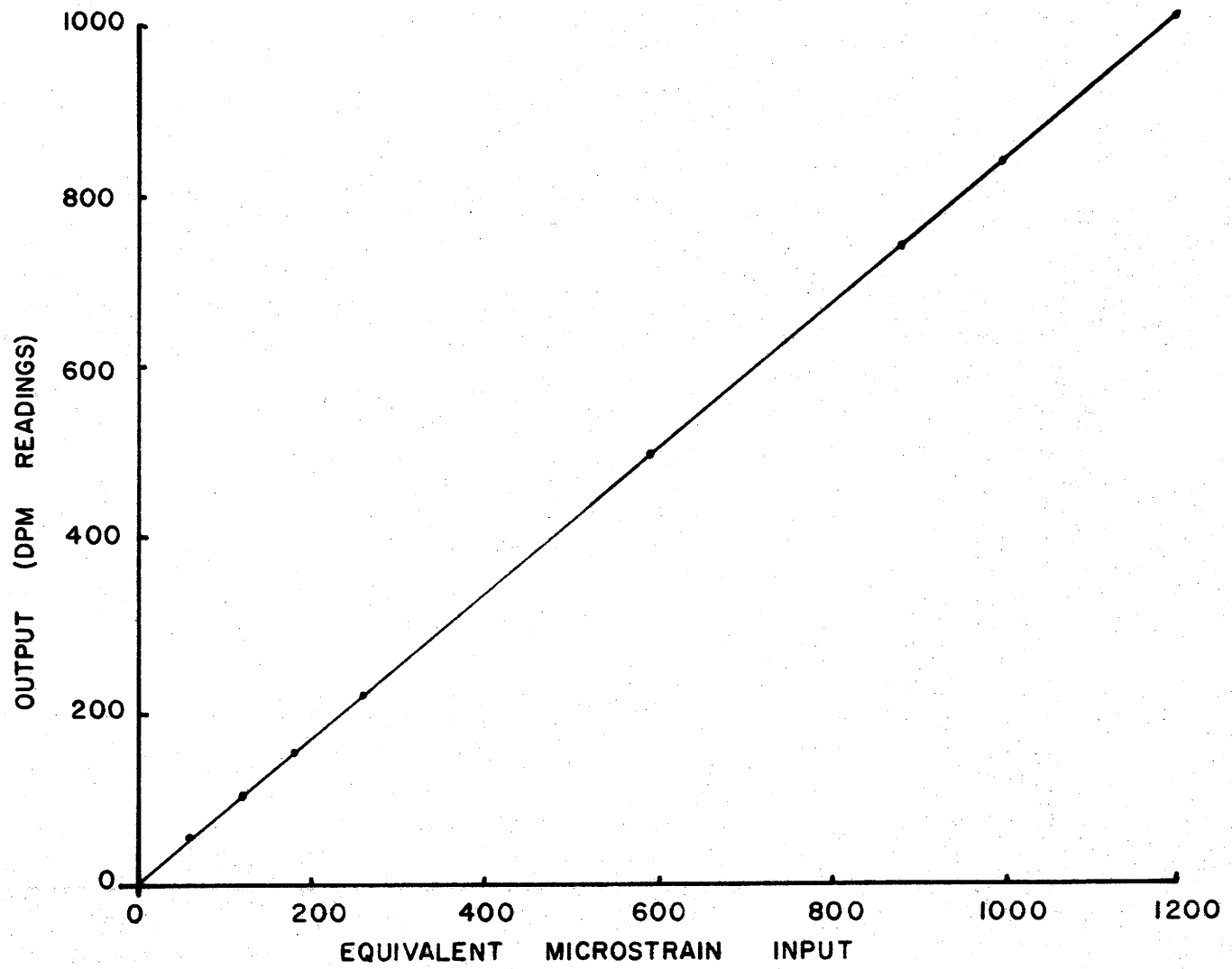

FIG. VII-1 – DYROD LINEARITY

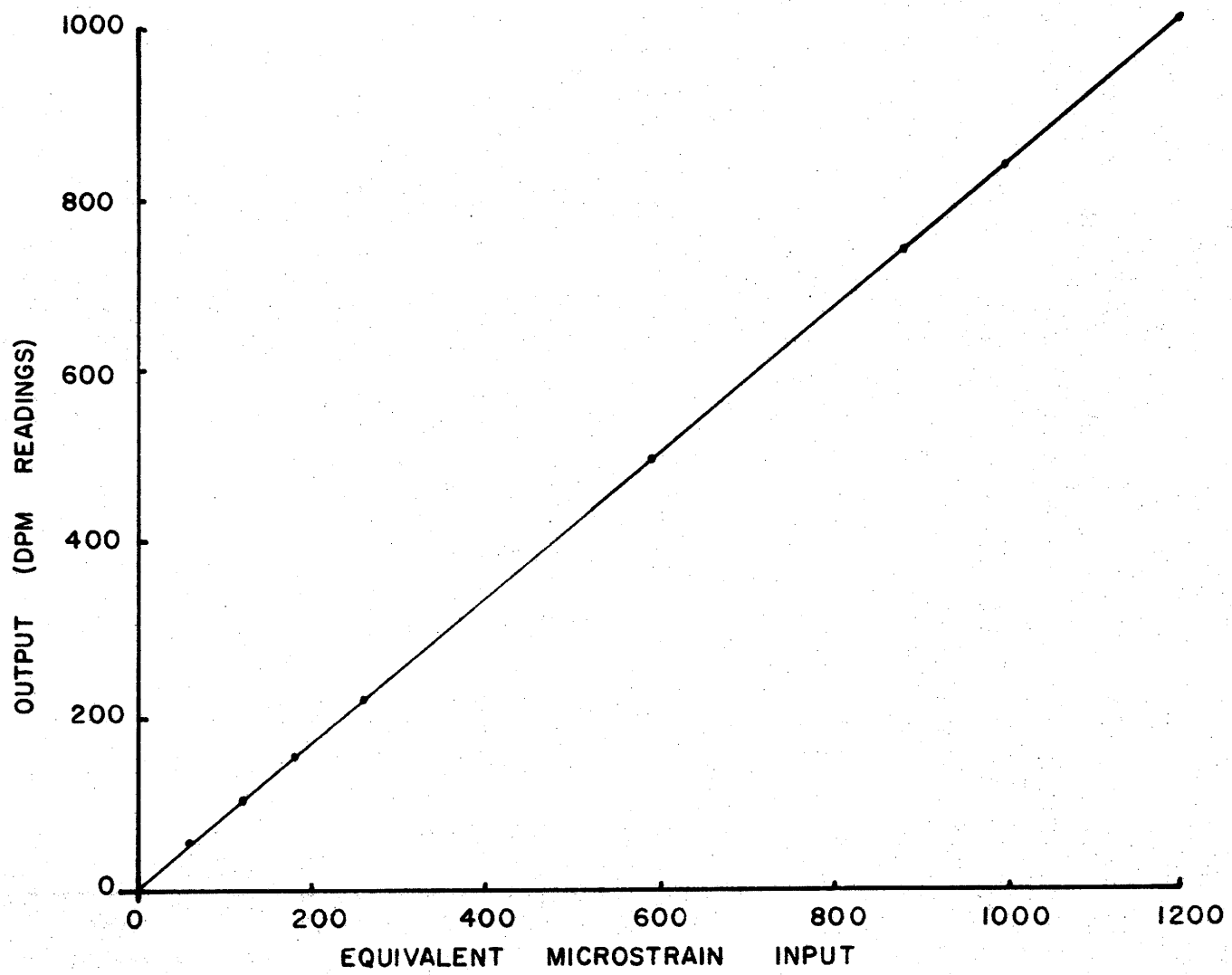

FIG. VII-1 – DYROD LINEARITY

strain was induced in the beam and the DYROD output was read using a digital volt meter (DVM). The induced strain was then removed and a reading was taken with the DVM for the various calibration resistor positions while depressing the calibrate button. The value of each of the resistors was then calculated using the relationship above and the results are shown in table VII-1. Close agreement between the measured value and the manufacturer's stated value was achieved.

TABLE VII-1.-- VALUES OF DYROD CALIBRATION RESISTORS

Calibration Resistor Number	Calculated Resistance From Test (ohms)	Specified Resistance (ohms)
1	15,171	15,000
2	19,987	20,000
3	49,587	49,900
4	59,940	60,000
5	67,950	68,100
6	101,695	102,000
7	230,769	232,000
8	331,492	332,000
9	495,868	499,000
10	998,336	1,000,000

NOTES